NACA TN 3174

NATIONAL ADVISORY COMMITTEE FOR AERONAUTICS

TECHNICAL NOTE 3174

INFLUENCE OF AIRFOIL TRAILING-EDGE ANGLE AND TRAILING-EDGE-THICKNESS VARIATION ON THE EFFECTIVENESS OF A PLAIN FLAP AT HIGH SUBSONIC MACH NUMBERS

By Albert D. Hemenover and Donald J. Graham

Ames Aeronautical Laboratory
Moffett Field, Calif.

Washington
June 1954

NATIONAL ADVISORY COMMITTEE FOR AERONAUTICS

TECHNICAL NOTE 3174

INFLUENCE OF AIRFOIL TRAILING-EDGE ANGLE AND TRAILING-EDGE-THICKNESS VARIATION ON THE EFFECTIVENESS OF A PLAIN FLAP AT HIGH SUBSONIC MACH NUMBERS

By Albert D. Hemenover and Donald J. Graham

SUMMARY

The effects of variation of trailing-edge angle and trailing-edge thickness on the lift characteristics of a 10-percent-chord thick symmetrical NACA airfoil section with a 25-percent-chord plain flap are appraised from wind-tunnel tests at Mach numbers from 0.3 to 0.9 and Reynolds numbers varying correspondingly from 1 to 2 million. The airfoil trailing-edge angle was varied from approximately 18° to 6°, and the trailing-edge thickness from zero to the thickness at the flap hinge line.

Reduction of the trailing-edge angle decreases, at moderate angles of attack, the loss of flap effectiveness for small deflections ordinarily noted at high subsonic Mach numbers for airfoils of conventional profile. At zero angle of attack, reduction of the trailing-edge angle has no effect on the variation of flap effectiveness with Mach number but has the favorable result of decreasing the range of flap deflections for which the effectiveness is zero or negative.

An increase of the airfoil trailing-edge thickness results in an increase of flap effectiveness at virtually all Mach numbers. The results indicate further that, at zero angle of attack, an increase of trailing-edge thickness promotes, in general, an increase of lift effectiveness from the low-speed value in the range of Mach numbers for which the effectiveness of a sharp trailing-edge flap decreases sharply. For the particular thickened trailing-edge flaps investigated, however, the variation of effectiveness with Mach number would appear to be undesirably large.

INTRODUCTION

The influence of two elements of airfoil geometry, trailing-edge angle and trailing-edge thickness, on the lift characteristics of airfoil

sections and the effectiveness of trailing-edge control surfaces at transonic Mach numbers has recently become the subject of considerable interest. In the investigation of reference 1, the aerodynamic characteristics of an airfoil section 10-percent chord thick at Mach numbers from 0.3 to 0.9 were determined for trailing-edge angles of 6°, 12°, and 18°. The first part of the present investigation extends this study to an appraisal of the effects of this trailing-edge-angle variation on the characteristics of the same airfoil section with a 25-percent-chord plain flap.

The second part of the investigation was prompted by reports from free-flight investigations of generally improved effectiveness at transonic Mach numbers of ailerons with thickened trailing edges as compared to that of sharp trailing-edge surfaces. To examine the effects of trailing-edge thickness on the variation of flap effectiveness with Mach number, the characteristics of the airfoil section of the trailing-edge-angle study were determined with 25-percent-chord plain straight-sided flaps having trailing-edge thicknesses equal to, and one-half of, the thickness at the flap hinge line.

NOTATION

c	chord of airfoil
c_d	section drag coefficient
c_l	section lift coefficient
$c_{m_{c/4}}$	section pitching-moment coefficient about the quarter-chord point
h	airfoil trailing-edge thickness
M	Mach number
R	Reynolds number
T.E.	trailing edge
$t_{0.75c}$	airfoil-section thickness at 0.75c
α_0	section angle of attack, degrees
δ_f	flap deflection, degrees
$\frac{dc_l}{d\delta_f}$	section flap-effectiveness parameter, rate of change of section lift coefficient with flap deflection at constant α_0

AIRFOIL DESCRIPTION

The basic airfoil-thickness distribution for the investigation was that of the modified NACA four-digit series (see reference 2) with maximum thickness at the 40-percent-chord station. This thickness distribution permits the profile aft of the maximum-thickness location to be changed sufficiently to provide the desired variation in trailing-edge angle without changing essentially the forward portion of the airfoil section. The profiles investigated are illustrated in figure 1 and are designated as follows:

Profile	Trailing-Edge Angle
NACA 0010-0.70 40/1.575	17.9°
NACA 0010-0.70 40/1.051	12°
NACA 0010-0.70 40/0.524	6°
NACA 0010-0.70 40/1.575 (Mod. A)	0°
NACA 0010-0.70 40/1.575 (Mod. B)	7.5°

The first four digits have the same significance as the airfoil designation given in reference 2 and specify the camber and maximum thickness of the profile. The decimal number following the dash is the leading-edge-radius index; the leading-edge radius as a fraction of the airfoil chord is given by the product of the radius index and the square of the thickness-chord ratio. The two digits immediately preceding the slant represent the location of maximum thickness in percent of the chord from the leading edge. The last decimal number is the trailing-edge-angle index, the angle being twice the arc tangent of the product of the angle index and the thickness-chord ratio.

For the trailing-edge-thickness study, the profiles consisted of NACA 0010-0.70 40/1.575 airfoils modified aft of the 75-percent-chord point. Modification A consisted of the substitution of a parallel-sided section of thickness equal to that at the 75-percent-chord station for the normal contour aft of this point. Modification B was formed by substituting for the normal profile a straight-sided section with trailing-edge thickness equal to one-half that at the 75-percent-chord station.

The coordinates for the airfoils of the investigation are listed in tables I to V.

APPARATUS AND TESTS

The tests were made in the Ames 1- by 3-1/2-foot high-speed wind tunnel, a two-dimensional-flow wind tunnel of relatively low turbulence level.

Five 6-inch-chord airfoil models were constructed of aluminum alloy for the tests. The models completely spanned the short dimension of the wind-tunnel test section. End leakage at the model was prevented by the use of contoured sponge-rubber gaskets compressed between the ends of the models and the tunnel walls. Flap deflection was simulated by progressively bending the aft 25 percent of the profile through a total angular range of as much as 16°. For each of the profiles, the thickness at the 75-percent-chord position (representative of the hinge line of an actual 25-percent-chord plain flap) was relieved to facilitate the bending. Surface continuity was preserved by filling the resultant gap with glazing putty.

Measurements of lift, drag, and pitching moment were made at Mach numbers from 0.3 to as high as 0.9 for the various models at angles of attack ranging in general from -2° to 12°. Flap deflection was varied by small increments from approximately -1° to approximately 6° for the greatest part of the investigation. In the case of the NACA 0010-0.70 40/1.575 section, the deflections were extended in the positive direction to approximately 14°. It was not possible, by the means employed, to obtain uniform increments of flap deflection. Sufficient data were obtained, however, to permit, with reasonable accuracy, the determination of the effectiveness of the various flaps for small deflections.

Lift and pitching moments were measured by a method similar to that described in reference 3 from integrations of the pressure reactions on the tunnel walls of the forces on the airfoils. Drag was determined from wake-survey measurements made with a rake of total head tubes.

The variation of Reynolds number with Mach number for the tests is illustrated in figure 2.

RESULTS AND DISCUSSION

Section lift and pitching-moment coefficients at constant angles of attack are presented as functions of Mach number for the various profiles and flap deflections in figures 3 to 12. Drag coefficients for the sharp trailing-edge airfoil sections are similarly presented in figures 13 to 15. The drag characteristics of the thickened trailing-edge

airfoils are not included in the report. Schlieren observations disclosed the existence of strongly developed Karman vortex streets in the wakes of these sections, and wake total pressure measurements made under such conditions have been found to yield erroneous drag results. Section lift coefficients as functions of angle of attack for constant Mach numbers and flap deflections are shown in figures 16 to 20 for the various airfoil sections.

All the characteristics have been corrected for tunnel-wall interference by the methods of reference 4. Dashed lines have been used in figures 3 through 20 to indicate the region of possible influence of wind-tunnel choking on the results.

The pitching-moment and drag characteristics will not be analyzed inasmuch as the object of the present investigation is to determine the lift effectiveness of a plain flap as affected by variations of the trailing-edge geometry.

The variations of section lift coefficient with flap deflection at constant angles of attack for various Mach numbers are illustrated in figures 21 to 23, respectively, for the profiles having trailing-edge angles of 17.9°, 12°, and 6°, and in figures 24 and 25, respectively, for the sections with trailing-edge thickness equal to, and one-half of, the thickness at the flap hinge line. The slopes $dc_l/d\delta_f$ of these curves at zero flap deflection provide a measure of flap effectiveness and are presented in figure 26 as functions of Mach number for angles of attack of 0°, 4°, and 6°.

Focusing attention first upon the airfoils with sharp trailing-edge flaps, it is noted from figure 26 that the effects of trailing-edge-angle variation are confined to Mach numbers above 0.75. At zero angle of attack, an abrupt loss of effectiveness beginning at a Mach number in the vicinity of 0.8 is evident for all three trailing-edge angles. The interesting feature of the results in this case is the very small benefit derived from reduction of the trailing-edge angle even to a value as low as 6°.

From schlieren photographs (fig. 27) of the flow fields about the models at approximately 0.88 Mach number and zero angle of attack and flap deflection, it is noted that the flaps lay entirely within the region of separated flow aft of the compression shocks on the airfoil, and therefore could develop virtually no lifting pressures. A similar observation was made by Göthert in reference 5 from pressure-distribution measurements for a 9-percent-thick airfoil section. It would be anticipated from a study of the flow fields that at higher angles of attack or larger flap deflections the flaps would again become effective.

Furthermore, it would be expected that, by virtue of less extensive flow separation, the flap with the smallest trailing-edge angle would display the greatest improvement. The results to follow confirm these expectations.

In parts (b) and (c) of figure 26 a successive improvement of the variation of flap effectiveness with Mach number with reduction of the trailing-edge angle is indicated at angles of attack of 4° and 6°. Even at 6° angle of attack, however, the 17.9° trailing-edge-angle flap lost effectiveness for small deflections at the highest Mach numbers.

Another important aspect of the problem of control-surface effectiveness is the extent of the range of deflections for which the surface is ineffective. Figure 28 has been prepared to illustrate the effect of airfoil profile on this characteristic. Section lift coefficients as functions of flap deflection at zero angle of attack are shown for each profile at the highest Mach numbers of the investigation. Again confining the discussion first to the sharp trailing-edge flaps, it is noted that the 17.9° trailing-edge-angle flap at 0.875 Mach number is relatively ineffective for deflections from 0° to approximately 4°. The extent of this ineffective range is seen to become successively smaller with reduction of the trailing-edge angle and is not evident for the 6° trailing-edge angle. At 0.9 Mach number a favorable effect of trailing-edge-angle reduction is also evident. For both the 17.9° and the 12° trailing-edge angles a reversal of effectiveness occurs, extending to $4\text{-}1/2^\circ$ deflection for the former and to approximately 3° for the latter. The 6° trailing-edge-angle flap is ineffective up to 3° deflection but experiences no reversal of effectiveness at this Mach number.

From these results it is evident that for conventional airfoil sections some improvement in flap-effectiveness characteristics at high subsonic Mach numbers may ordinarily be expected from reduction of the trailing-edge angle. At angles of attack near zero, the smaller the trailing-edge angle the smaller will be the range of flap deflections for zero or negative effectiveness. At higher angles of attack, the smaller the trailing-edge angle the less adverse will be the effects of Mach number on the flap effectiveness.

If now the case of trailing-edge-thickness variation is considered, it is observed in figure 26 that the thickened trailing-edge flaps are markedly more effective than the sharp trailing-edge flaps at all but the highest Mach numbers. The greater effectiveness is ascribed to the fact that without the trailing-edge closure the loading on the flap does not fall to zero at the trailing edge as in the conventional case. The hinge moments of these flaps could be expected to be correspondingly larger than for the sharp trailing-edge flaps.

At zero angle of attack, in the Mach number range where the effectiveness of the sharp trailing-edge flaps commenced to decrease, the effectiveness of the thickened trailing-edge flaps increased very sharply. Schlieren photographs (fig. 27) of the flow at 0.88 Mach number disclose very much smaller regions of separated flow over the blunt trailing-edge flaps than over the sharp trailing-edge flaps. (The asymmetry of the shock-wave pattern for the model with the thicker trailing edge is probably due to a small asymmetry in the airfoil model which is also evident in the lift curves of fig. 6 (c)). Between the Mach numbers of 0.88 and 0.9, the value of $dc_l/d\delta_f$ for the flap with trailing-edge thickness equal to one-half the thickness at the hinge line dropped to virtually zero, whereas that for the flap with double this trailing-edge thickness apparently continued to increase. A virtually infinite slope of the curve of lift coefficient as a function of flap deflection at zero deflection is indicated in figure 28 at 0.9 Mach number for the latter flap. In either case the variation of effectiveness with Mach number is undesirably large and, from the standpoint of airplane controllability, possibly even more unfavorable than that for the sharp trailing-edge profiles.

With increasing angle of attack (cf. parts (a), (b), and (c) of fig. 26), the variation with Mach number of the effectiveness of the blunt trailing-edge flaps becomes much less severe, but is still considerably greater than for the sharp trailing-edge flaps with small trailing-edge angles.

CONCLUDING REMARKS

From a wind-tunnel investigation at Mach numbers from 0.3 to 0.9 (1 to 2 million Reynolds number) of the effects of trailing-edge-angle variation from 18° to 6°, and trailing-edge-thickness variation from zero to that at the flap hinge line, on the lift effectiveness of a 25-percent-chord plain flap on a 10-percent-thick airfoil section, the following specific conclusions are drawn:

1. Reduction of the trailing-edge angle decreases, at moderate angles of attack, the loss of flap effectiveness for small deflections at high subsonic Mach numbers.

2. At zero angle of attack, reduction of the trailing-edge angle has no effect on the variation of flap effectiveness with Mach number but has the favorable result of decreasing the range of flap deflections for which the effectiveness is zero or negative.

3. A general increase of flap effectiveness is promoted by an increase of trailing-edge thickness. The increase is ascribed to the fact that the loading on the thickened trailing-edge profiles does not fall to zero at the trailing edge as is the case for sharp trailing-edge profiles.

4. At zero angle of attack, an increase of trailing-edge thickness results, in general, in an increase of lift effectiveness from the low-speed value in the range of Mach numbers for which the effectiveness of a sharp trailing-edge flap usually decreases. For the particular thickened trailing-edge profiles investigated, however, the over-all variation of effectiveness with Mach number is so large as to be distinctly unfavorable from the standpoint of airplane controllability.

It would appear from the results of this investigation that the variation with Mach number of the effectiveness of a plain flap cannot be satisfactorily controlled by variation of such parameters as the trailing-edge angle and the trailing-edge thickness independently. In order to maintain a satisfactory degree of flap effectiveness throughout the subsonic Mach number range by variation of airfoil geometry, the airfoil shape should be such as to prevent flow separation from the surface appreciably ahead of the trailing edge. This can readily be accomplished by placing the airfoil maximum thickness at the trailing edge, but the attendant penalty in drag would be large. To approach the desired objective for an airfoil on which some pressure recovery is to be made ahead of the trailing edge, present indications are that the profile should embody some trailing-edge thickness in conjunction with a relatively small trailing-edge angle.

It should be borne in mind that for Reynolds numbers substantially larger than those of the present investigation the foregoing conclusions might be considerably modified.

Ames Aeronautical Laboratory,
National Advisory Committee for Aeronautics,
Moffett Field, Calif.

REFERENCES

1. Summers, James L., and Graham, Donald J.: Effects of Systematic Changes of Trailing-Edge Angle and Leading-Edge Radius on the Variation with Mach Number of the Aerodynamic Characteristics of a 10-Percent Chord Thick NACA Airfoil Section. NACA RM A9G18, 1949.

2. Stack, John, and von Doenhoff, Albert E.: Tests of 16 Related Airfoils at High Speeds, NACA Rep. 492, 1934.

3. Abbott, Ira H., von Doenhoff, Albert E., and Stivers, Louis S., Jr.: Summary of Airfoil Data. NACA Rep. 824, 1945.

4. Allen H. Julian, and Vincenti, Walter G.: Wall interference in a Two-Dimensional-Flow Wind Tunnel, with Consideration of the Effect of Compressibility. NACA Rep. 782, 1944.

5. Göthert, B.: Control Effectiveness at High Subsonic Speeds. British M.O.S. Völkenrode Reports and Translations No. 72, February 1947.

TABLE I

COORDINATES OF THE NACA 0010-0.70 40/1.575 AIRFOIL SECTION
[Coordinates given in percent of airfoil chord]

Station	Upper or lower surface ordinate
0	0
.5	.820
.75	.999
1.25	1.279
2.5	1.782
5.0	2.460
7.5	2.949
10	3.338
15	3.926
20	4.347
25	4.648
30	4.848
40	5.000
50	4.856
60	4.433
70	3.733
80	2.767
90	1.556
95	.856
100	.100
L.E. radius: 0.70 percent c	

TABLE II

COORDINATES OF THE NACA 0010-0.70 40/1.051 AIRFOIL SECTION
[Coordinates given in percent of airfoil chord]

Station	Upper or lower surface ordinate
0	0
.5	.802
1.25	1.239
2.5	1.705
5.0	2.326
7.5	2.776
10	3.141
15	3.721
20	4.172
25	4.524
30	4.783
40	5.000
50	4.783
60	4.197
70	3.338
80	2.305
90	1.193
95	.638
100	.100
L.E. radius: 0.70 percent c	

TABLE III

COORDINATES OF THE NACA 0010-0.70 40/0.524 AIRFOIL SECTION
[Coordinates given in percent of airfoil chord]

Station	Upper or lower surface ordinate
0	0
.50	.786
1.25	1.198
2.5	1.628
5.0	2.191
7.5	2.602
10	2.943
15	3.515
20	3.995
25	4.401
30	4.717
40	5.000
50	4.709
60	3.962
70	2.943
80	1.836
90	.827
95	.416
100	.100
L.E. radius: 0.70 percent c	

TABLE IV

COORDINATES OF THE NACA 0010-0.70 40/1.575
(MODIFICATION A) AIRFOIL SECTION
[Coordinates given in percent of airfoil chord]

Station	Upper or lower surface ordinate
0	0
.5	.820
.75	.999
1.25	1.279
2.5	1.782
5.0	2.460
7.5	2.949
10	3.338
15	3.926
20	4.347
25	4.648
30	4.848
40	5.000
50	4.856
60	4.433
70	3.733
75	3.284
80	3.284
85	3.284
90	3.284
95	3.284
100	3.284
L.E. radius: 0.70 percent c	

TABLE V

COORDINATES OF THE NACA 0010-0.70 40/1.575
(MODIFICATION B) AIRFOIL SECTION
[Coordinates given in percent of airfoil chord]

Station	Upper or lower surface ordinate
0	0
.5	.820
.75	.999
1.25	1.279
2.5	1.782
5.0	2.460
7.5	2.949
10	3.338
15	3.926
20	4.347
25	4.648
30	4.848
40	5.000
50	4.856
60	4.433
70	3.733
75	3.284
80	2.956
85	2.627
90	2.299
95	1.970
100	1.642
L.E. radius: 0.70 percent c	

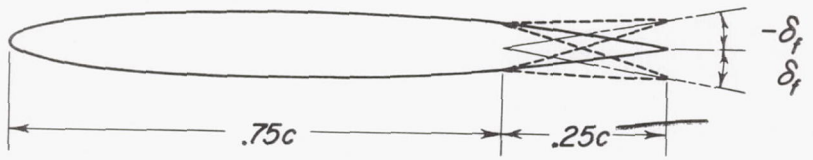

NACA 0010-0.70 40/1.575 section

T.E. Angle, 17.9°

NACA 0010-0.70 40/1.051 section

T.E. Angle, 12°

NACA 0010-0.70 40/0.524 section

T.E. Angle, 6°

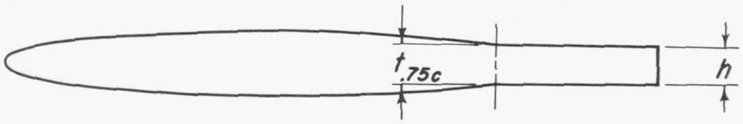

NACA 0010-0.70 40/1.575 section (modification A)

$h/t_{.75c} = 1.0$

NACA 0010-0.70 40/1.575 section (modification B)

$h/t_{.75c} = 0.5$

NACA

Figure 1.- Airfoil profiles with 25-percent-chord plain flaps.

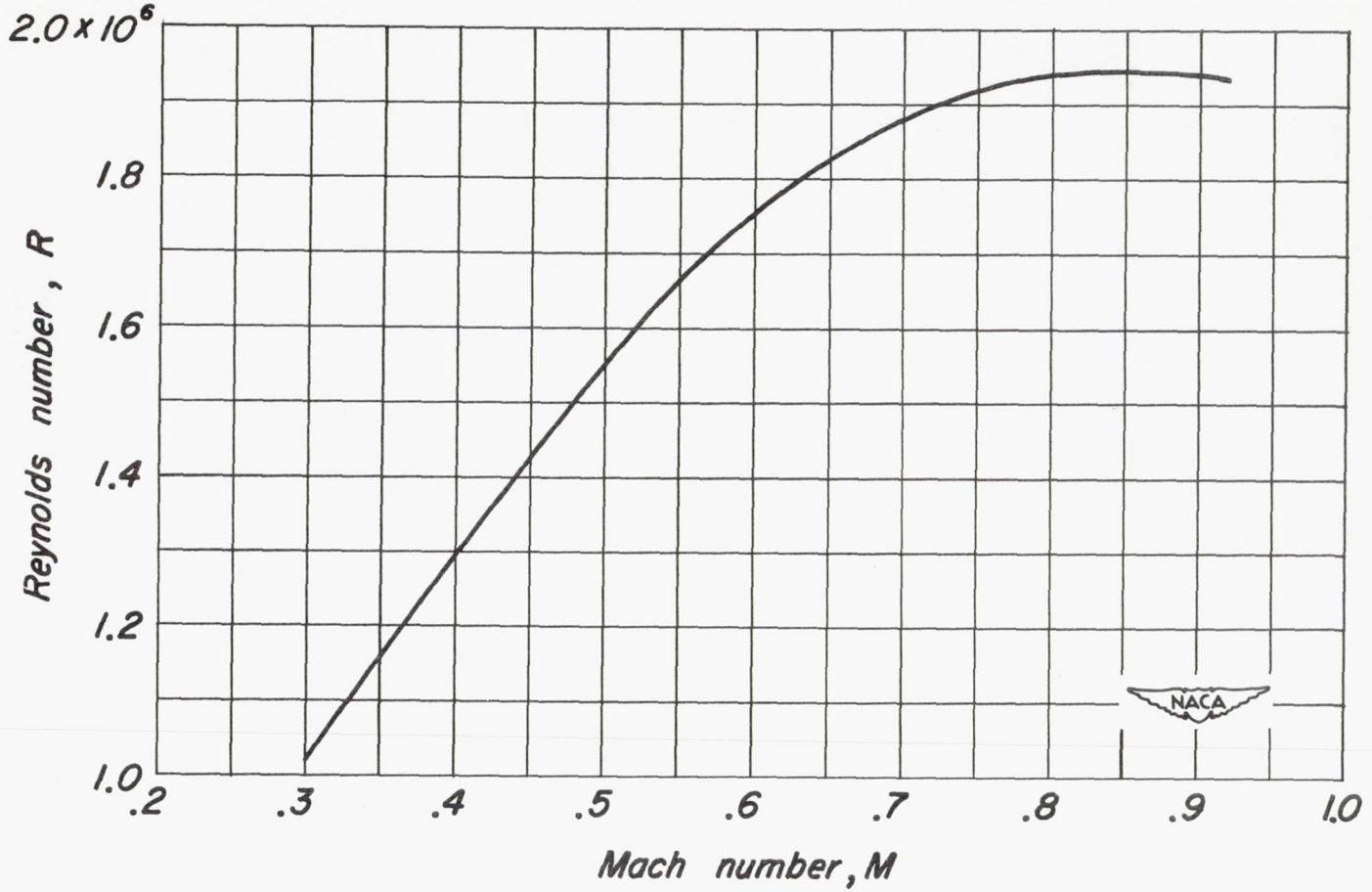

Figure 2.- Variation of Reynolds number with Mach number for 6-inch-chord airfoils in the Ames 1-by $3\frac{1}{2}$-foot high-speed wind tunnel.

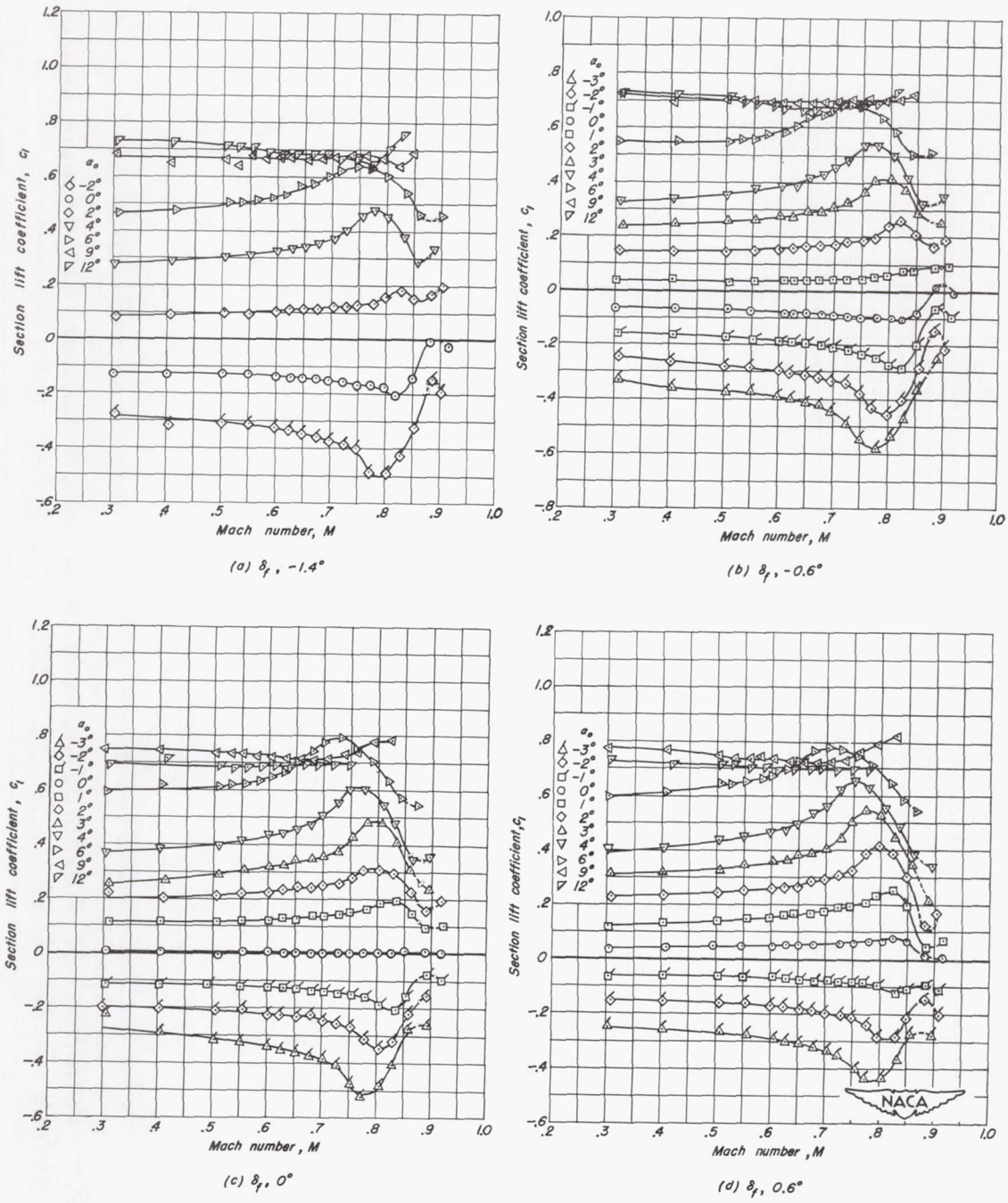

Figure 3.— Variation of section lift coefficient with Mach number at various angles of attack for the NACA 0010-0.70 40/1.575 airfoil section with a 25-percent-chord plain flap.

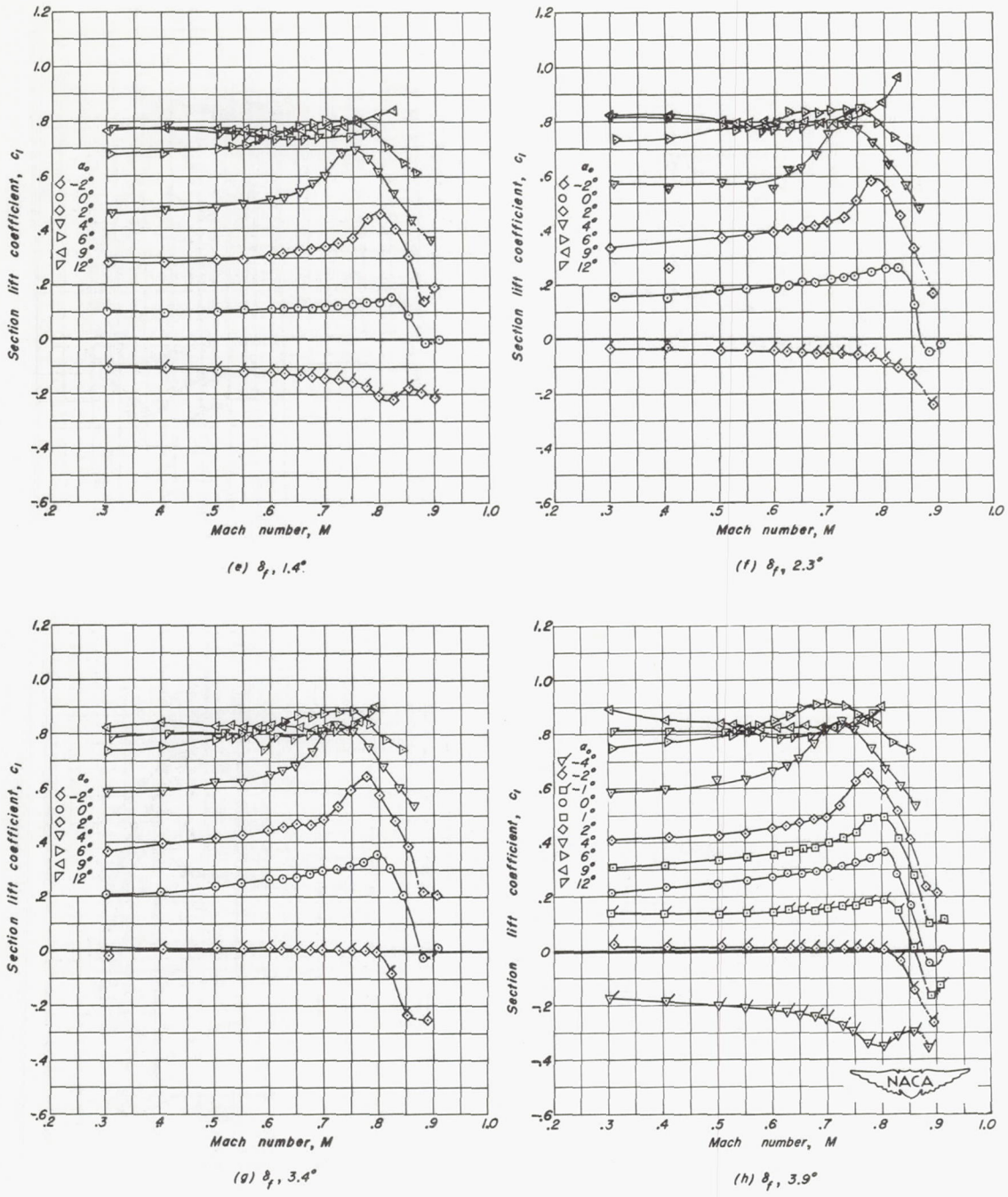

Figure 3.– Continued.

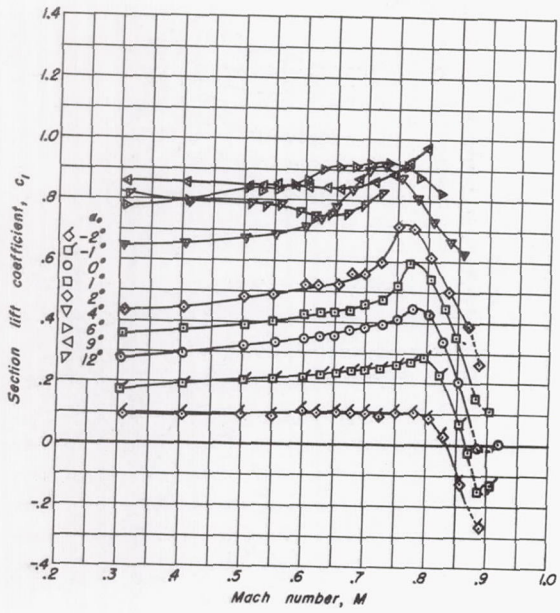

(i) δ_f, 4.6°

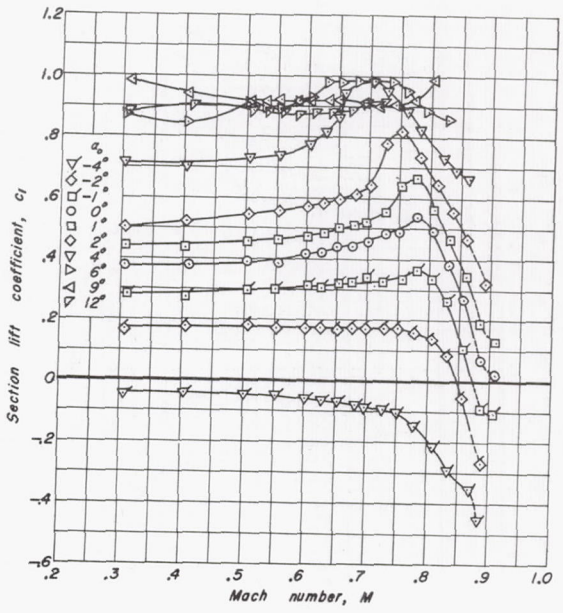

(j) δ_f, 6.1°

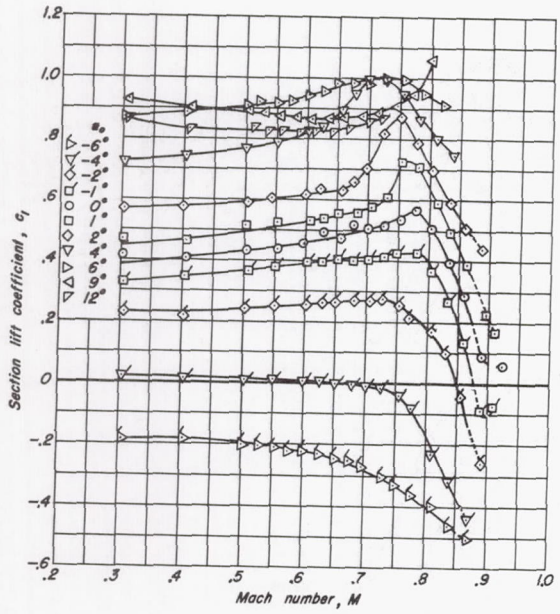

(k) δ_f, 6.8°

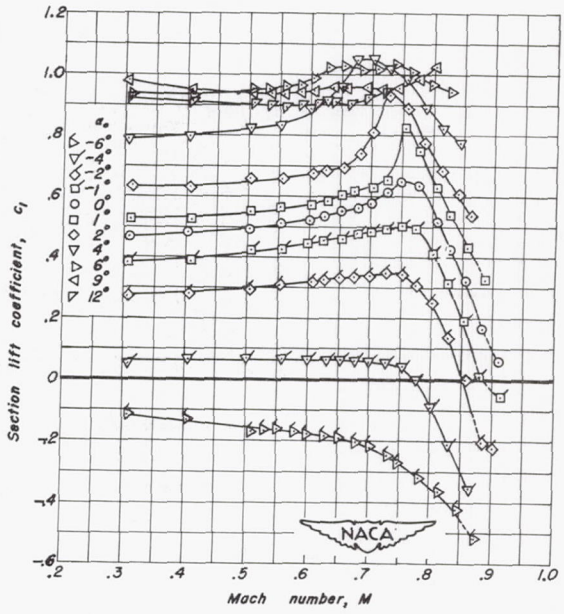

(l) δ_f, 8.1°

Figure 3. – Continued.

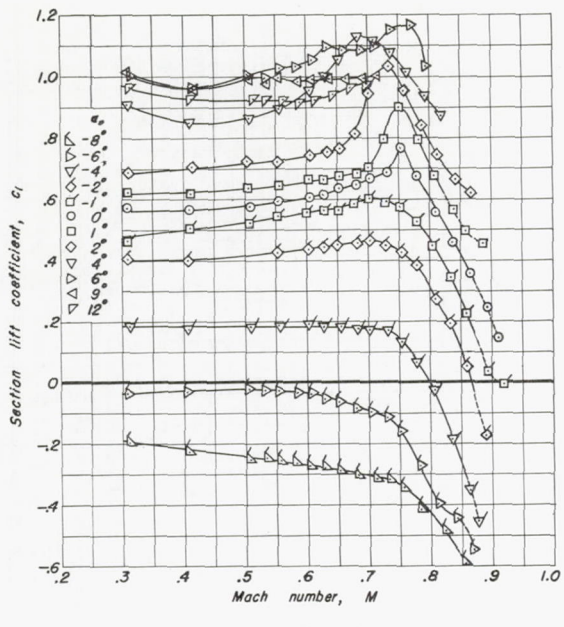

(m) δ_f, 10.1°

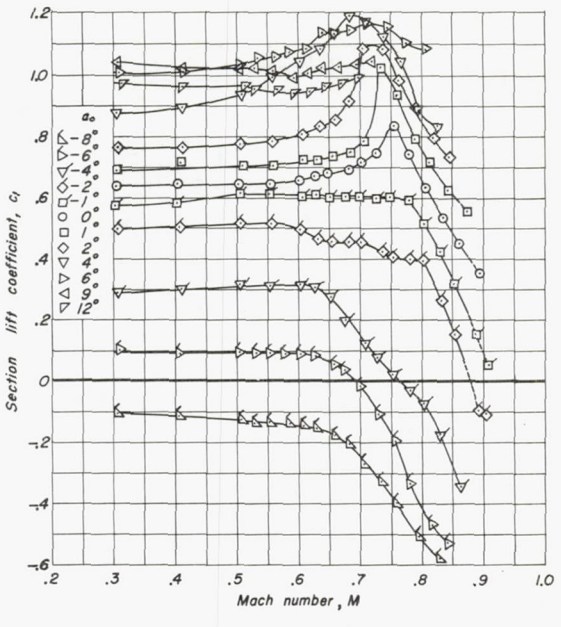

(n) δ_f, 12.1°

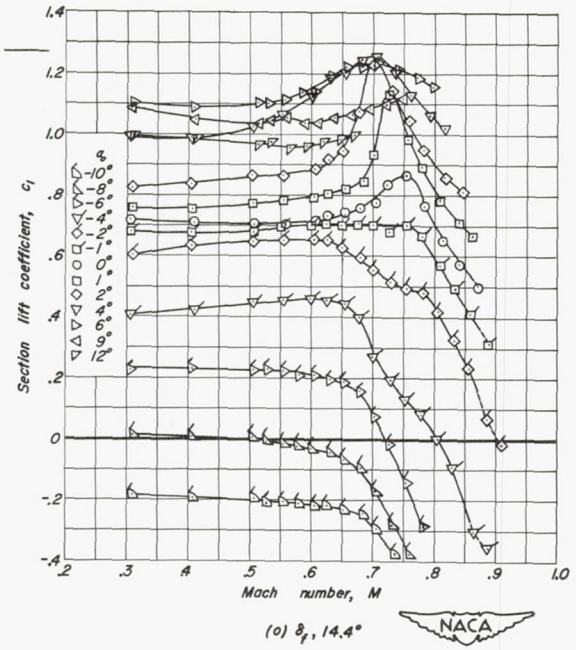

(o) δ_f, 14.4°

Figure 3.– Concluded.

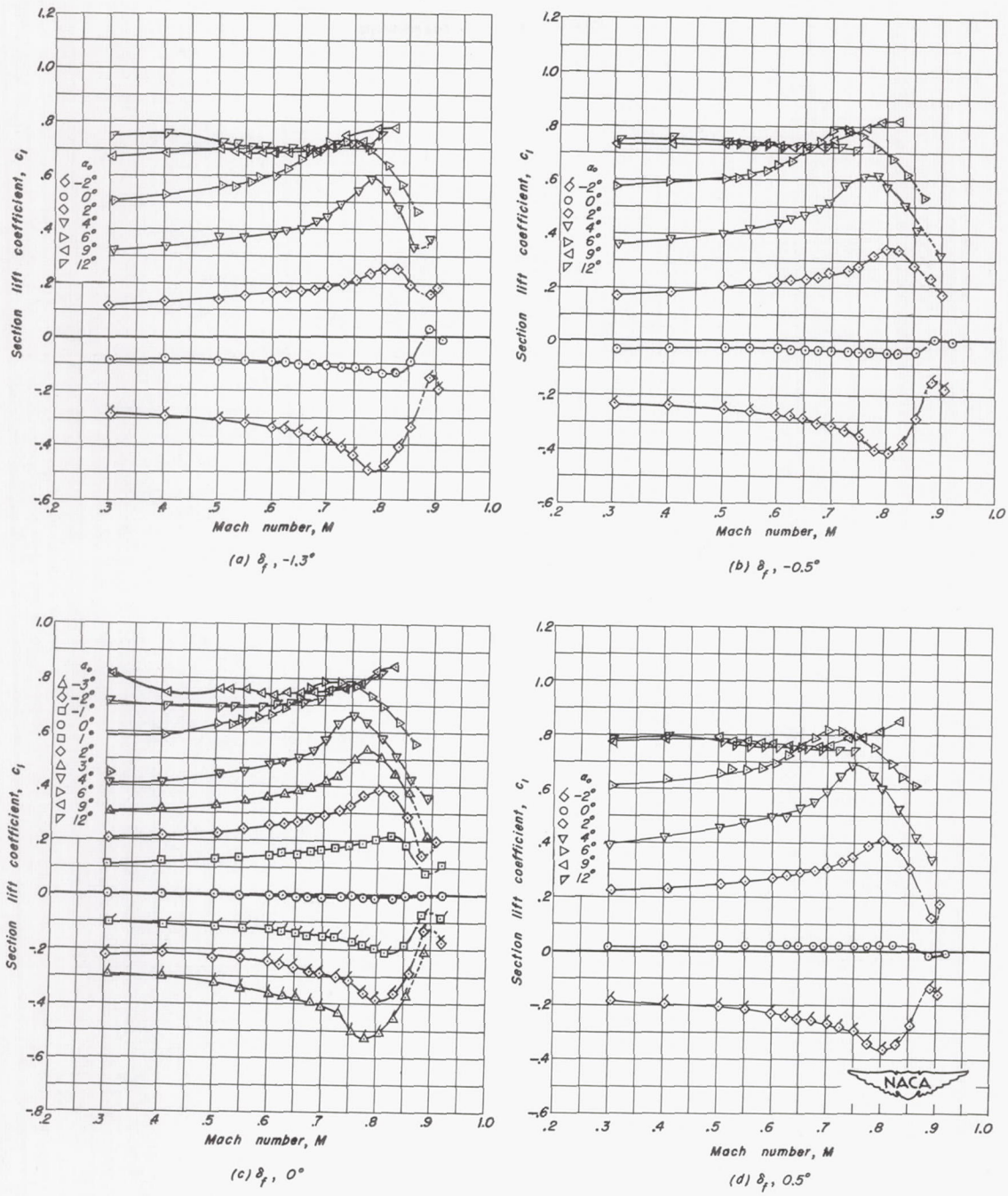

Figure 4.– Variation of section lift coefficient with Mach number at various angles of attack for the NACA 0010–0.70 40/1.051 airfoil section with a 25–percent–chord plain flap.

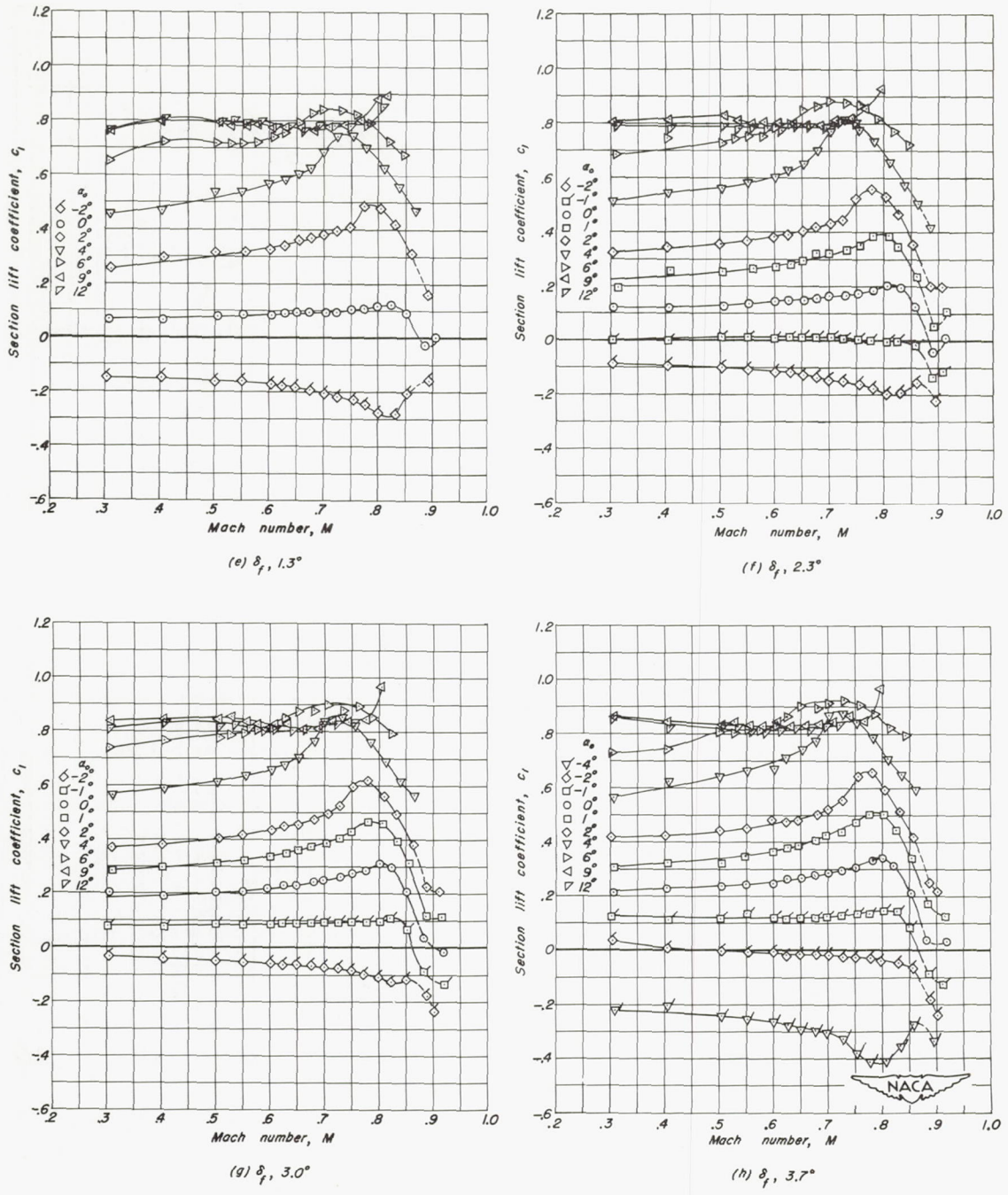

Figure 4.– Continued.

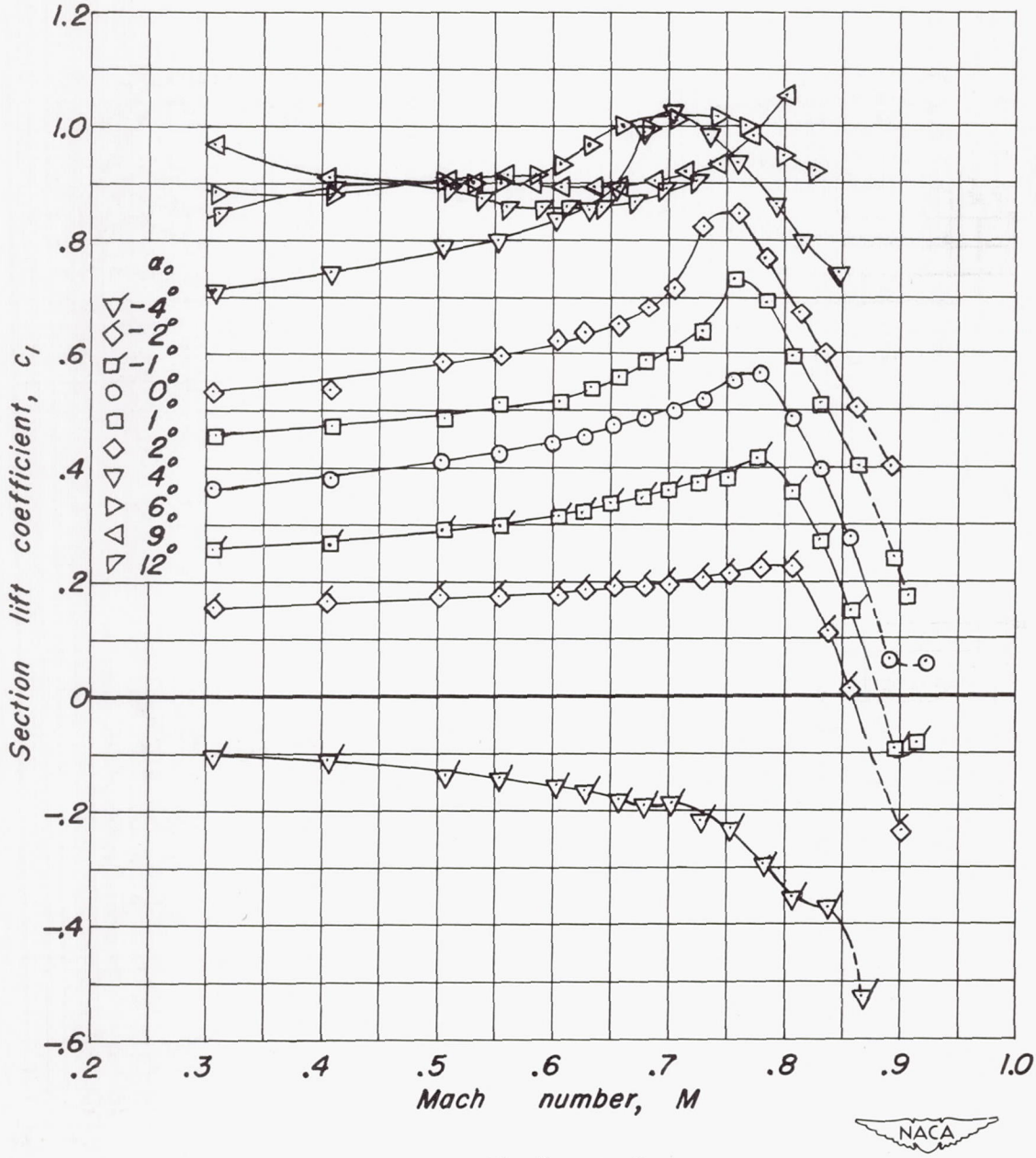

(i) δ_f, 6.1°

Figure 4.– Concluded.

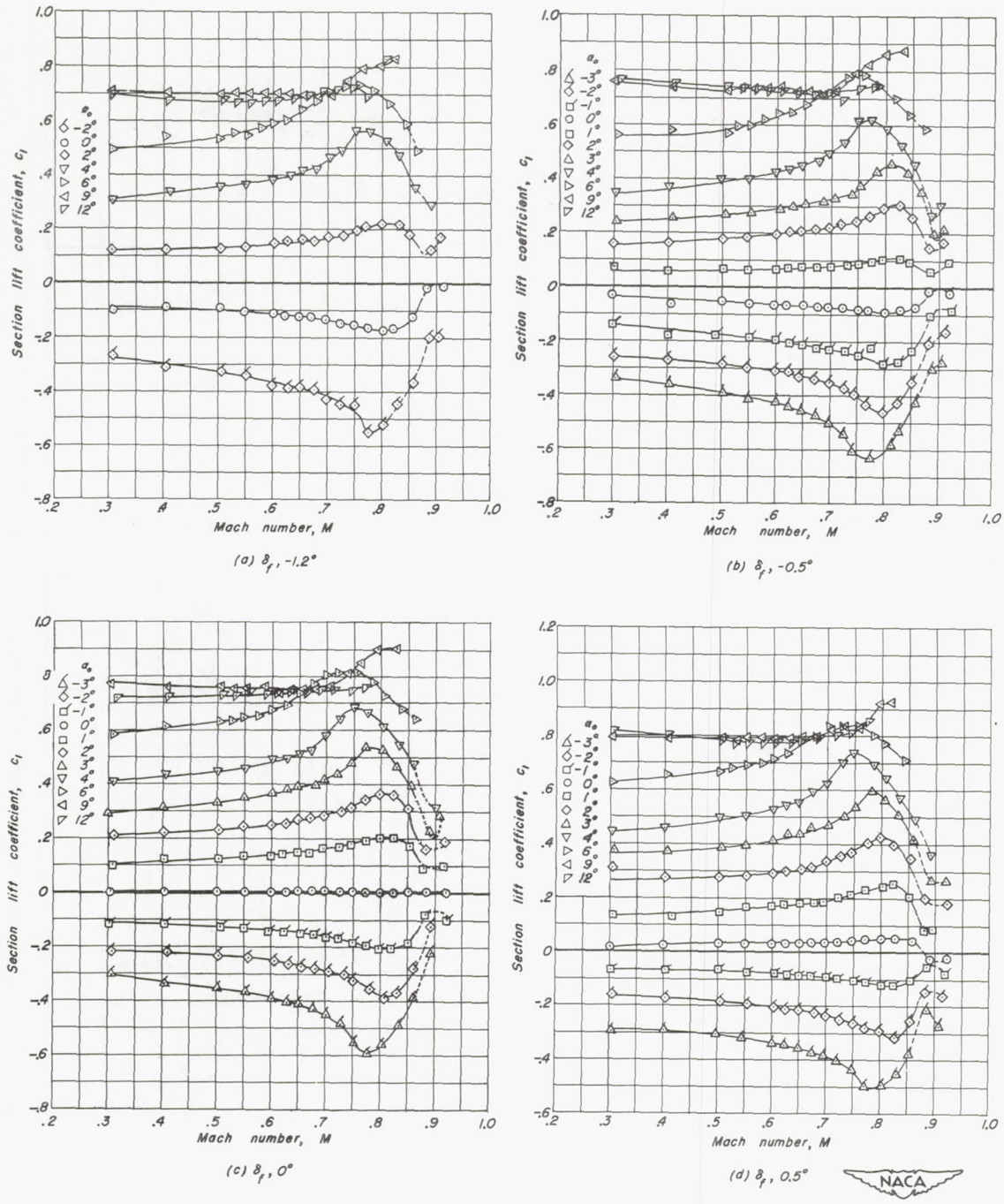

Figure 5.– Variation of section lift coefficient with Mach number at various angles of attack for the NACA 0010-0.70 40/0.524 airfoil section with a 25-percent-chord plain flap.

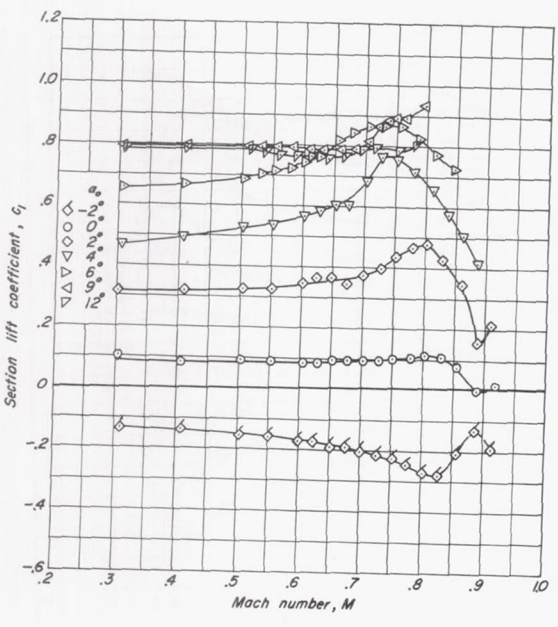

(e) δ_f, 1.2°

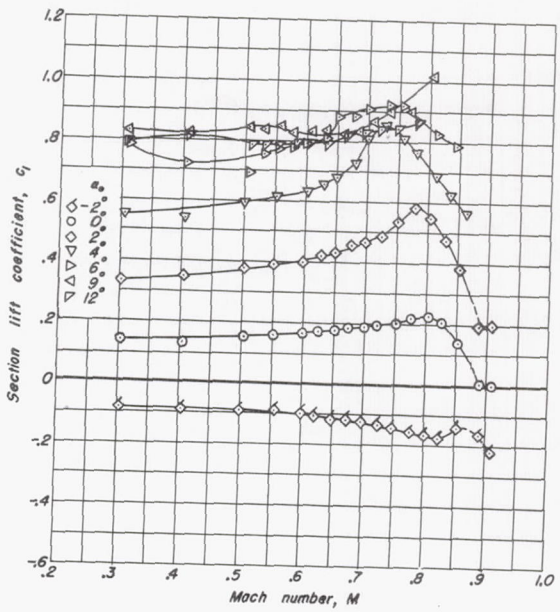

(f) δ_f, 2.3°

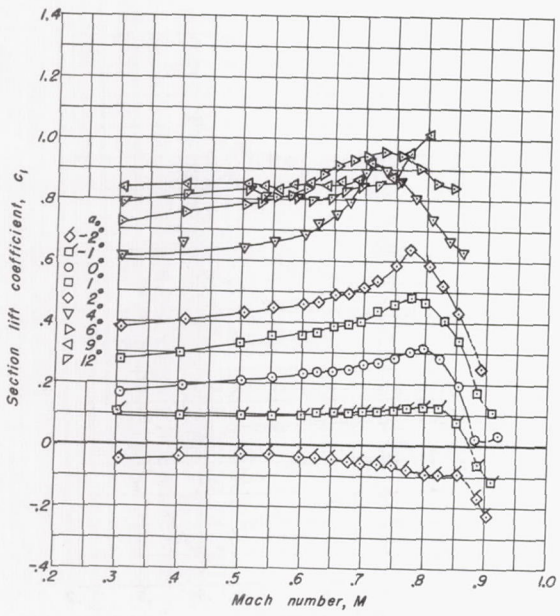

(g) δ_f, 3.4°

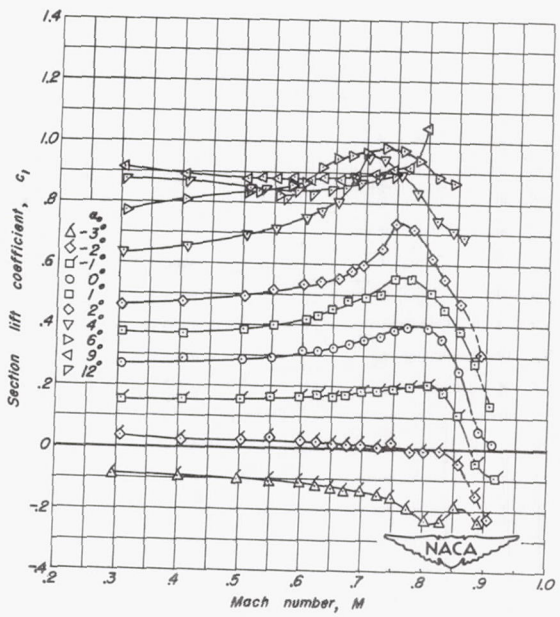

(h) δ_f, 4.2°

Figure 5. – Continued.

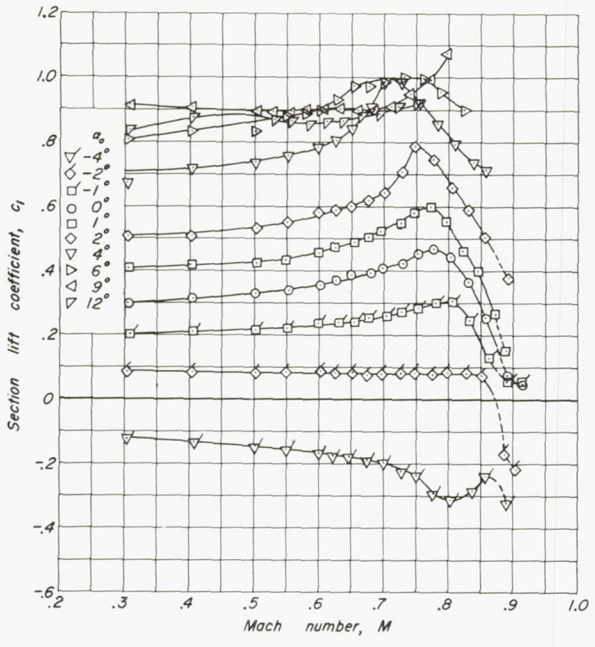

(i) δ_f, 5.0°

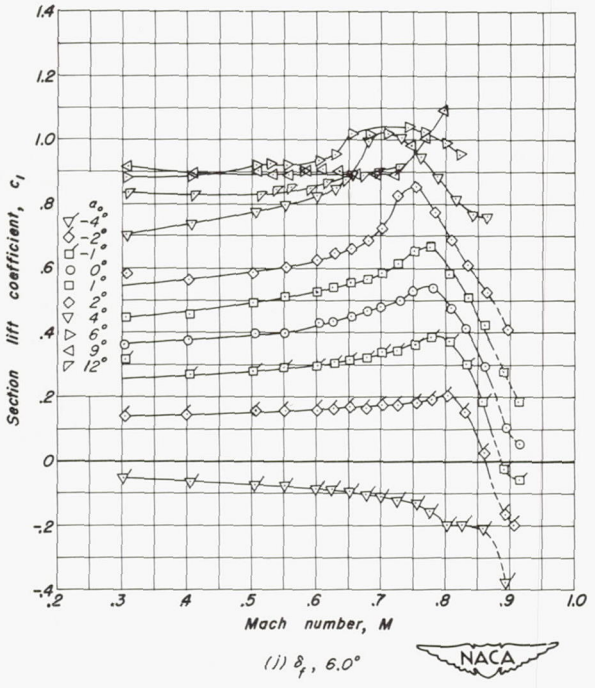

(j) δ_f, 6.0°

Figure 5.- Concluded.

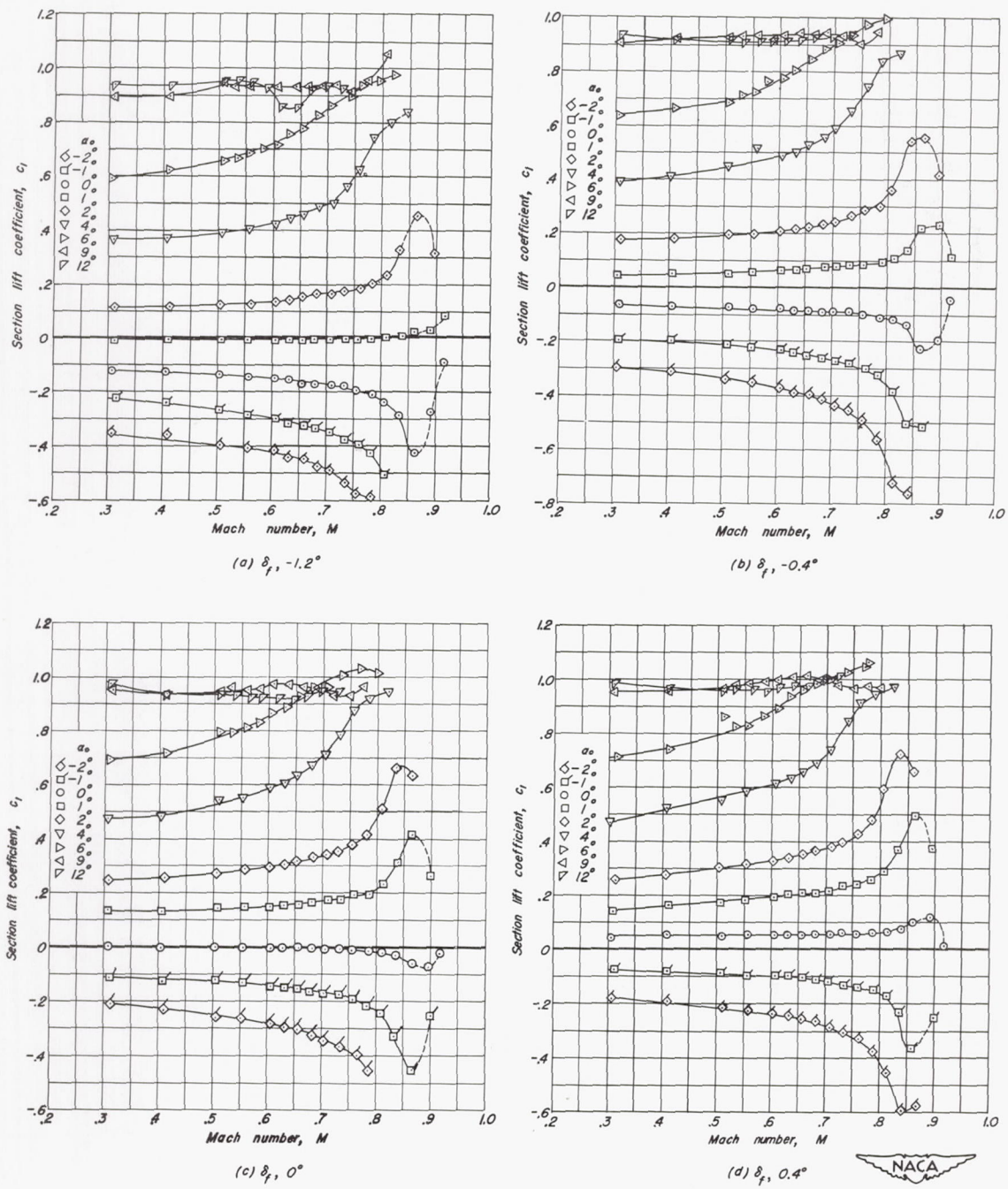

Figure 6.– Variation of section lift coefficient with Mach number at various angles of attack for the NACA 0010-0.70 40/1.575 (modification A) airfoil section with a 25-percent-chord plain flap.

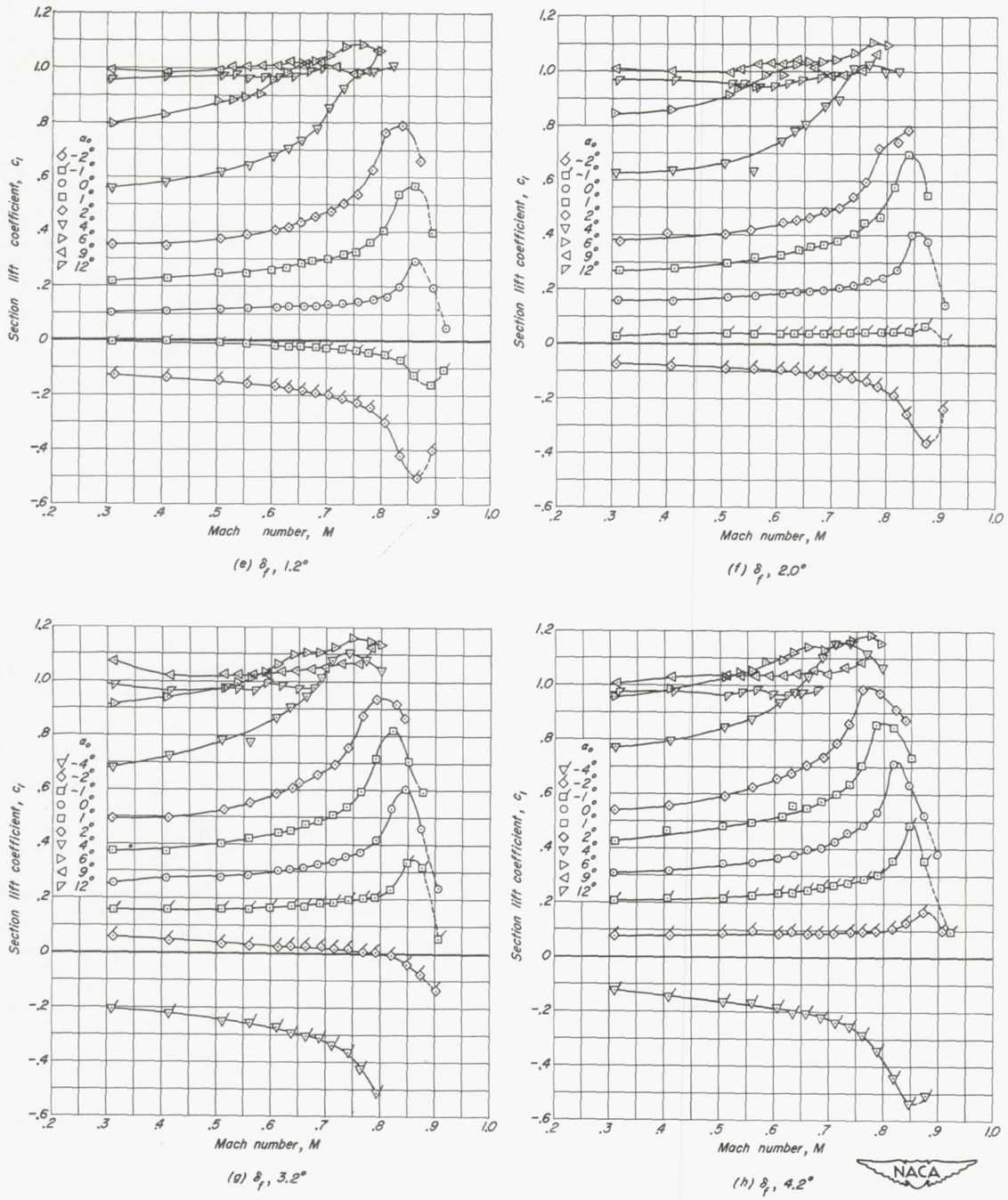

Figure 6.— Continued.

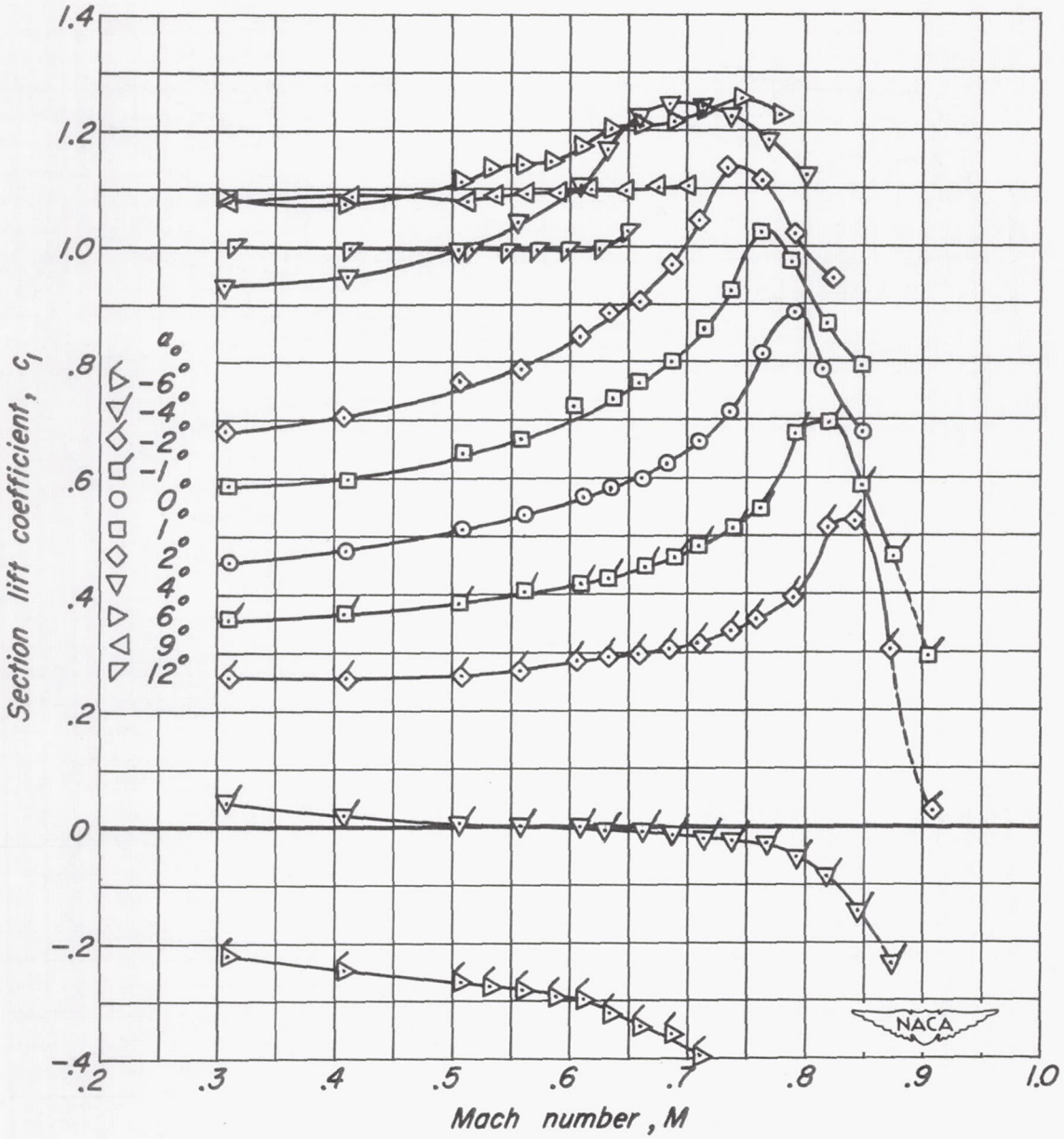

(i) δ_f, 6.8°

Figure 6.- Concluded.

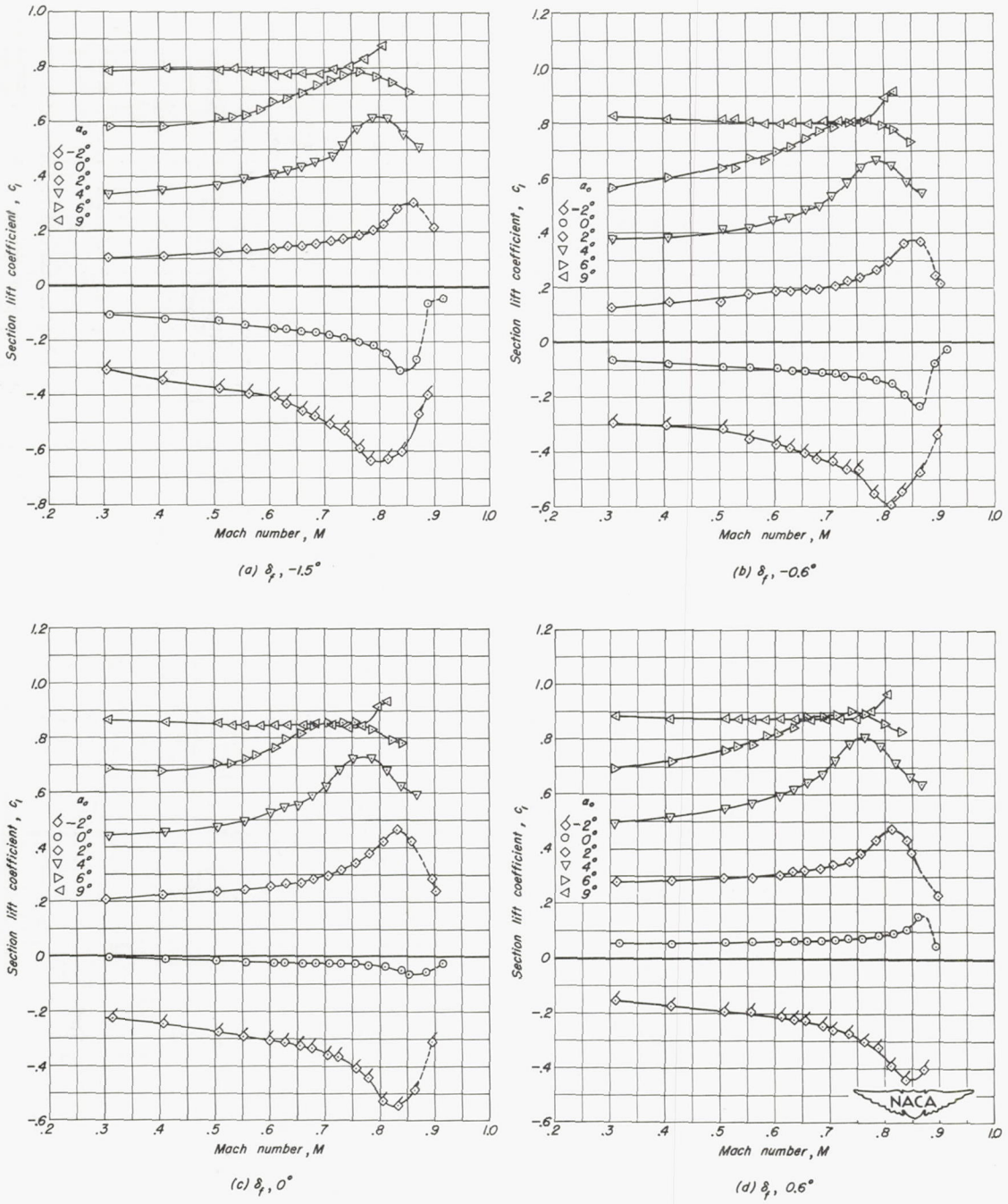

Figure 7.– Variation of section lift coefficient with Mach number at various angles of attack for the NACA 0010–0.70 40/1.575 (modification B) airfoil section with a 25–percent–chord plain flap.

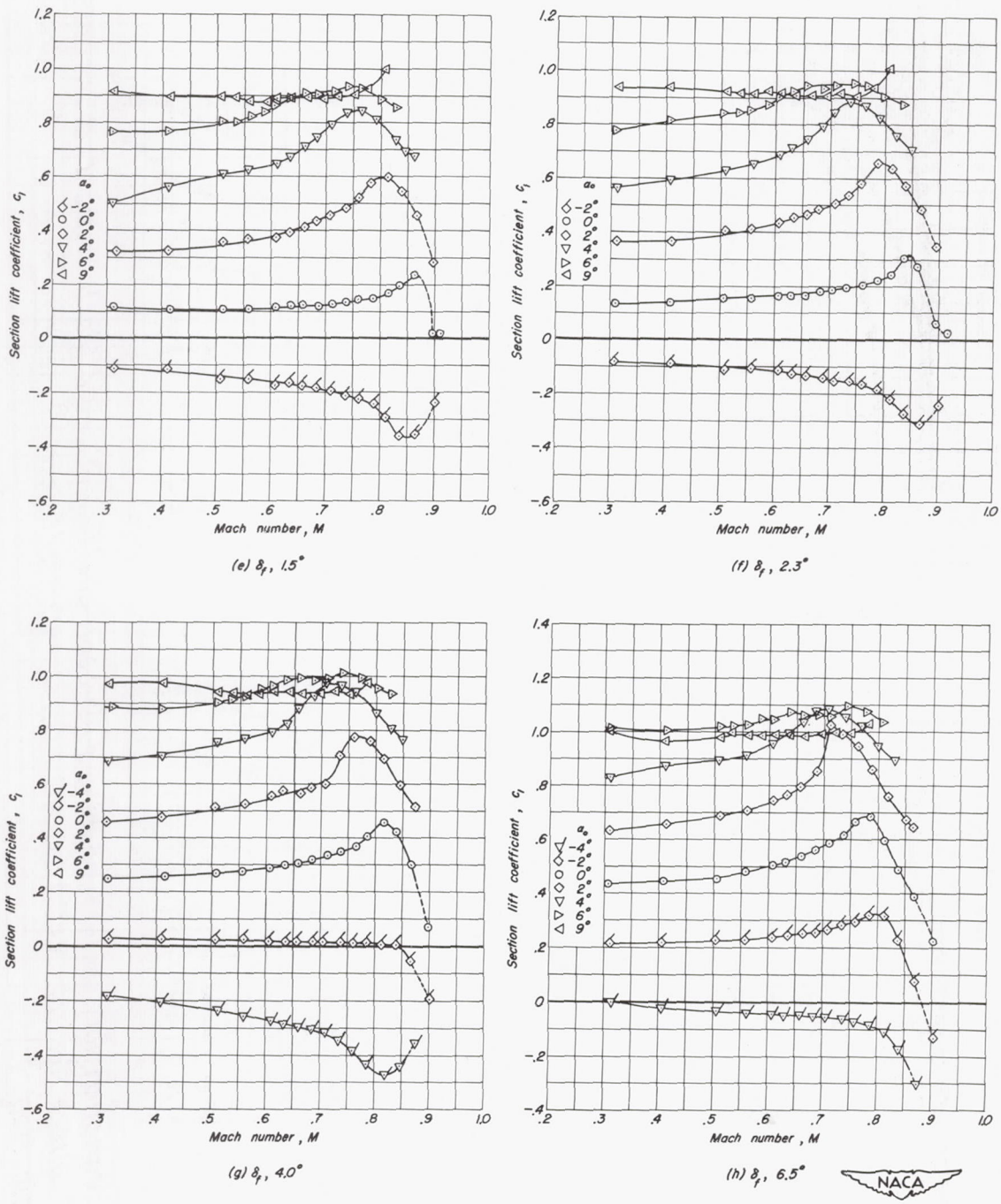

Figure 7.– Concluded.

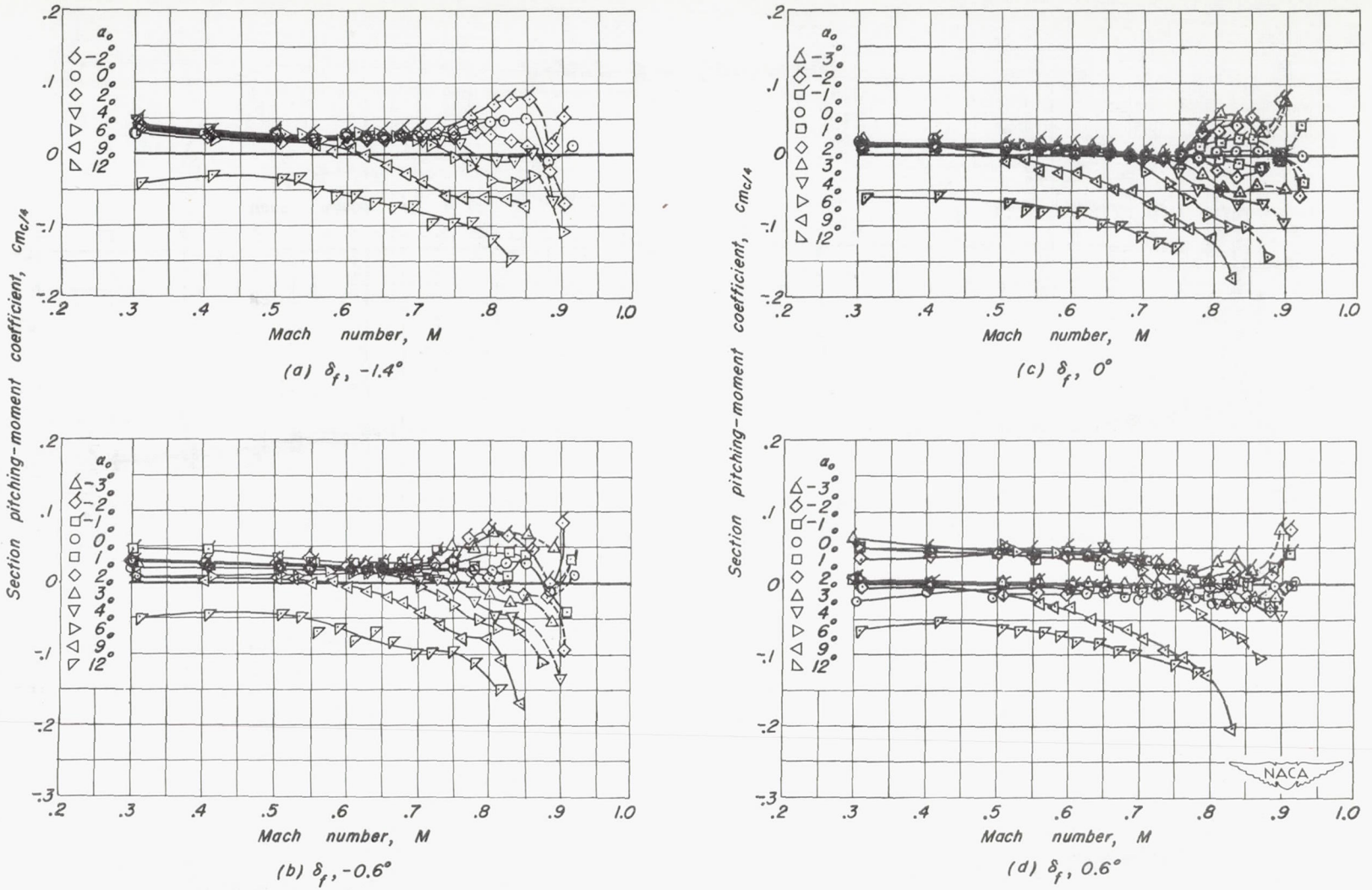

Figure 8.- Variation of section pitching-moment coefficient with Mach number at various angles of attack for the NACA 0010-0.70 40/1.575 airfoil section with a 25-percent-chord plain flap.

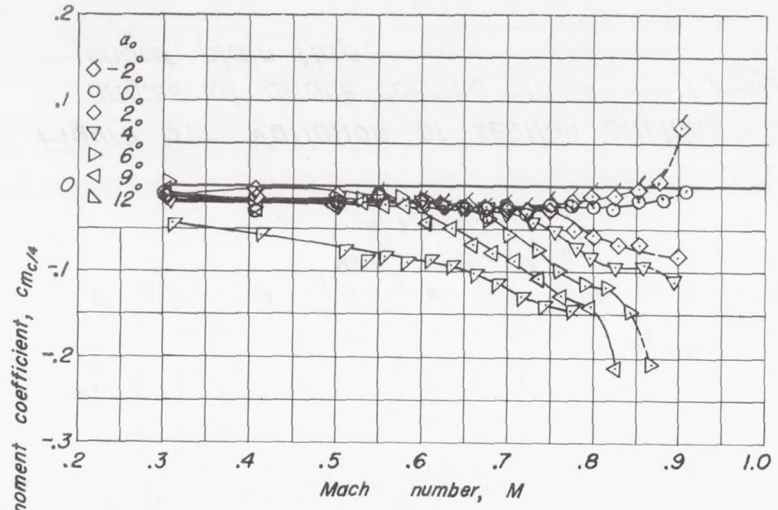

(e) δ_f, 1.4°

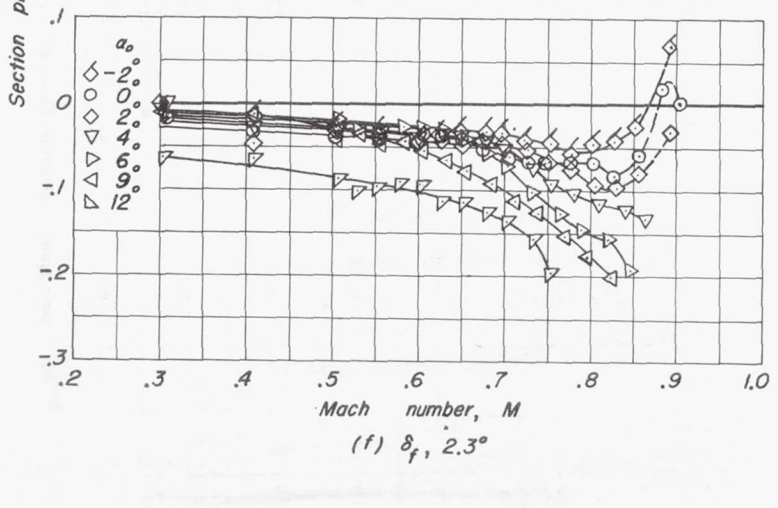

(f) δ_f, 2.3°

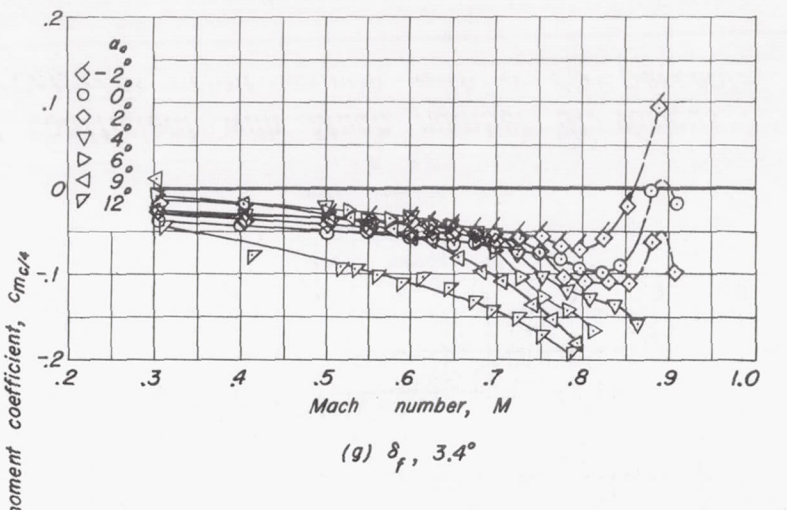

(g) δ_f, 3.4°

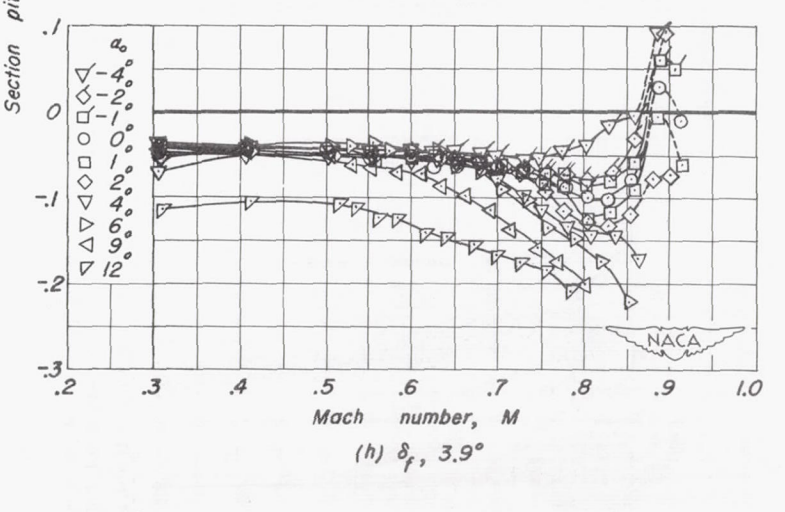

(h) δ_f, 3.9°

Figure 8.- Continued.

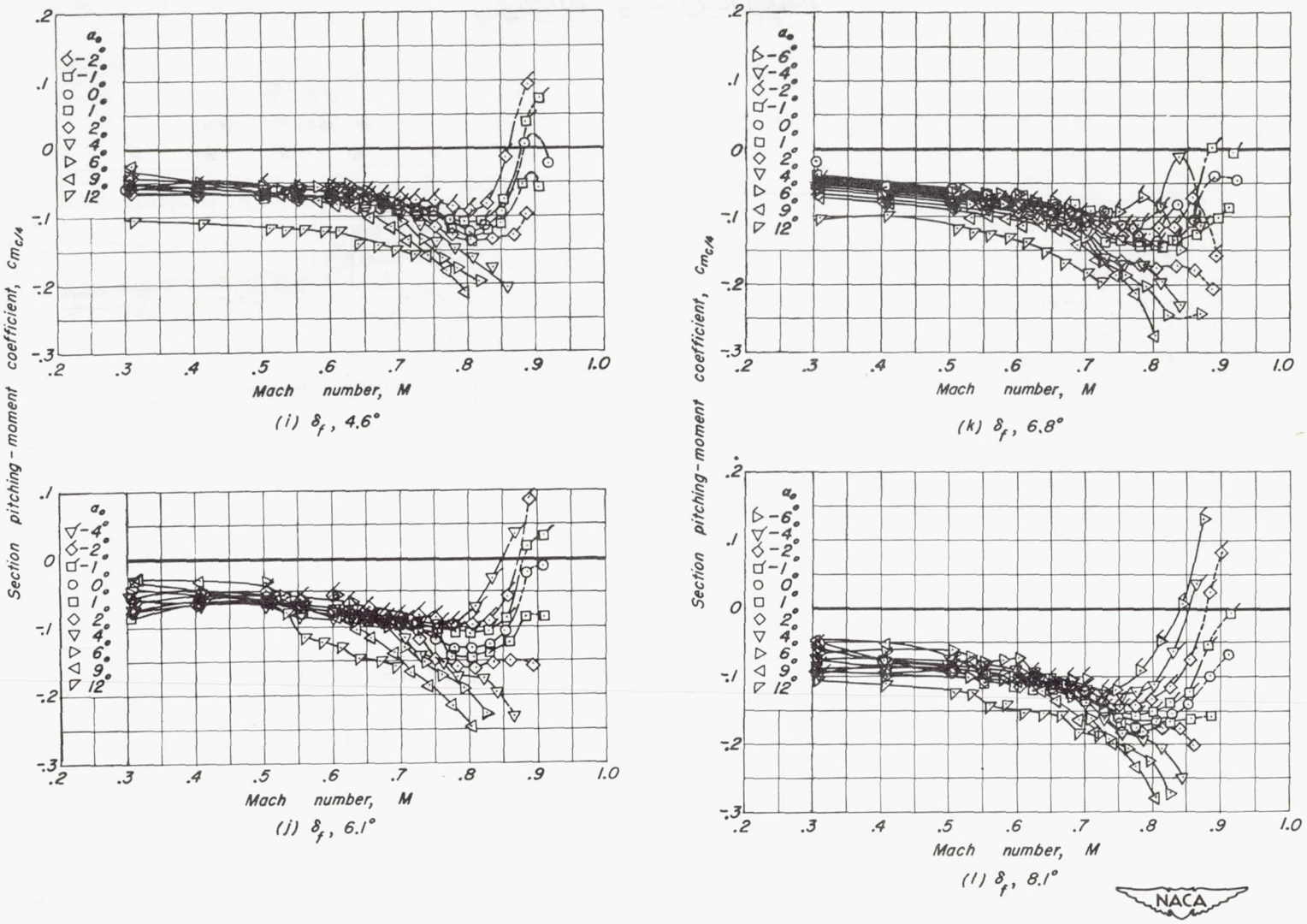

Figure 8.- Continued.

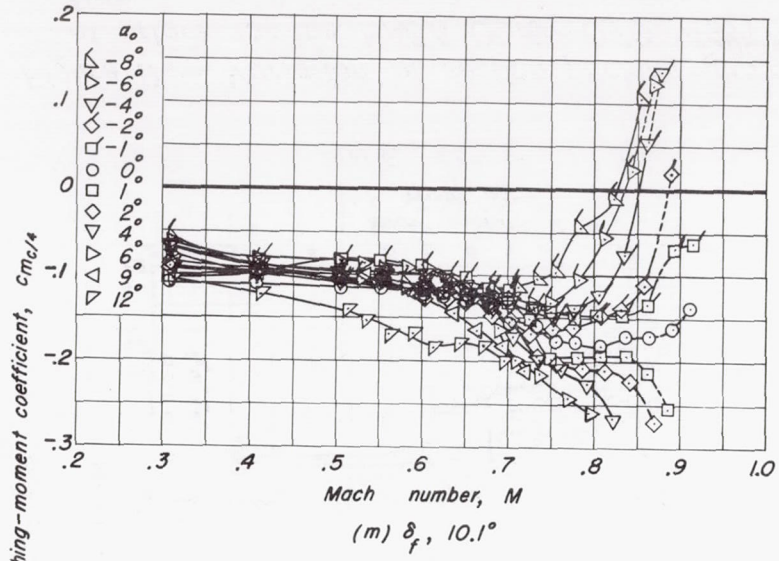

(m) δ_f, 10.1°

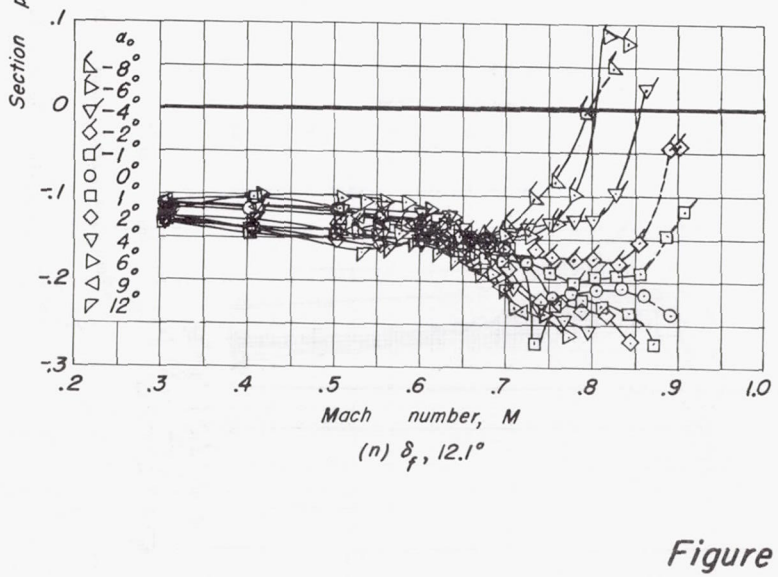

(n) δ_f, 12.1°

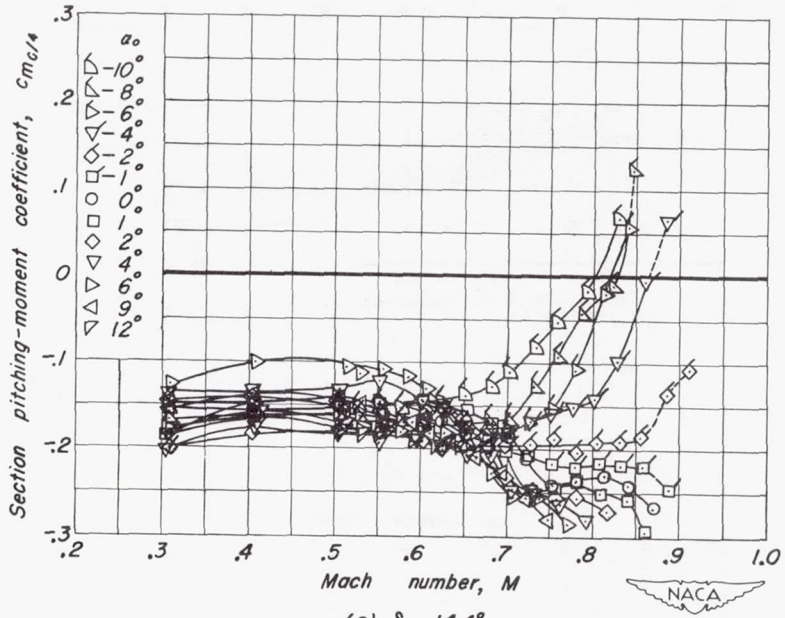

(o) δ_f, 14.4°

Figure 8. – Concluded.

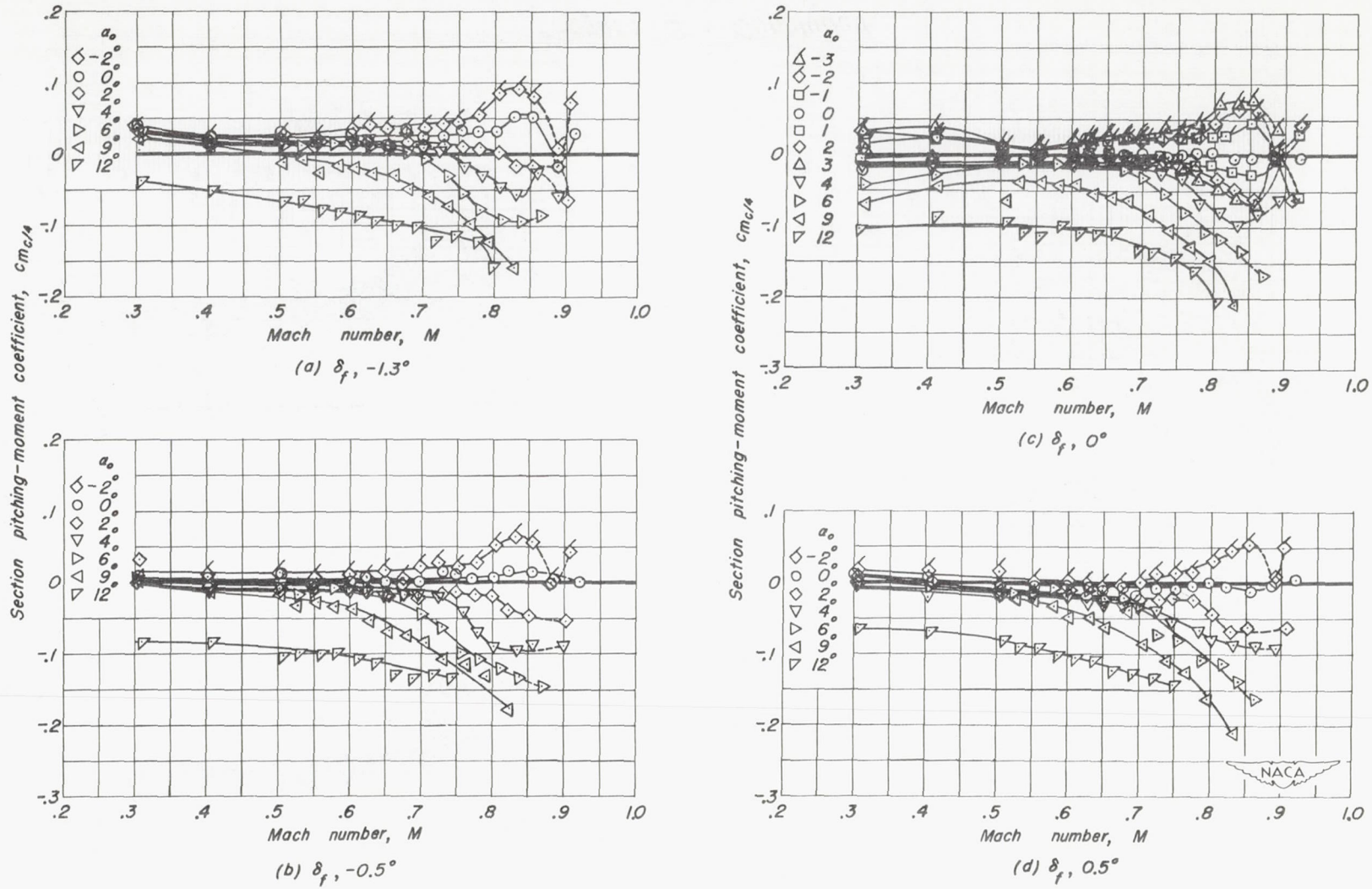

Figure 9.– Variation of section pitching-moment coefficient with Mach number at various angles of attack for the NACA 0010-0.70 40/1.051 airfoil section with a 25-percent-chord plain flap.

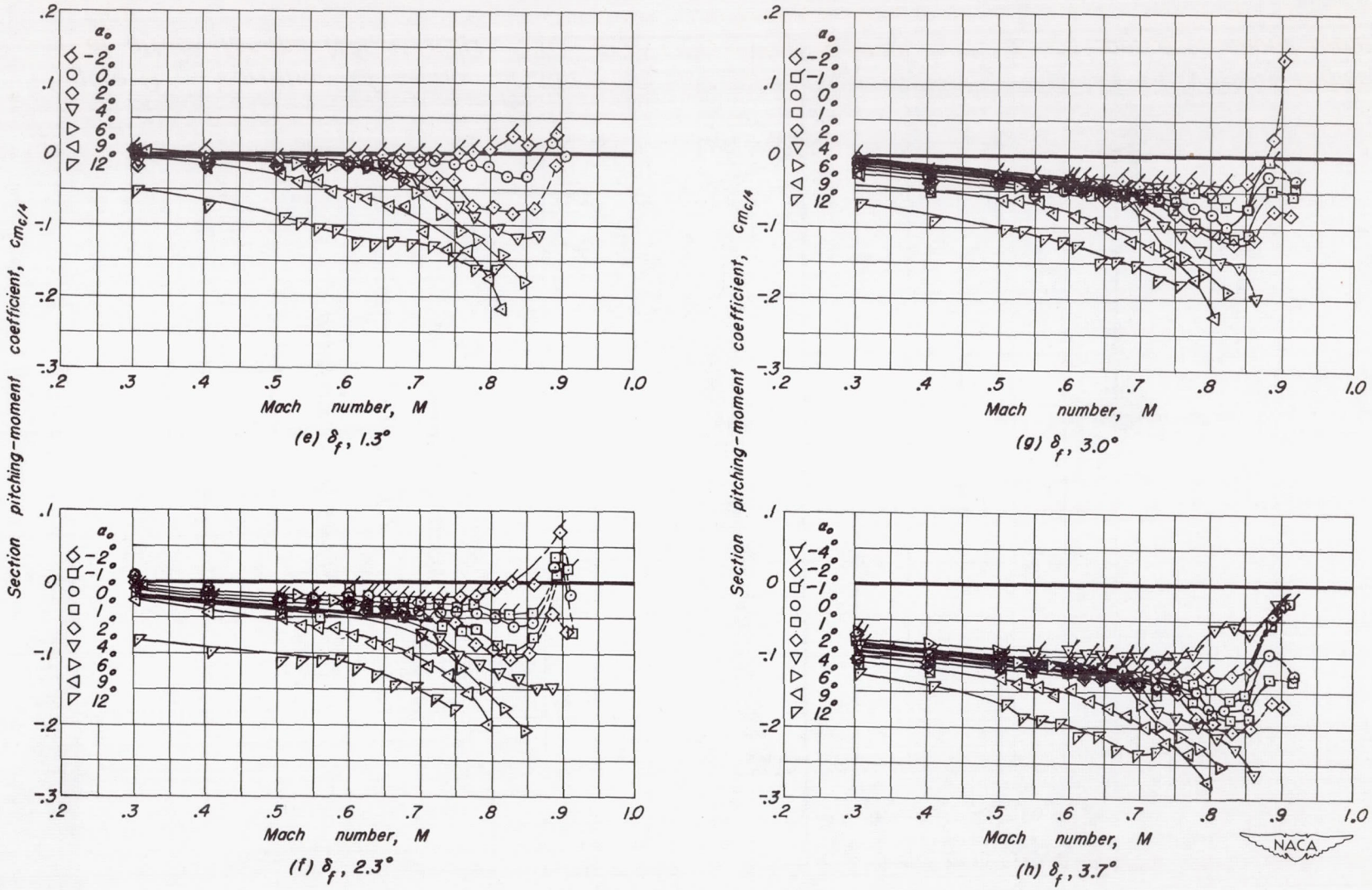

Figure 9.- Continued.

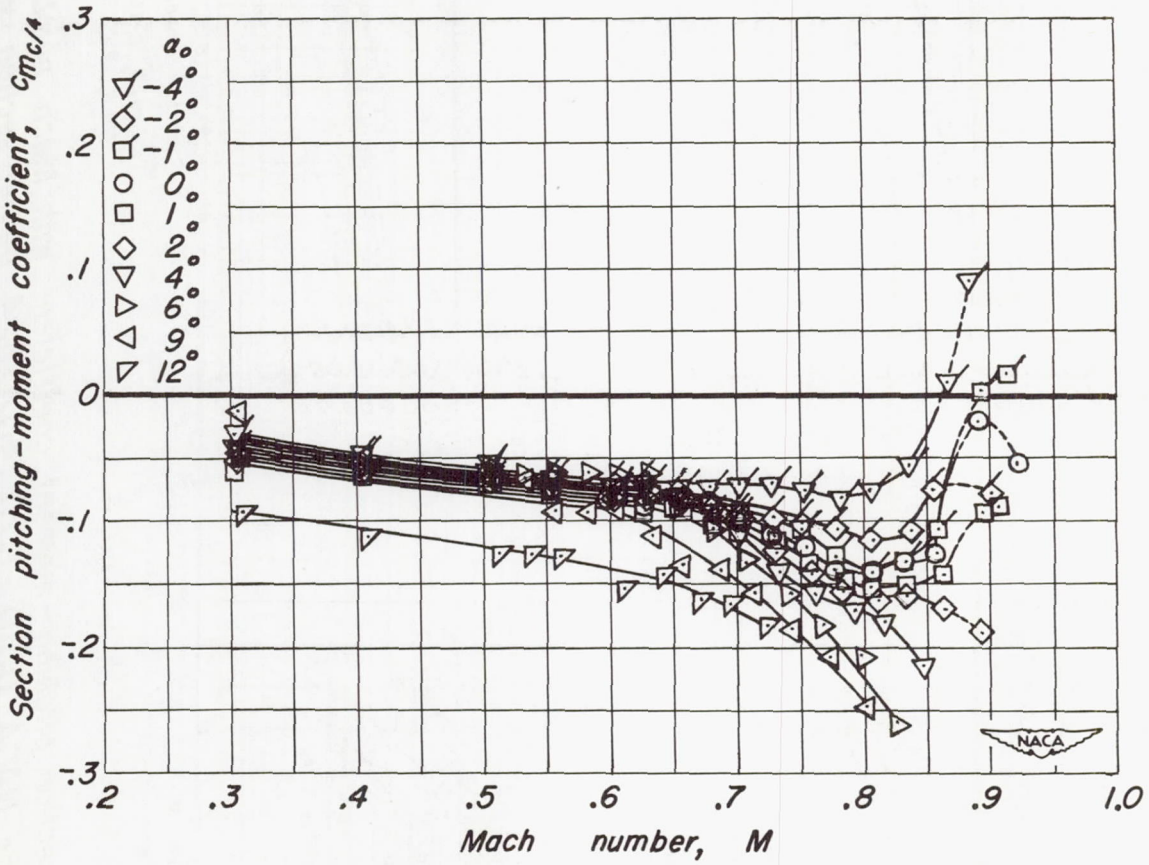

(i) δ_f, 6.1°

Figure 9. – Concluded.

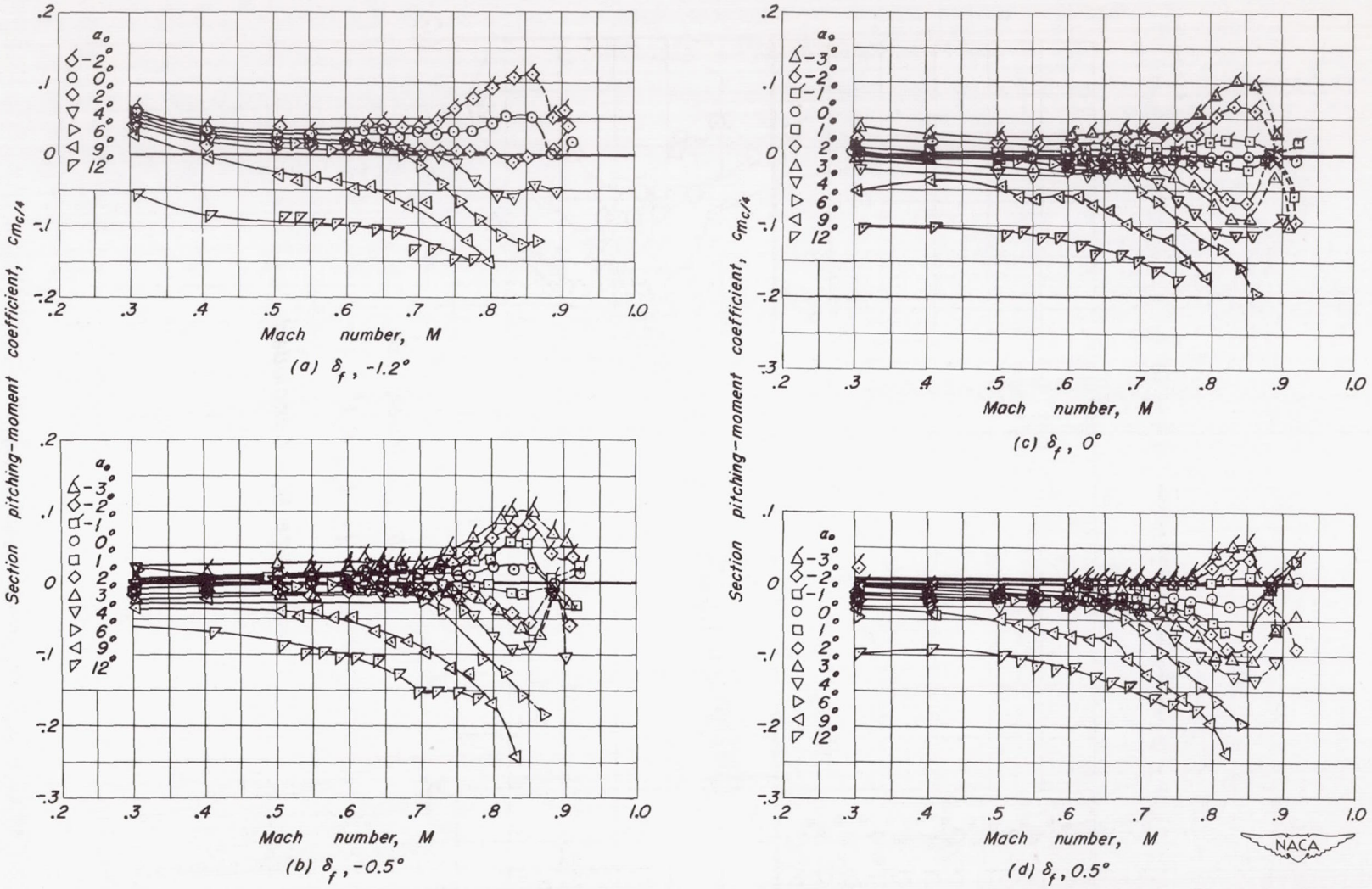

Figure 10.– Variation of section pitching-moment coefficient with Mach number at various angles of attack for the NACA 0010-0.70 40/0.524 airfoil section with a 25-percent-chord plain flap.

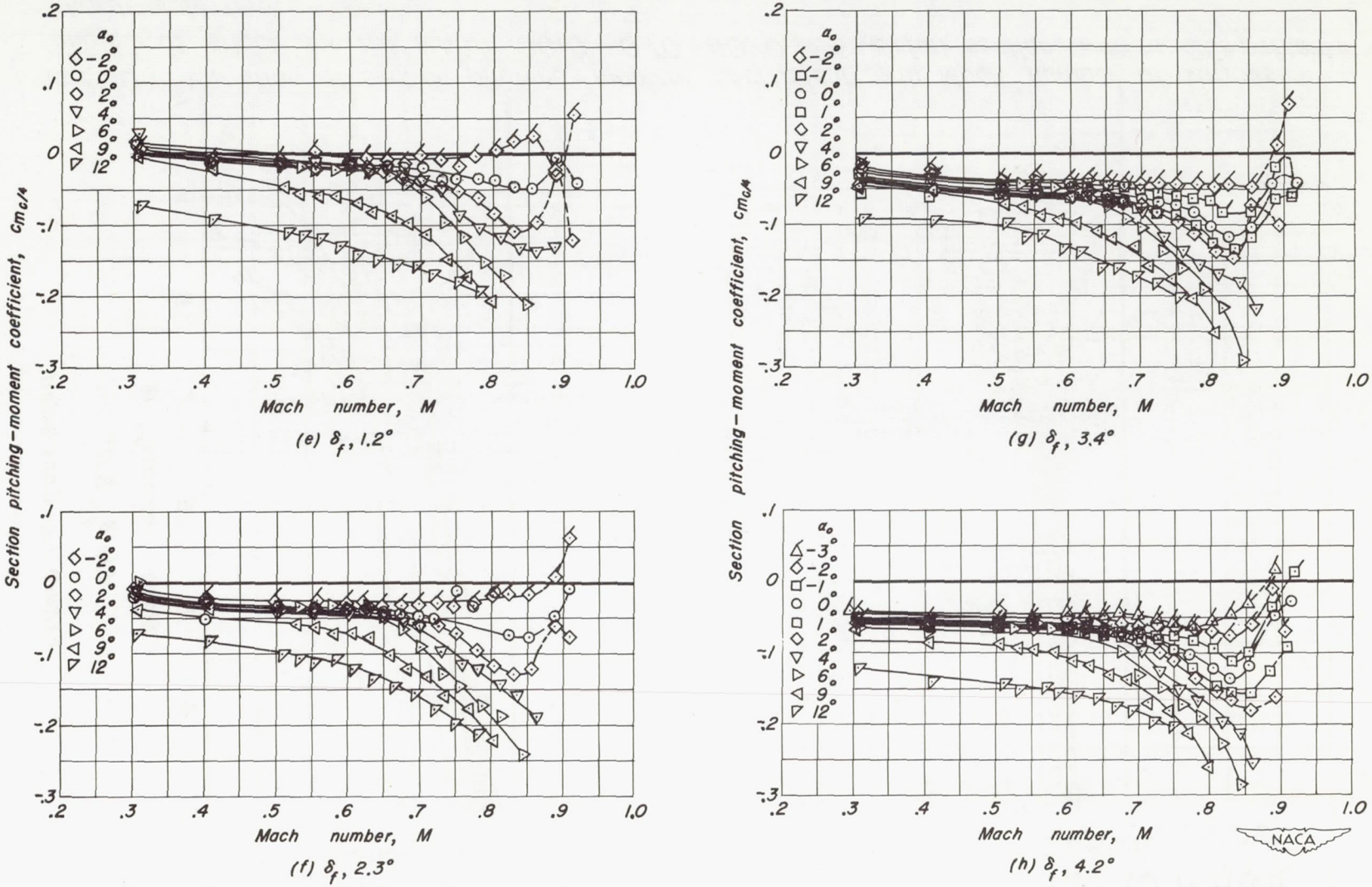

Figure 10. – Continued.

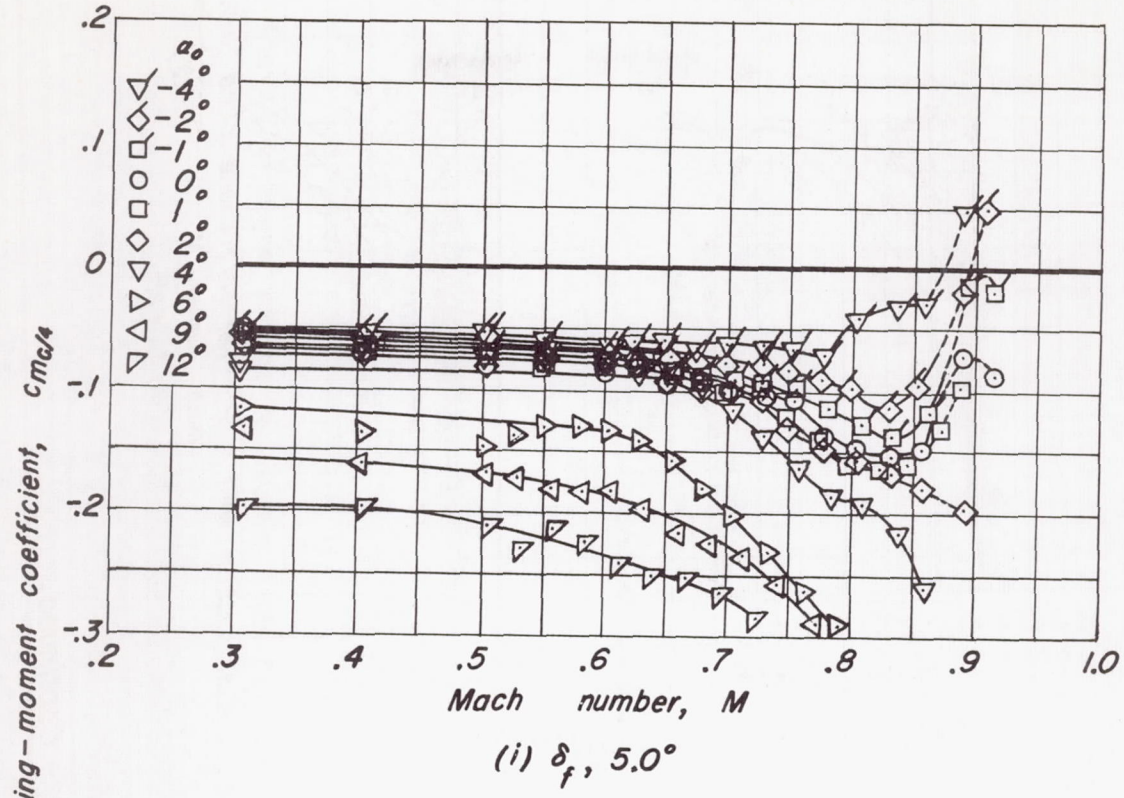

(i) δ_f, 5.0°

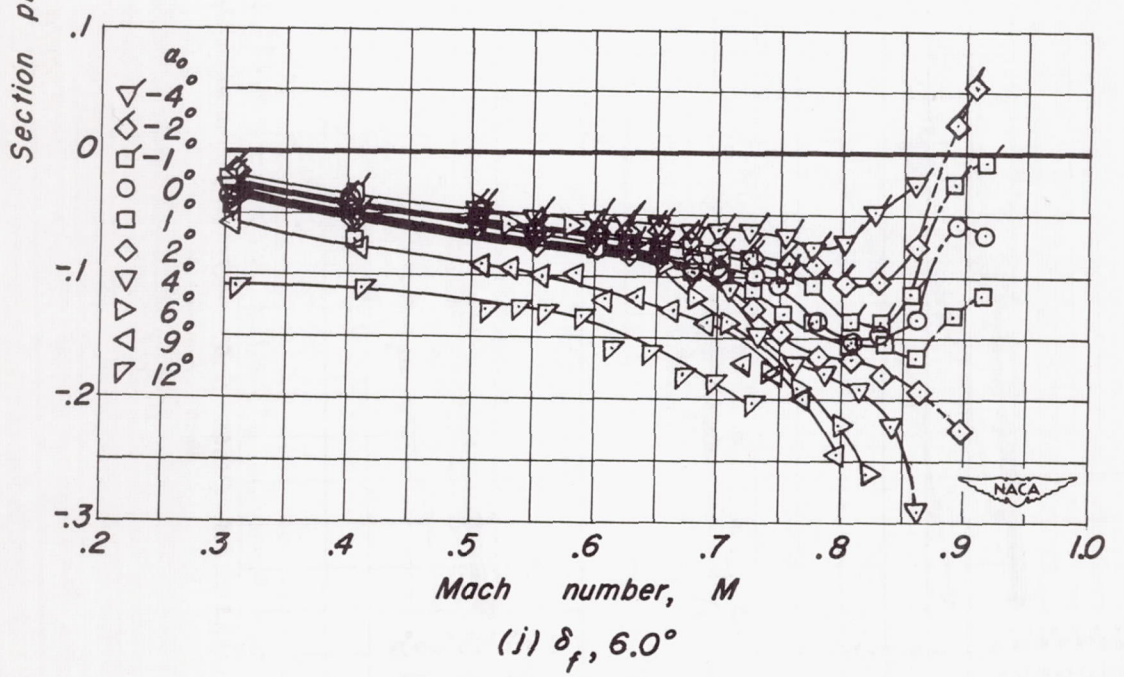

(j) δ_f, 6.0°

Figure 10.- Concluded.

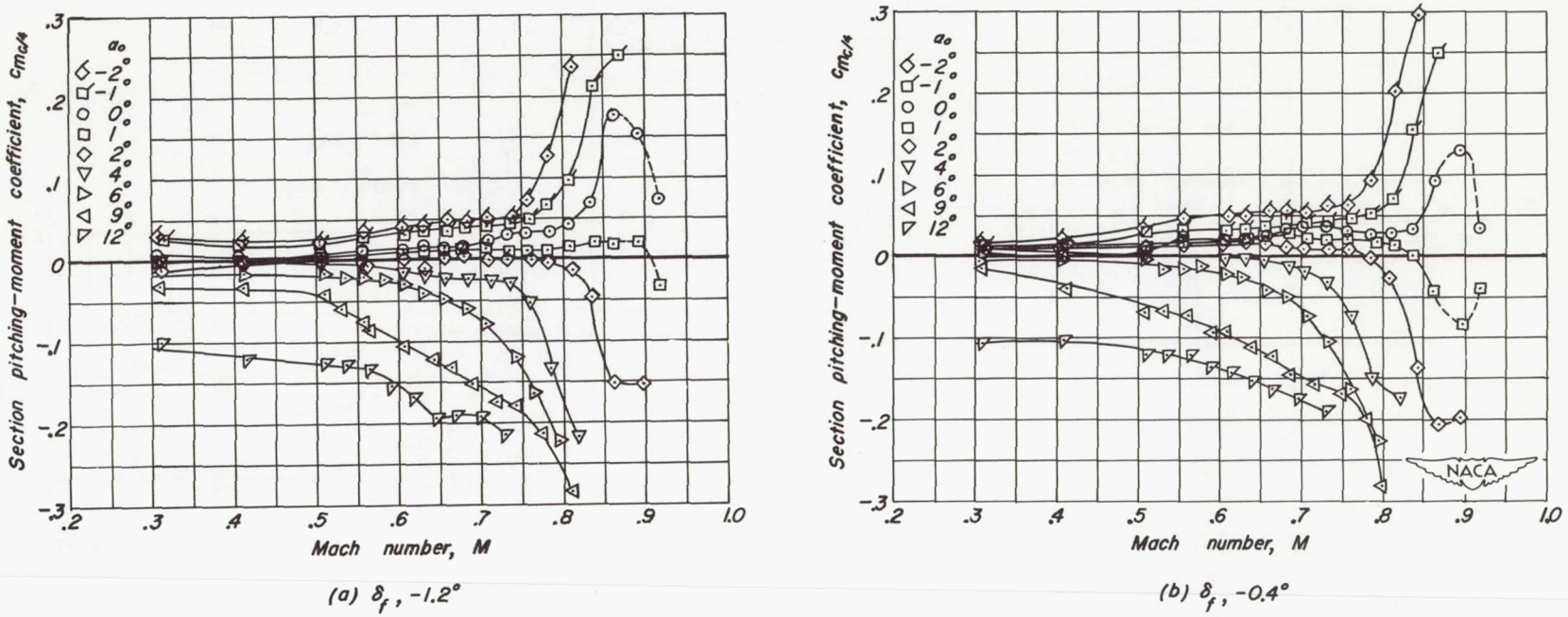

Figure 11.- Variation of section pitching-moment coefficient with Mach number at various angles of attack for the NACA 0010-0.70 40/1.575 (modification A) airfoil section with a 25-percent-chord plain flap.

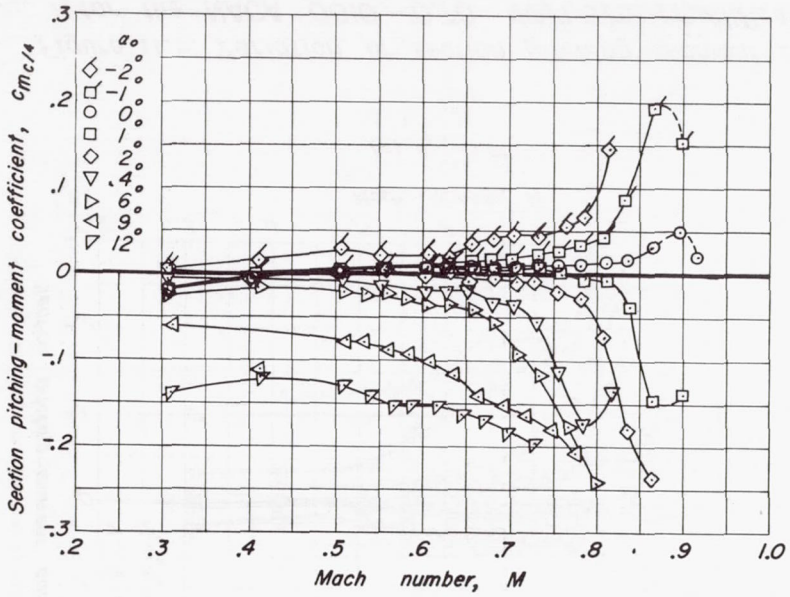

(c) δ_f, 0°

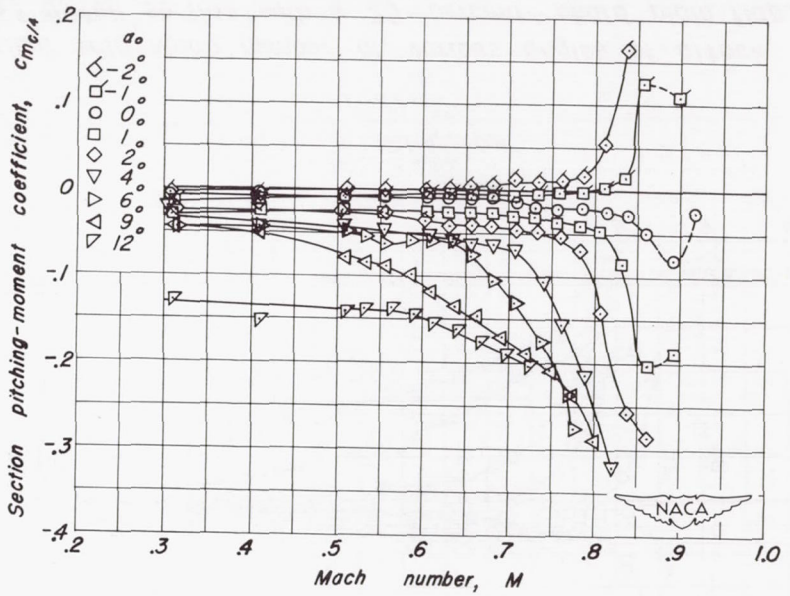

(d) δ_f, 0.4°

Figure 11.– Continued.

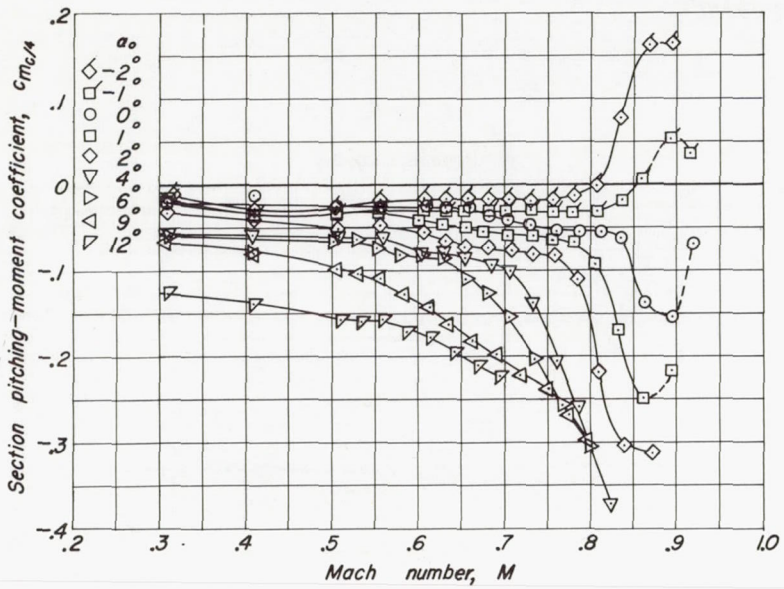

(e) δ_f, 1.2°

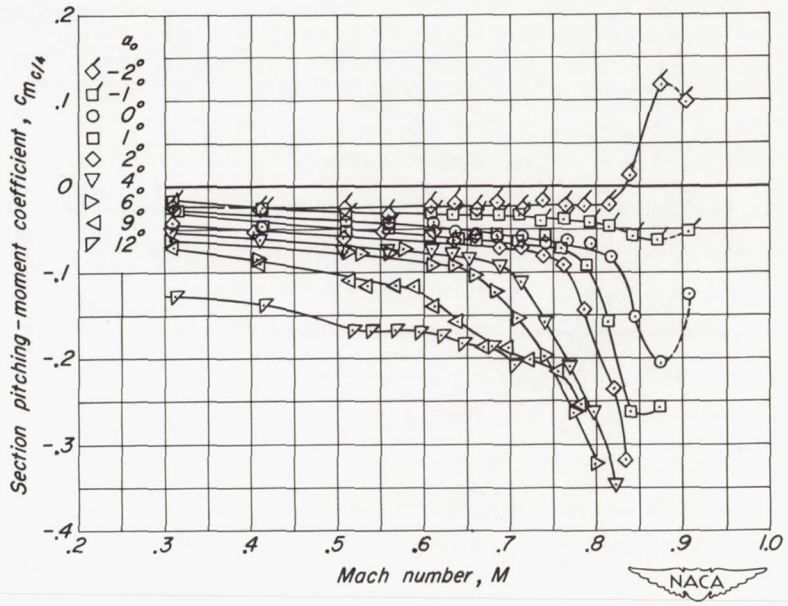

(f) δ_f, 2.0°

Figure 11.– Continued.

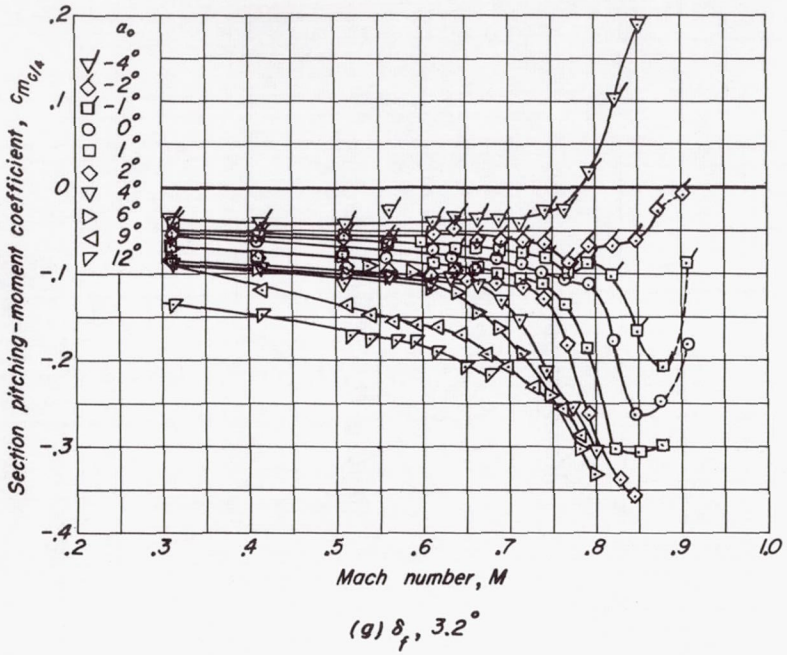

(g) δ_f, 3.2°

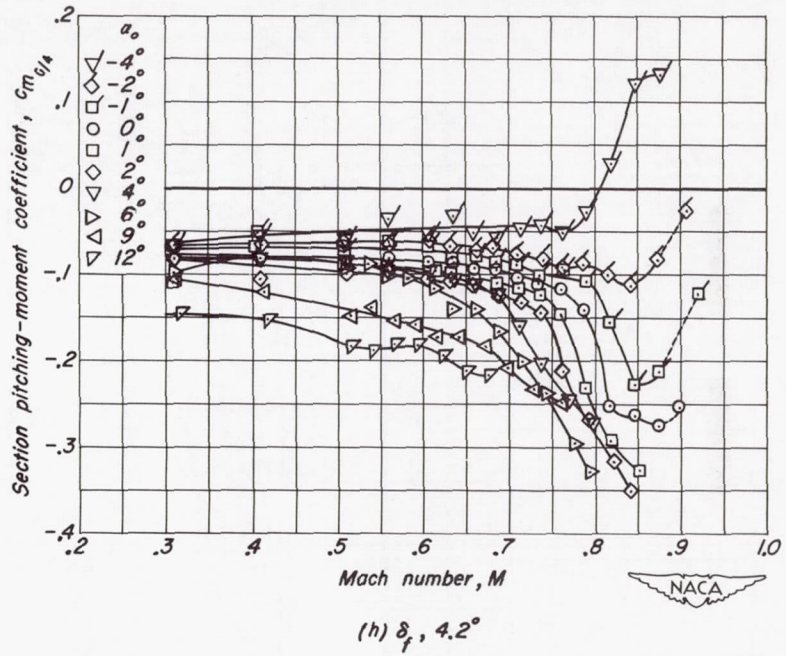

(h) δ_f, 4.2°

Figure 11. – Continued.

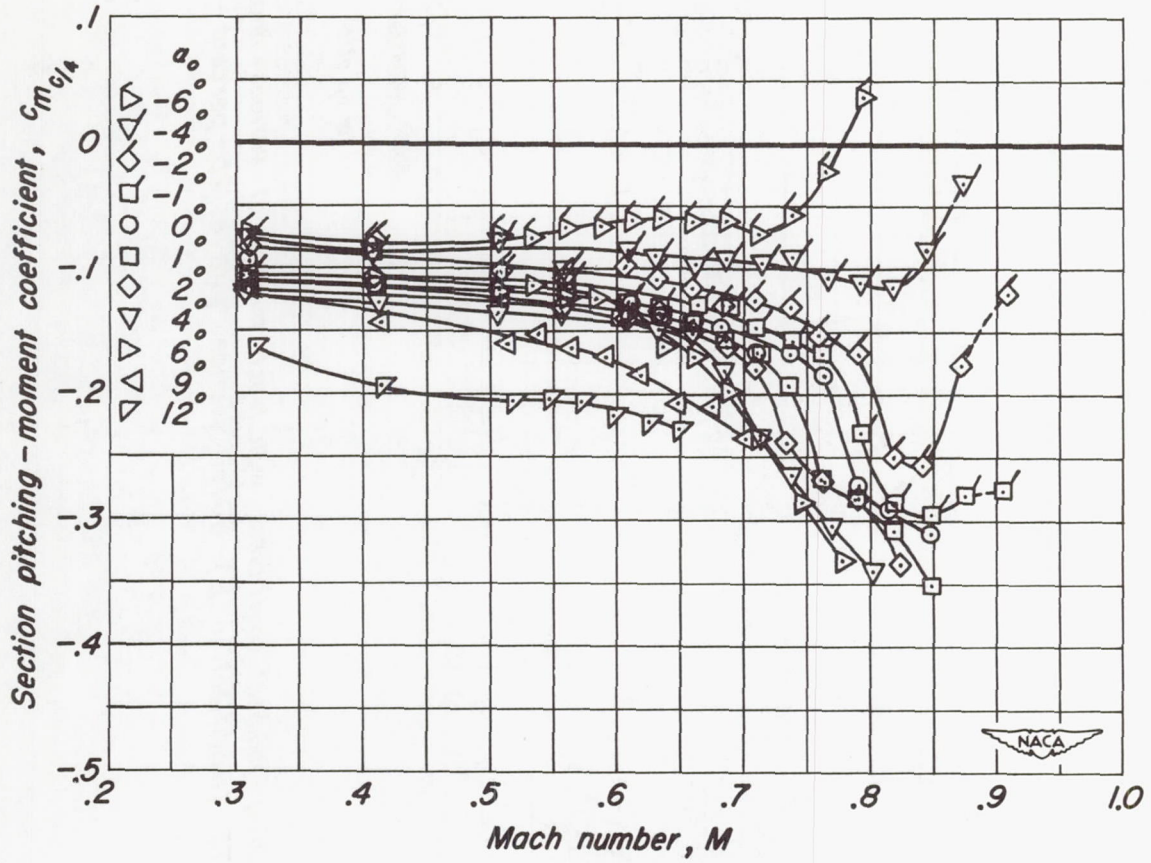

(i) δ_f, 6.8°

Figure 11. - Concluded.

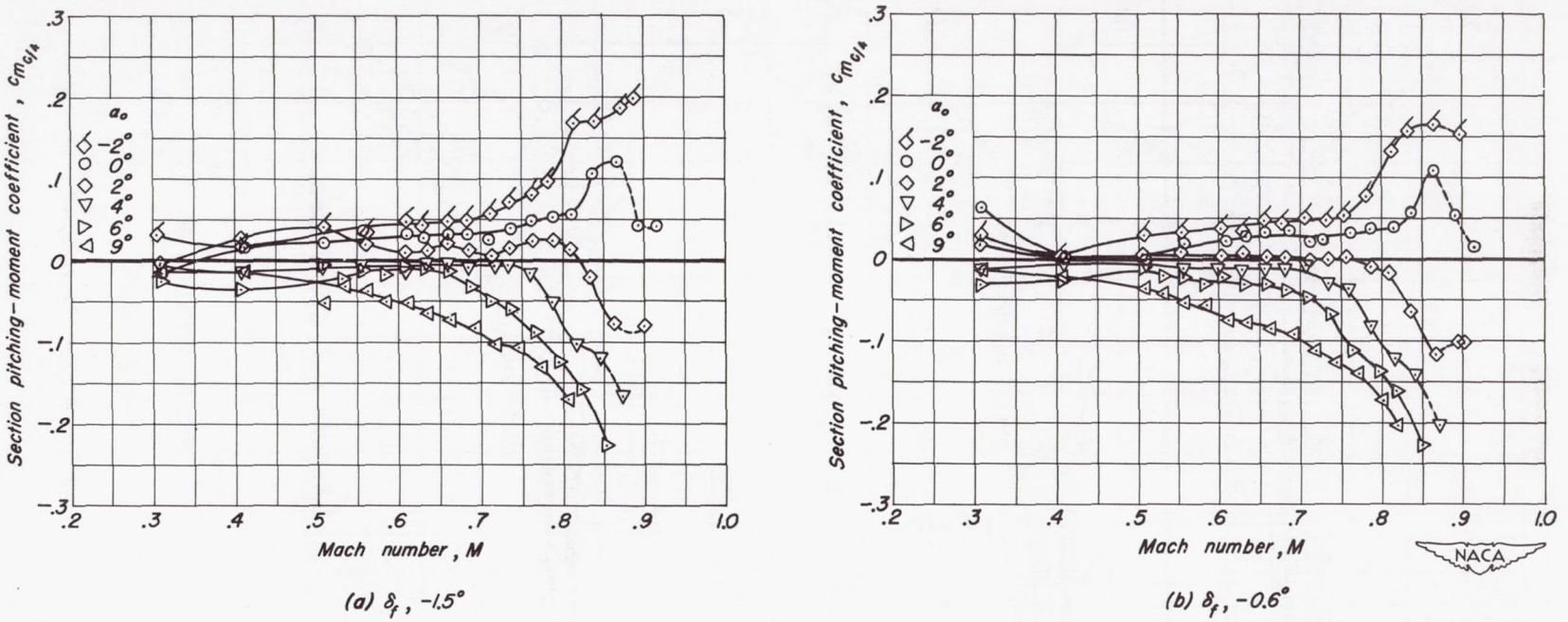

Figure 12.- Variation of section pitching-moment coefficient with Mach number at various angles of attack for the NACA 0010-0.70 40/1.575 (modification B) airfoil section with a 25-percent-chord plain flap.

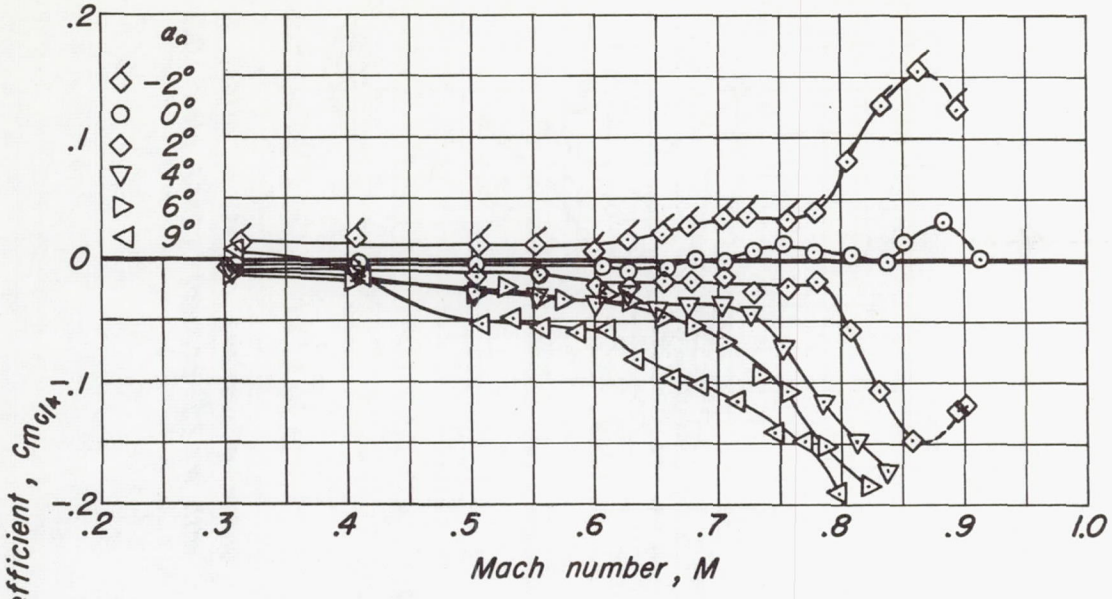

(c) δ_f, 0°

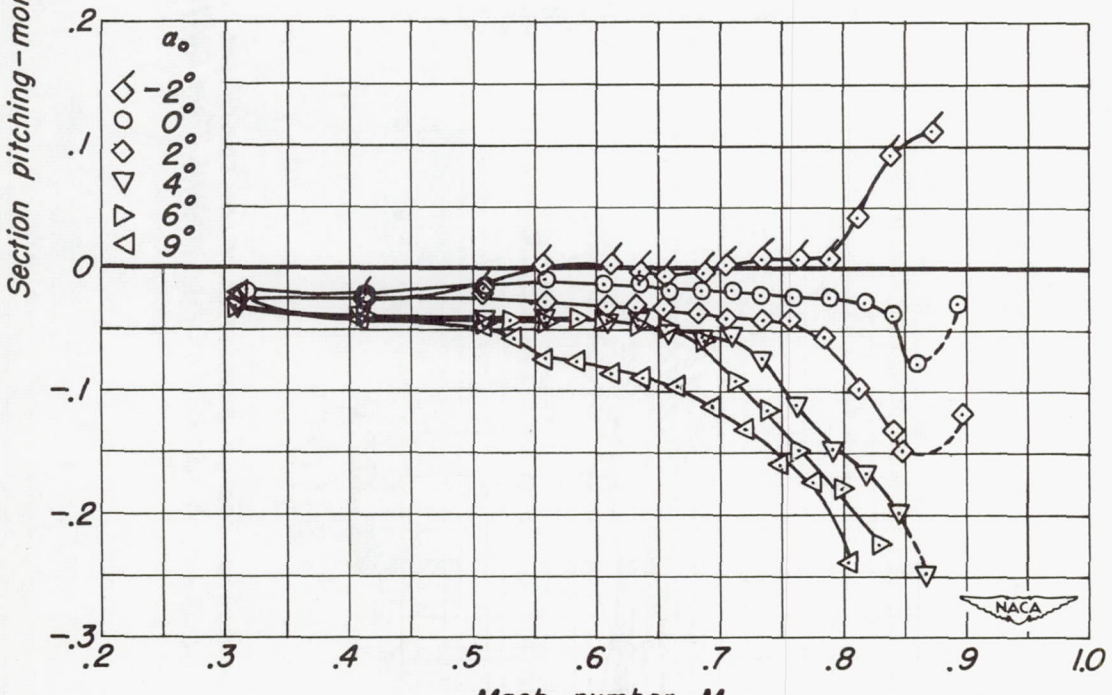

(d) δ_f, 0.6°

Figure 12.- Continued.

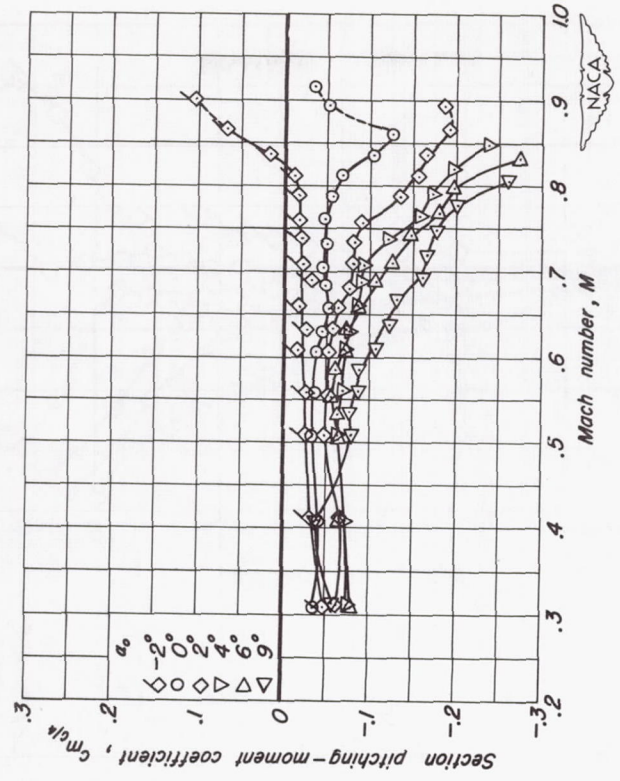

(f) δ_f, 2.3°

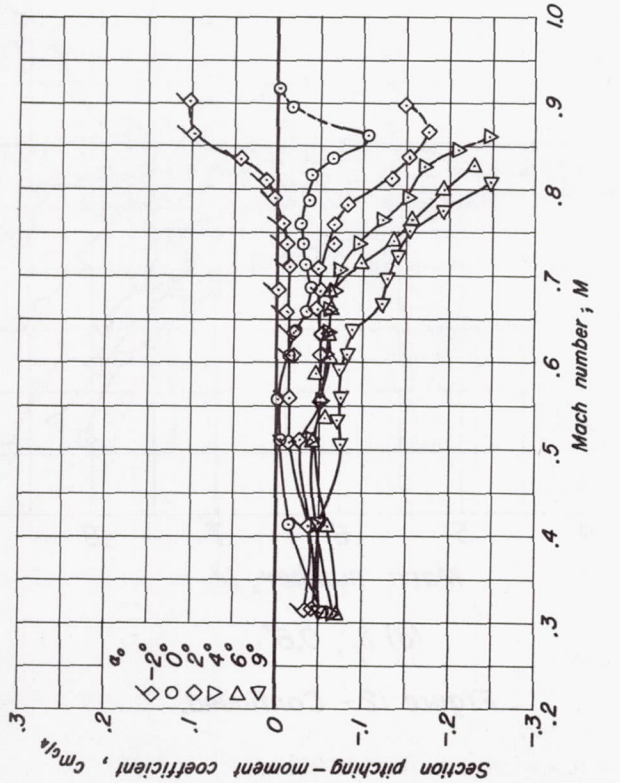

(e) δ_f, 1.5°

Figure 12.- Continued.

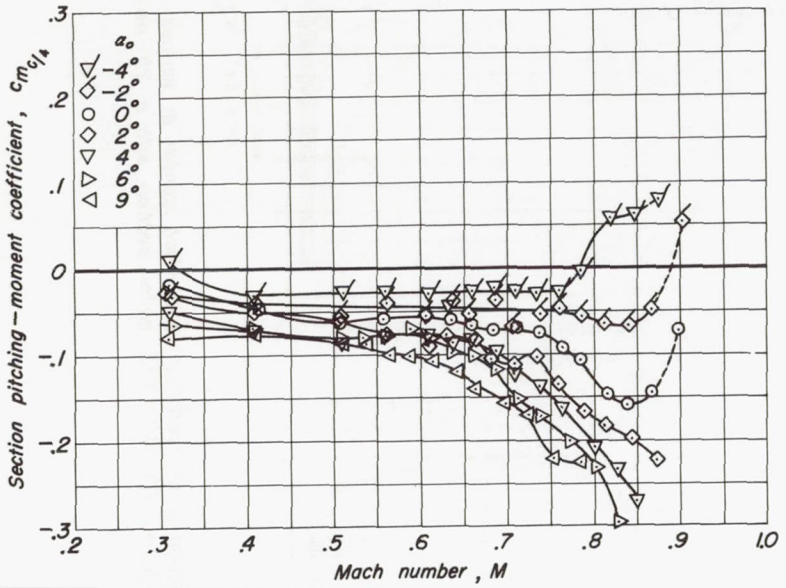

(g) δ_f, 4.0°

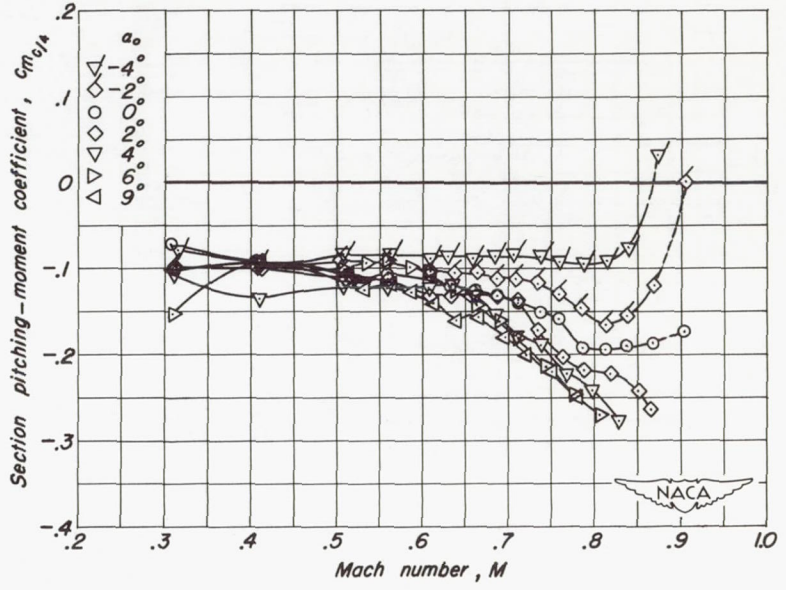

(h) δ_f, 6.5°

Figure 12.– Concluded.

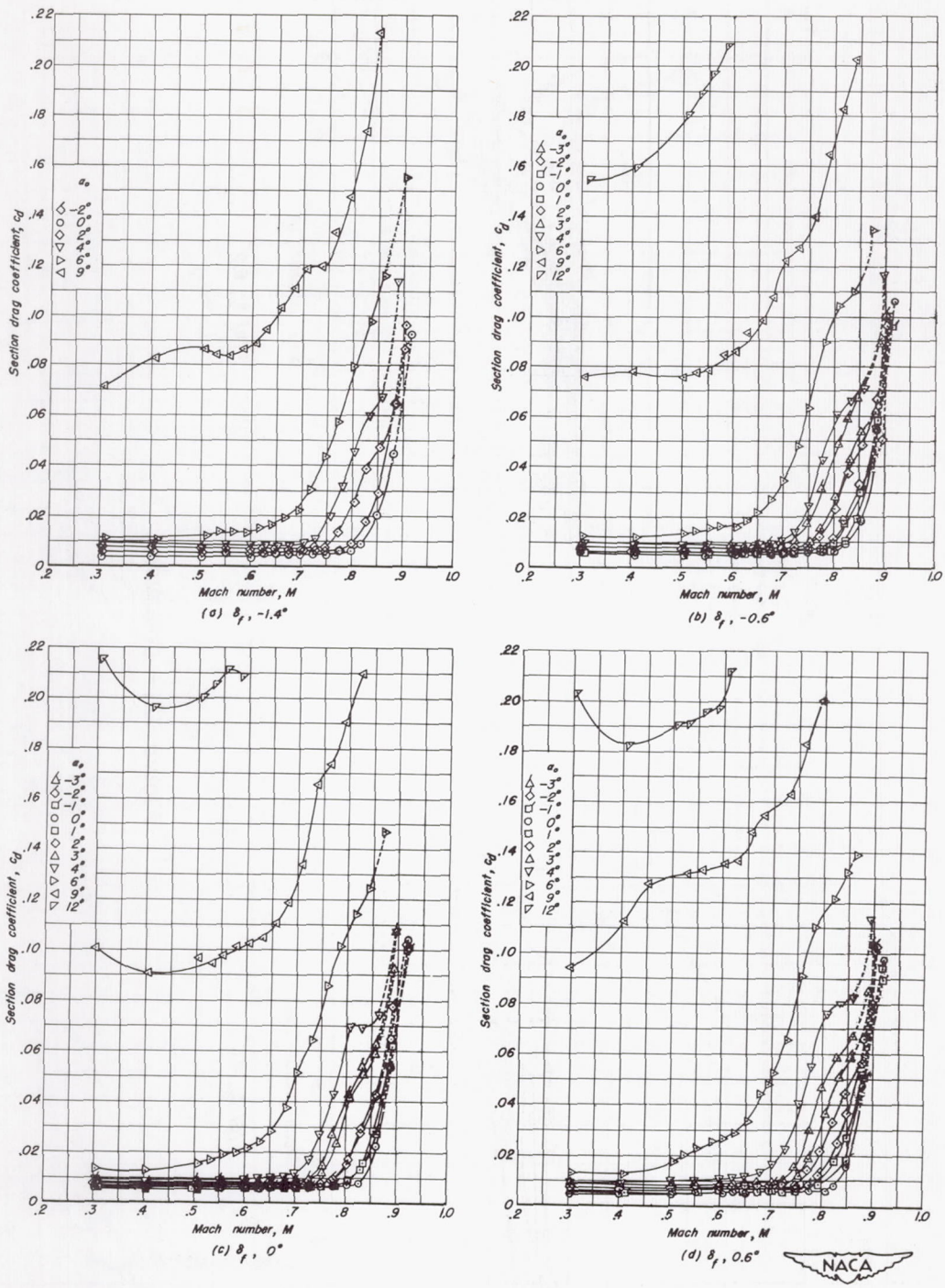

Figure 13.- Variation of section drag coefficient with Mach number at various angles of attack for the NACA 0010-0.70 40/1.575 airfoil section with a 25-percent-chord plain flap.

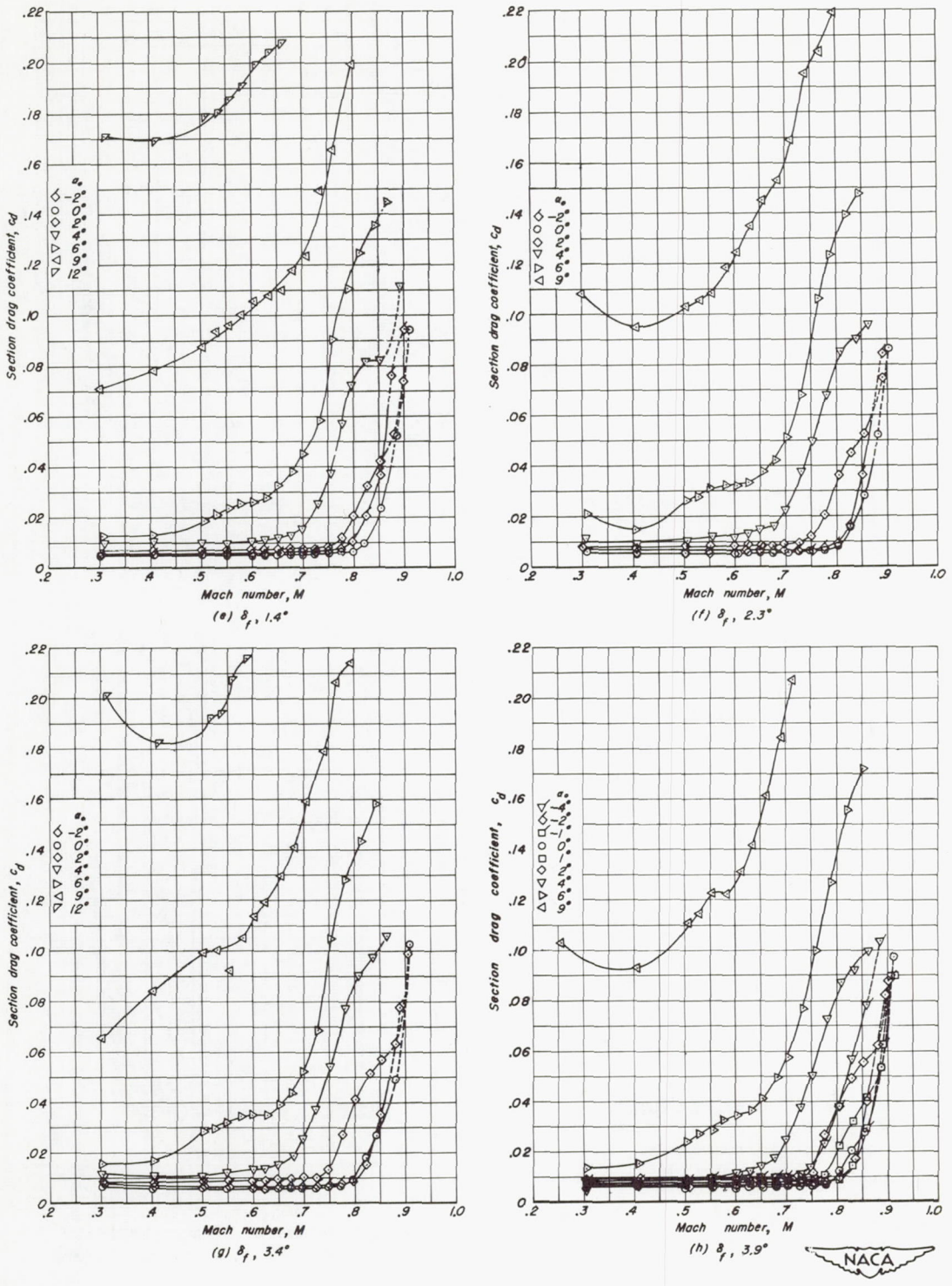

Figure 13.- Continued.

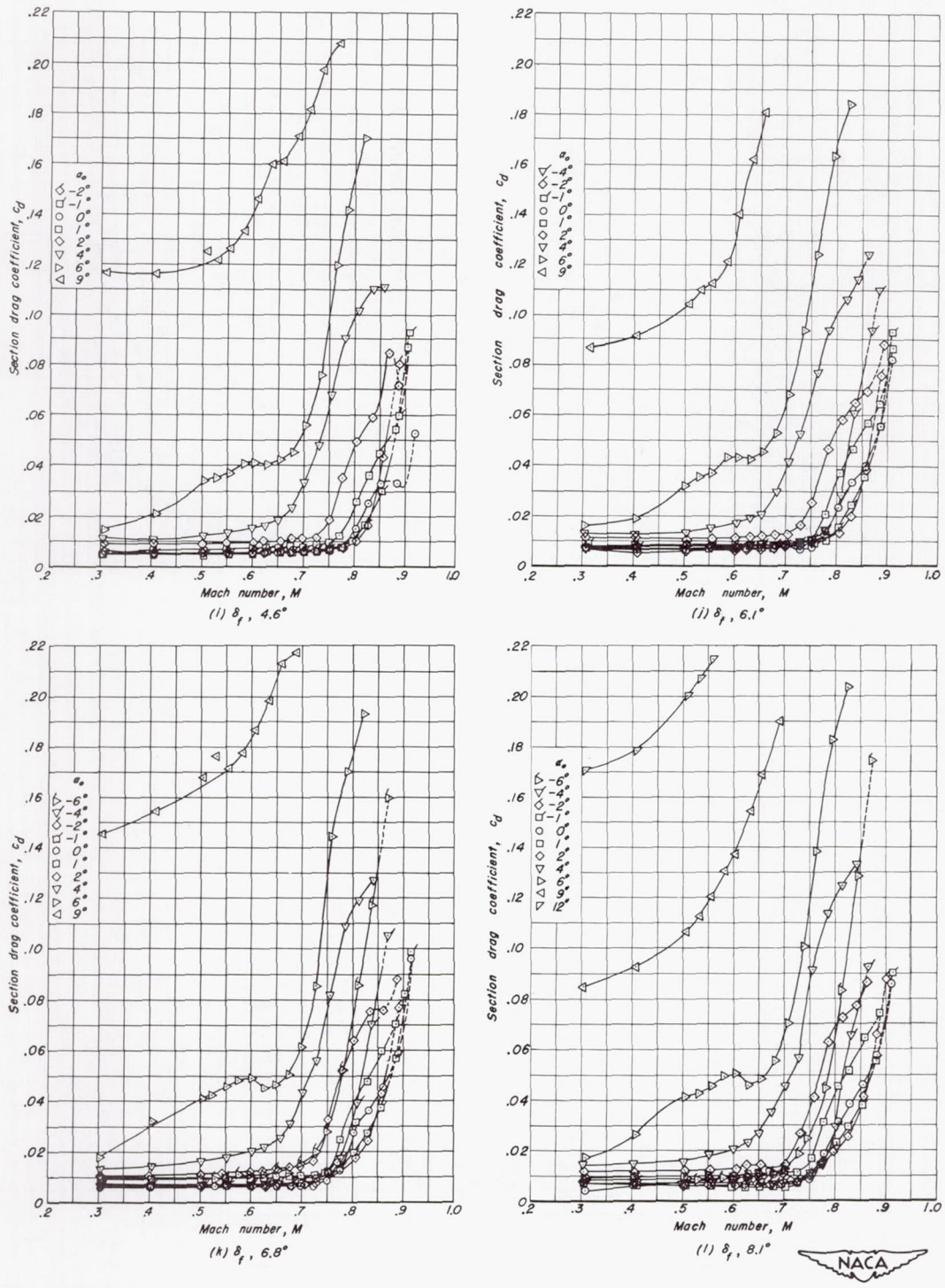

Figure 13.– Continued.

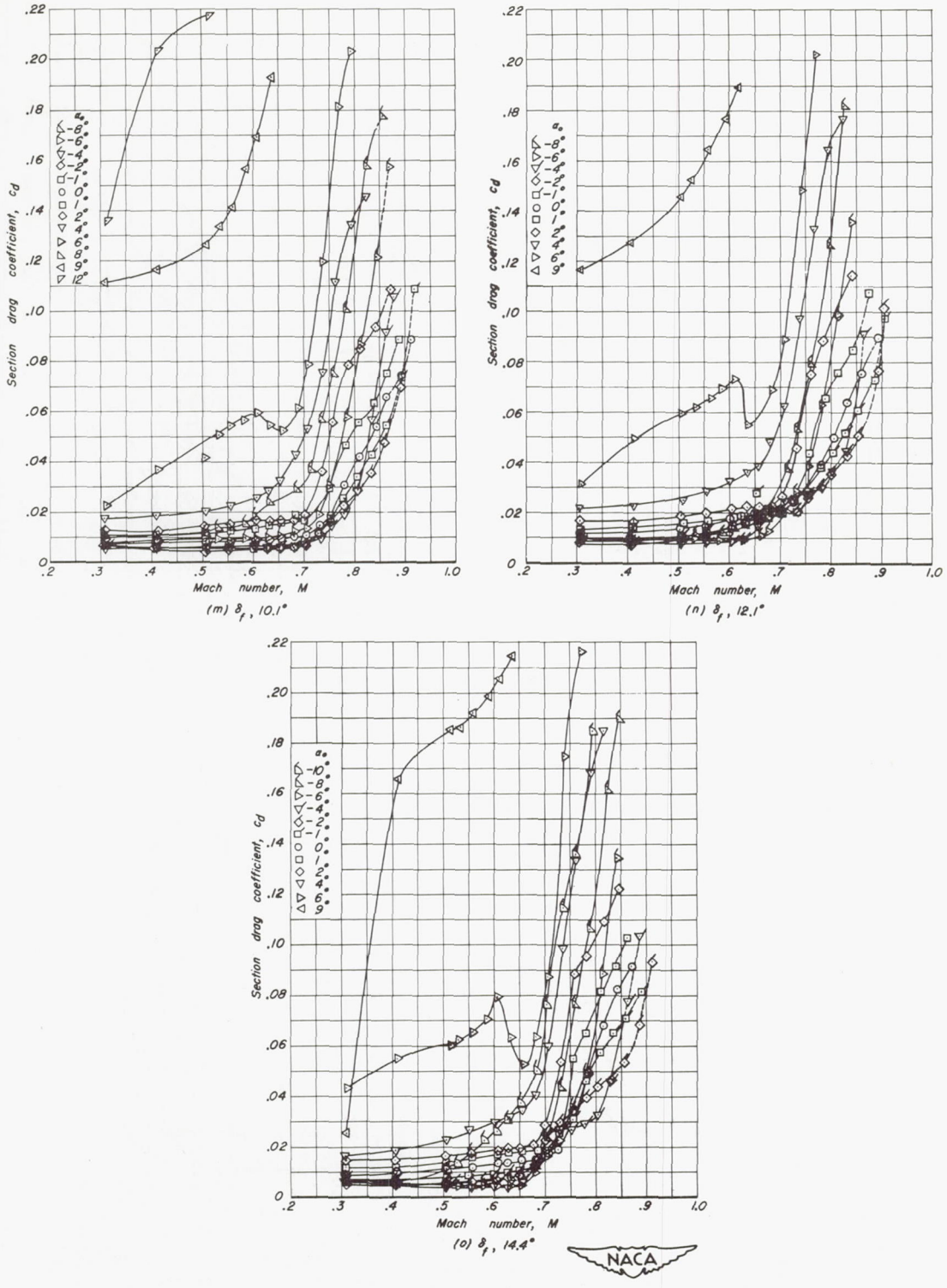

Figure 13.– Concluded.

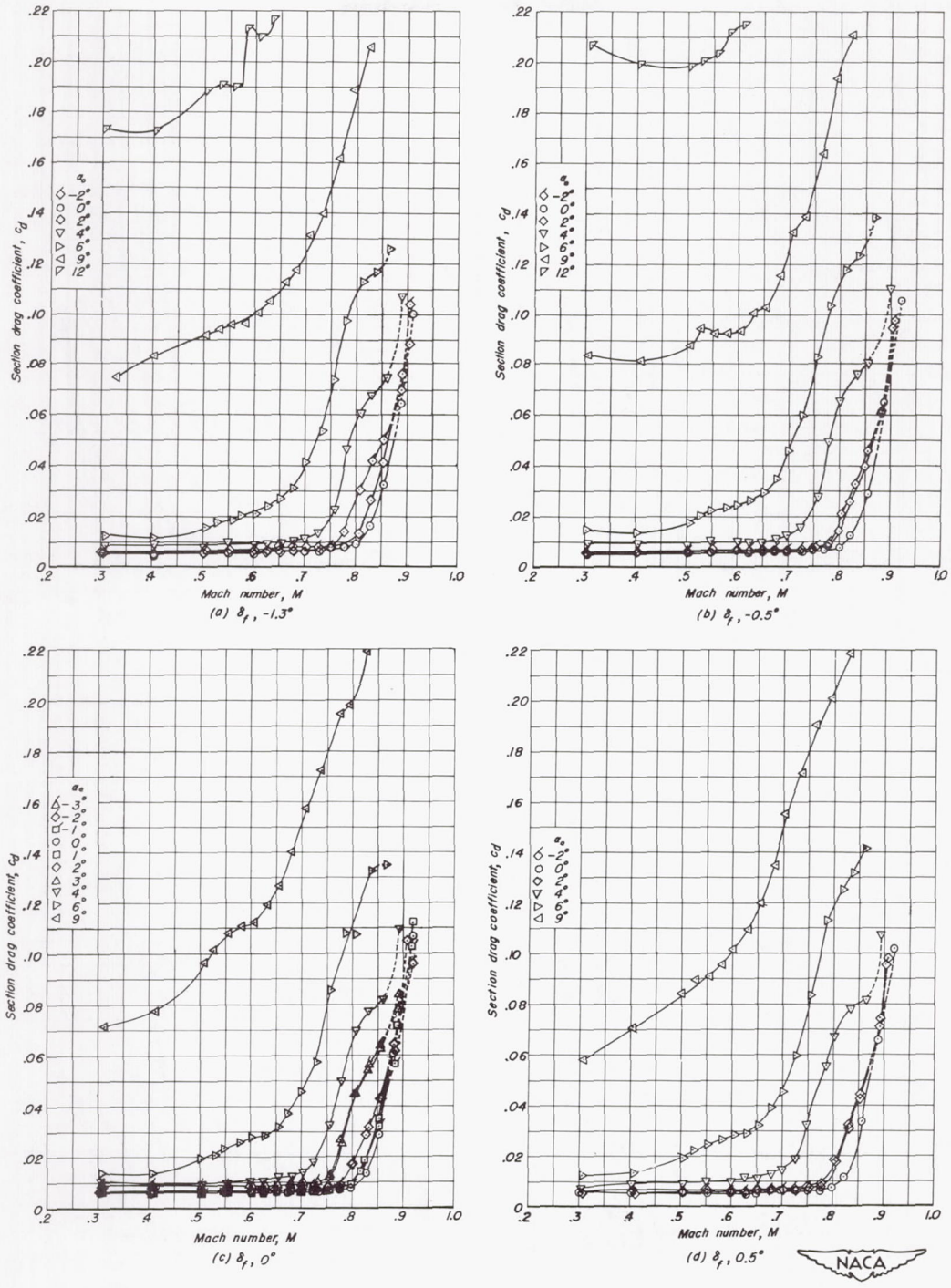

Figure 14.- Variation of section drag coefficient with Mach number at various angles of attack for the NACA 0010-0.70 40/1.051 airfoil section with a 25-percent-chord plain flap.

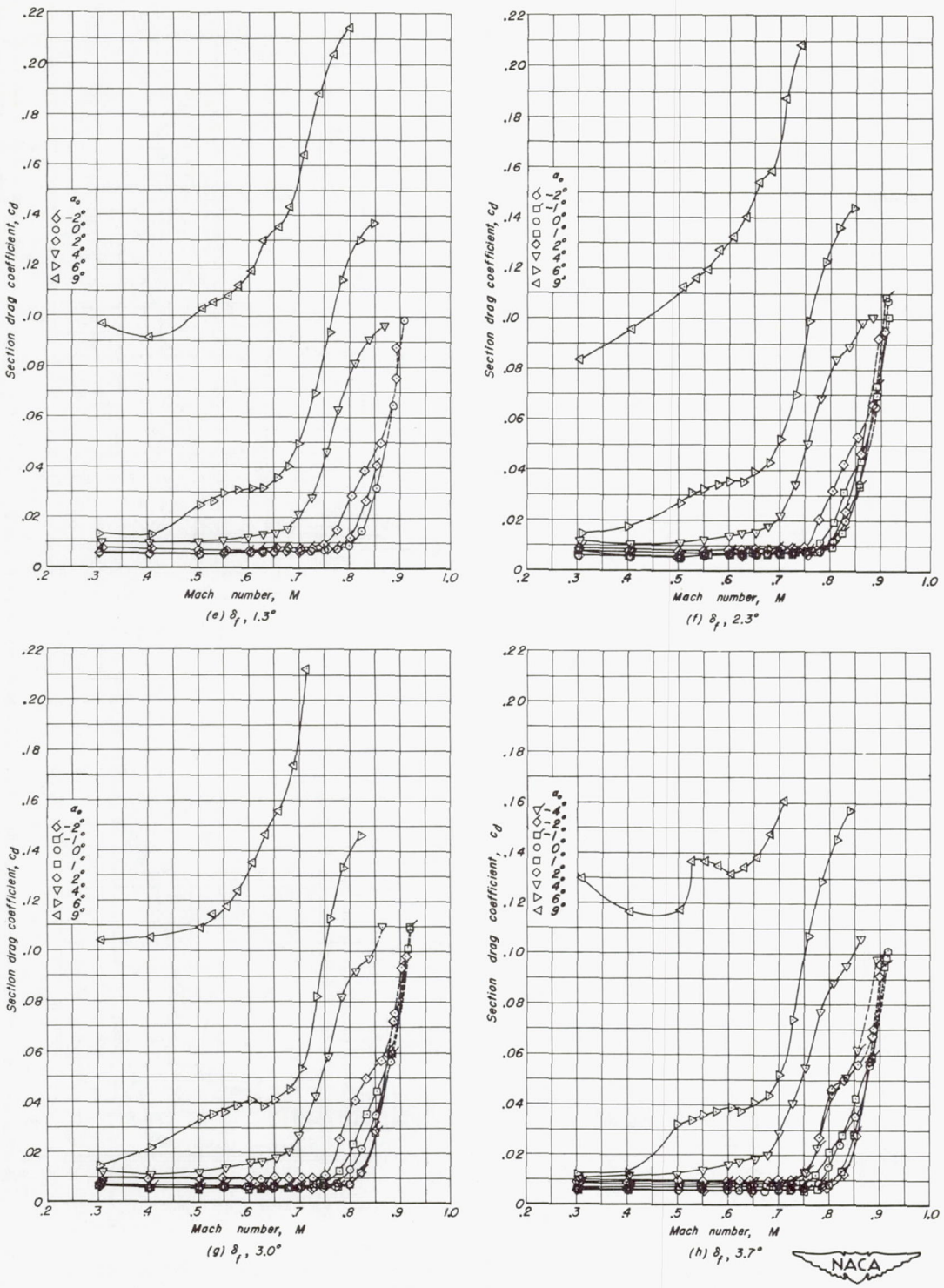

Figure 14.– Continued.

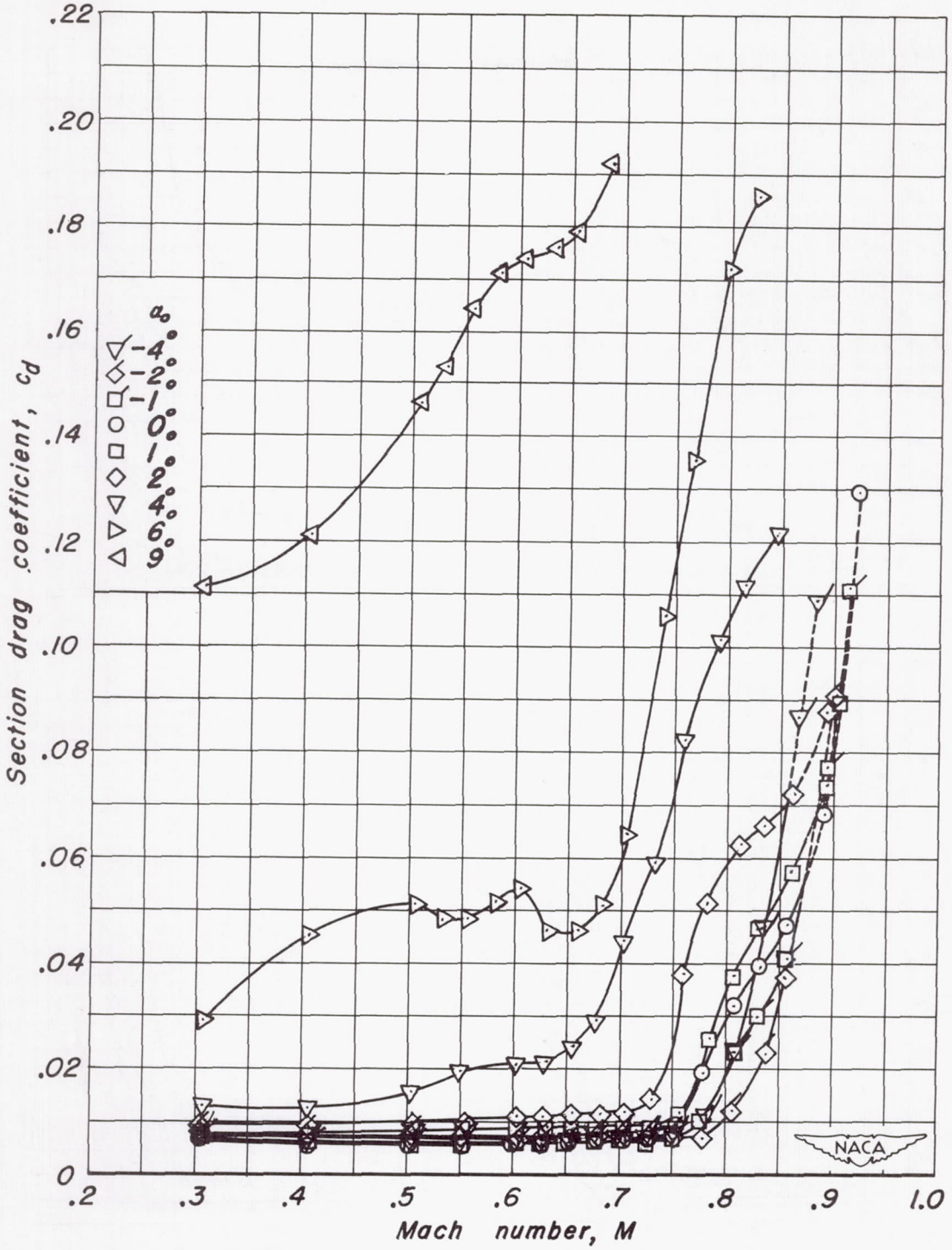

(i) δ_f, 6.1°

Figure 14.- Concluded.

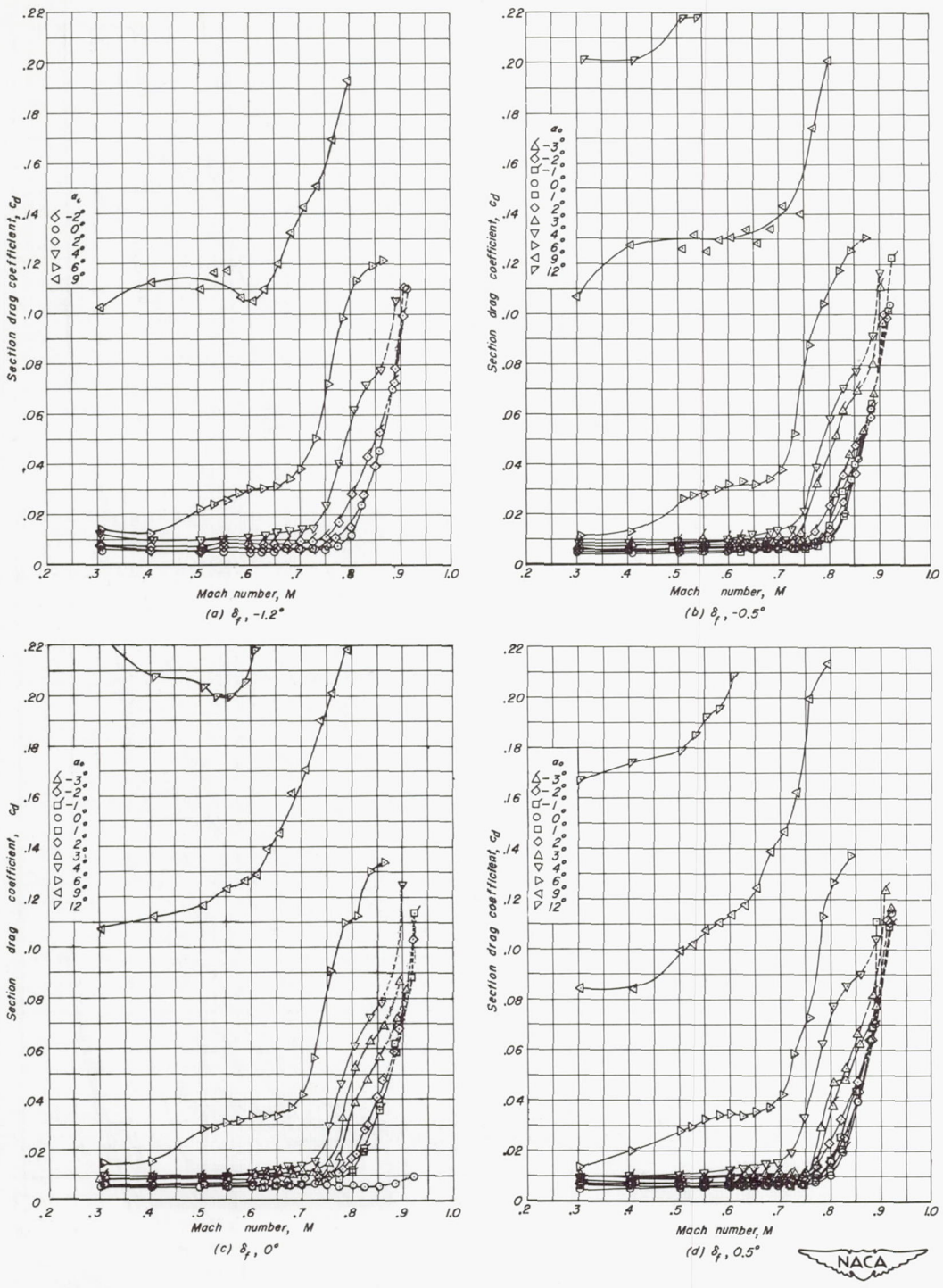

Figure 15:- Variation of section drag coefficient with Mach number at various angles of attack for the NACA 0010-0.70 40/0.524 airfoil section with a 25-percent-chord plain flap.

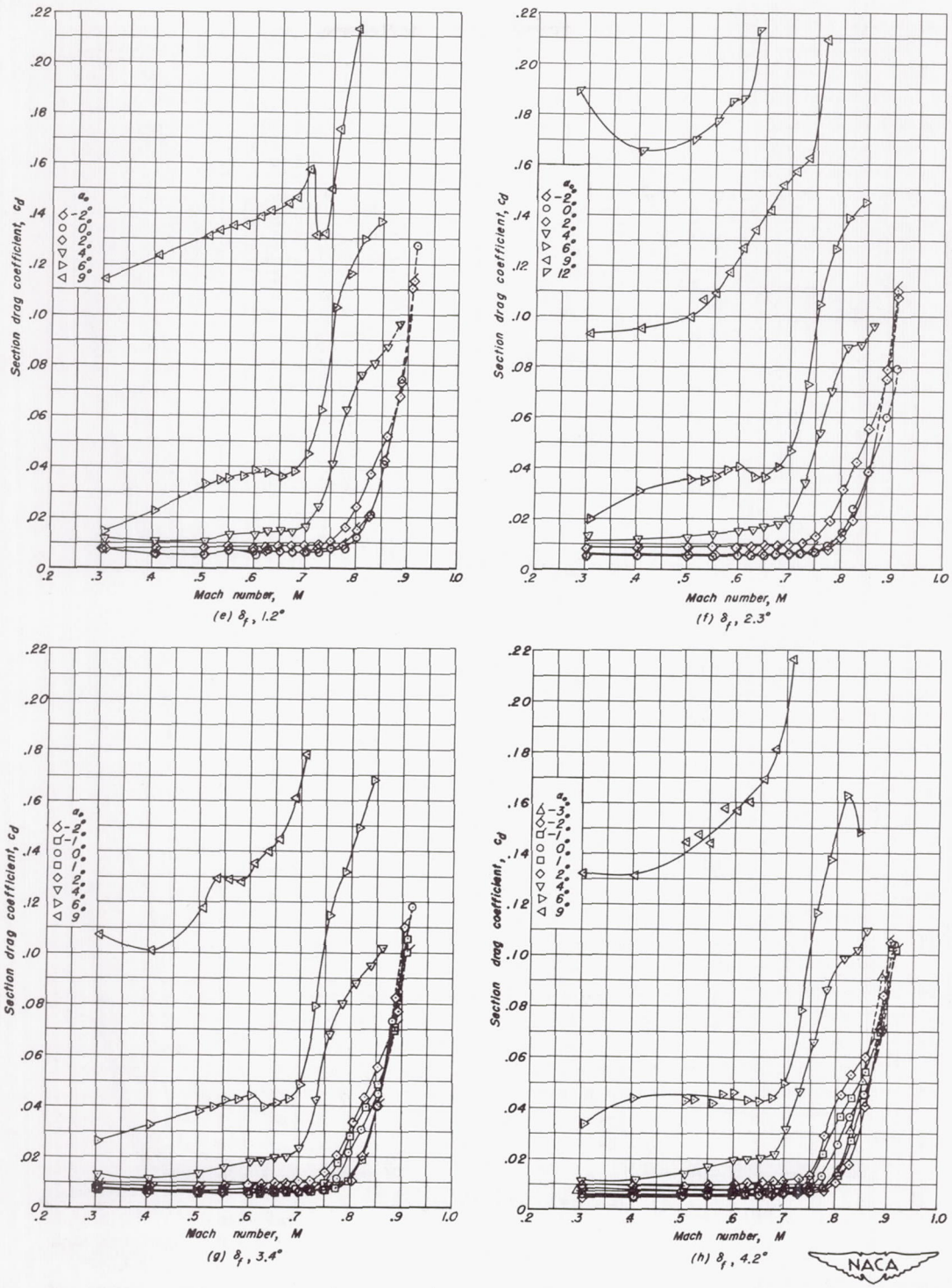

Figure 15.– Continued.

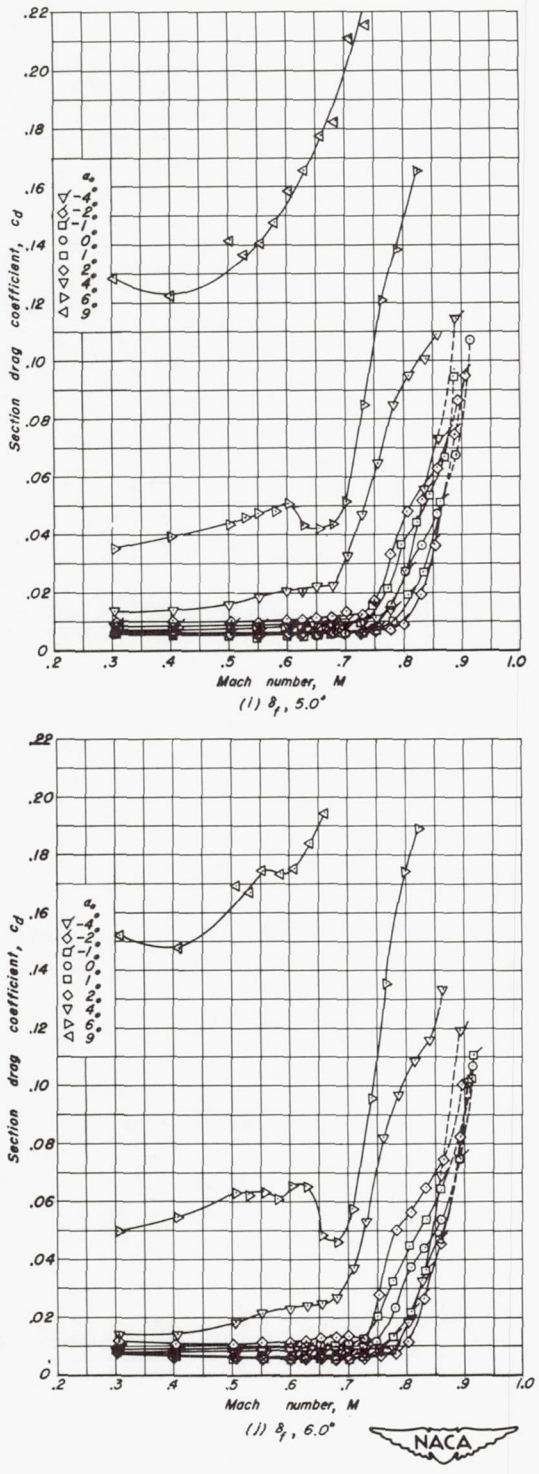

Figure 15.– Concluded.

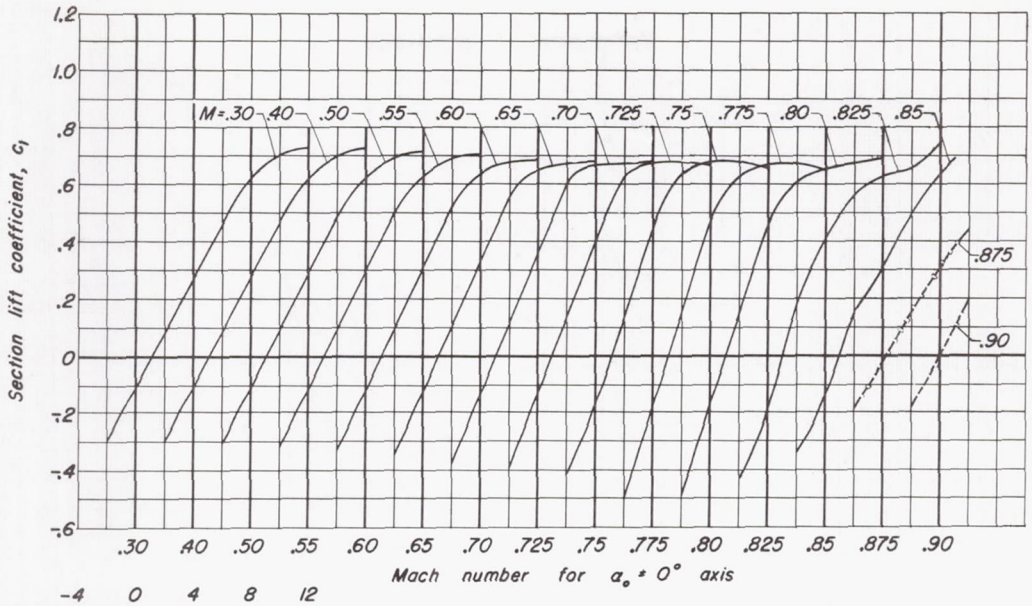

(a) δ_f, -1.4°

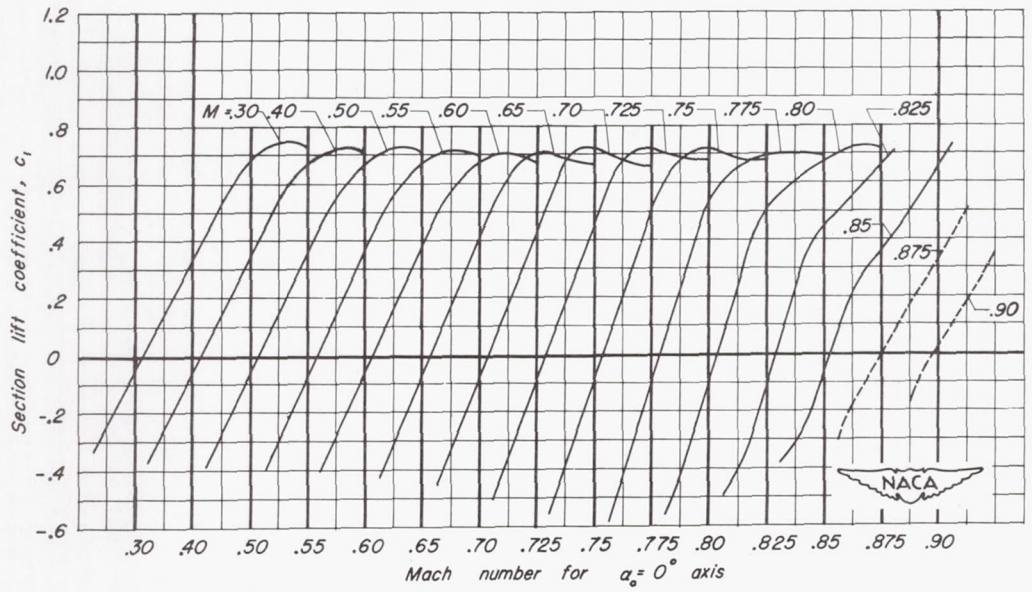

(b) δ_f, -0.6°

Figure 16.- Variation of section lift coefficient with angle of attack at various Mach numbers for the NACA 0010-0.70 40/1.575 airfoil section with a 25-percent-chord plain flap.

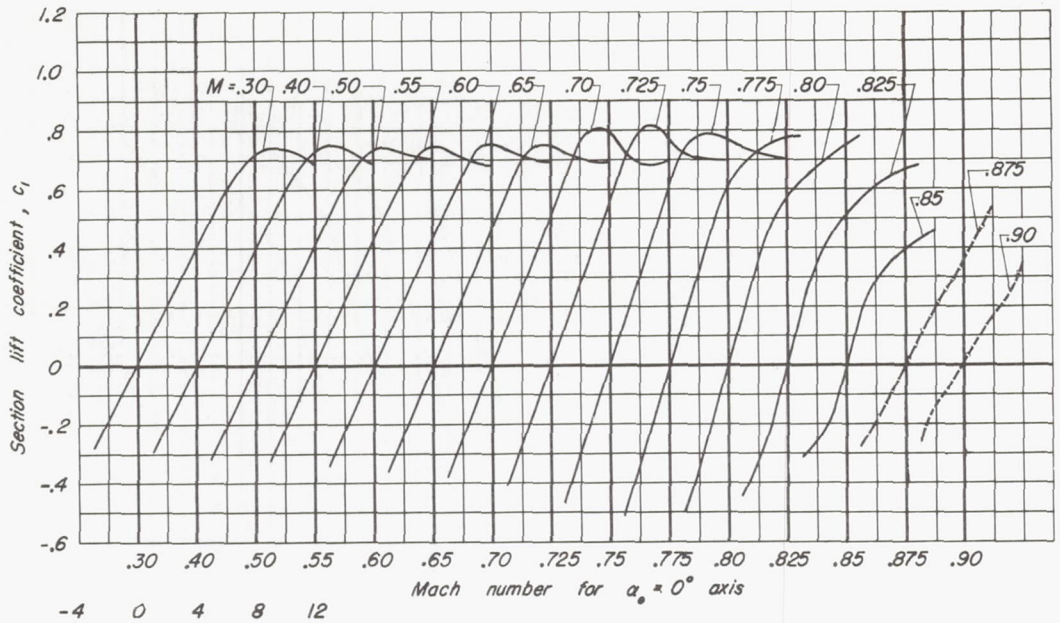

(c) δ_f, 0°

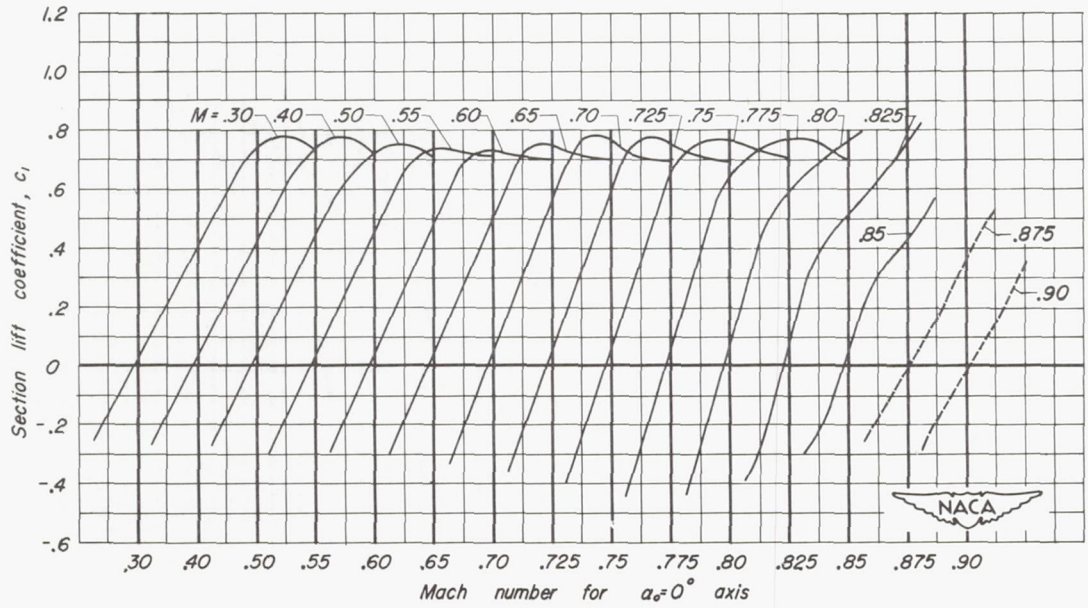

(d) δ_f, 0.6°

Figure 16.- Continued.

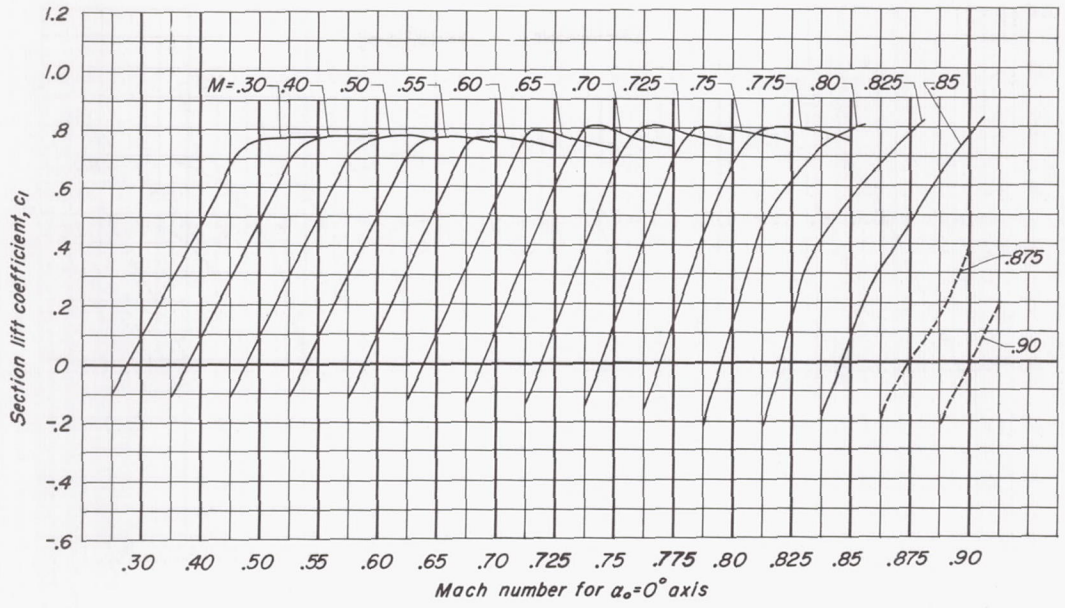

(e) δ_f, 1.4°

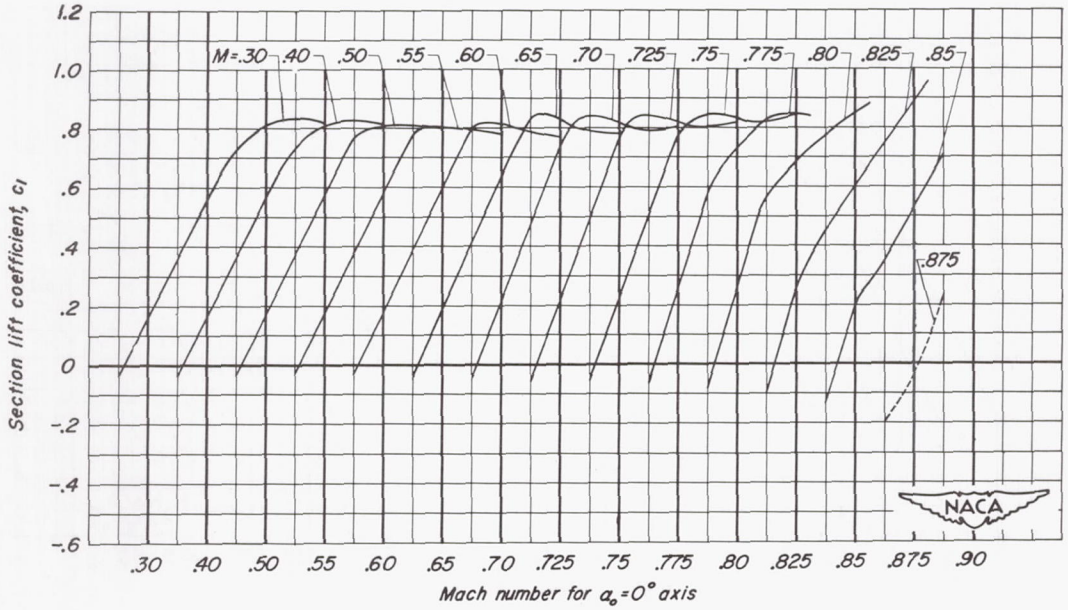

(f) δ_f, 2.3°

Figure 16.– Continued.

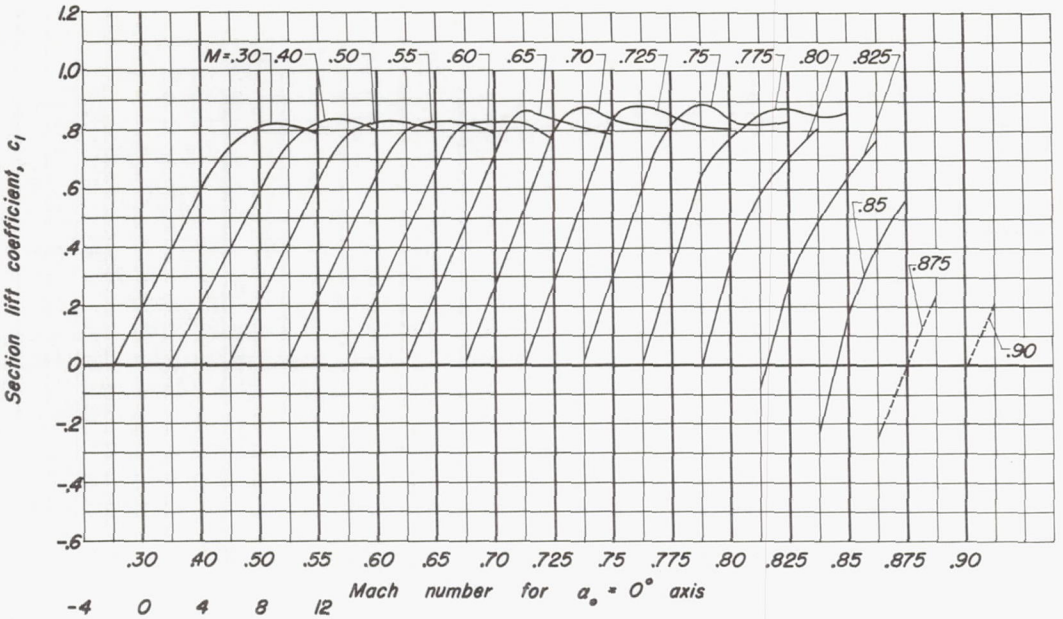

(g) δ_f, 3.4°

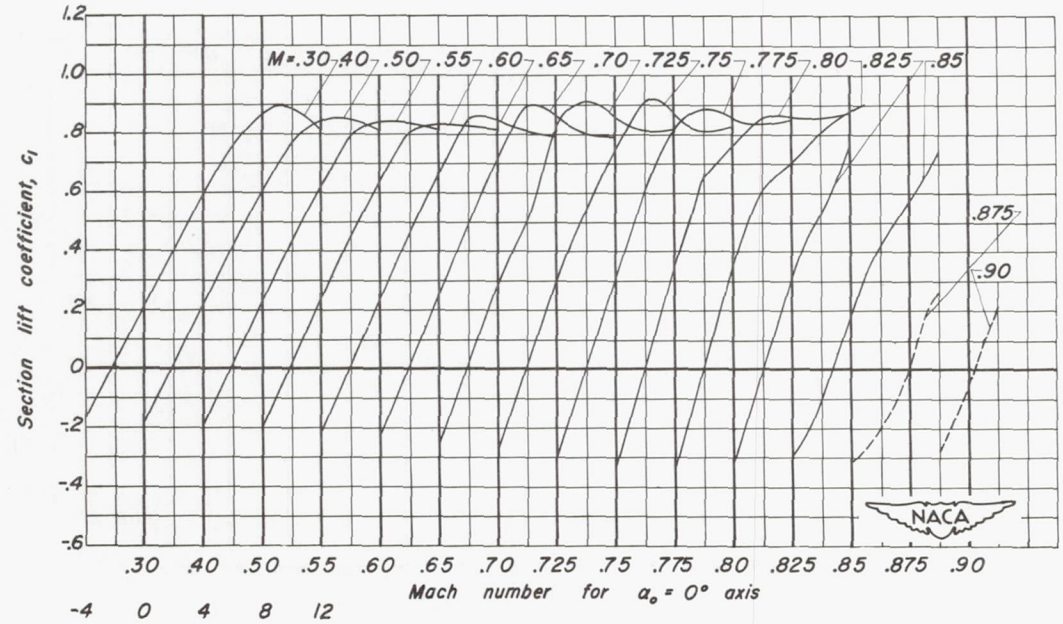

(h) δ_f, 3.9°

Figure 16.- Continued.

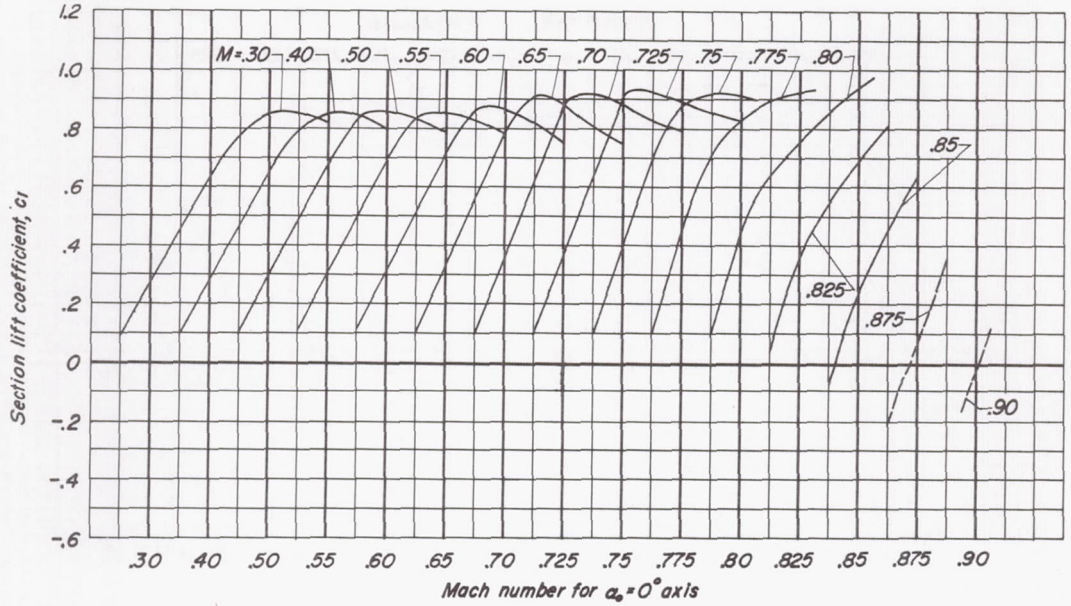

(i) δ_f, 4.6°

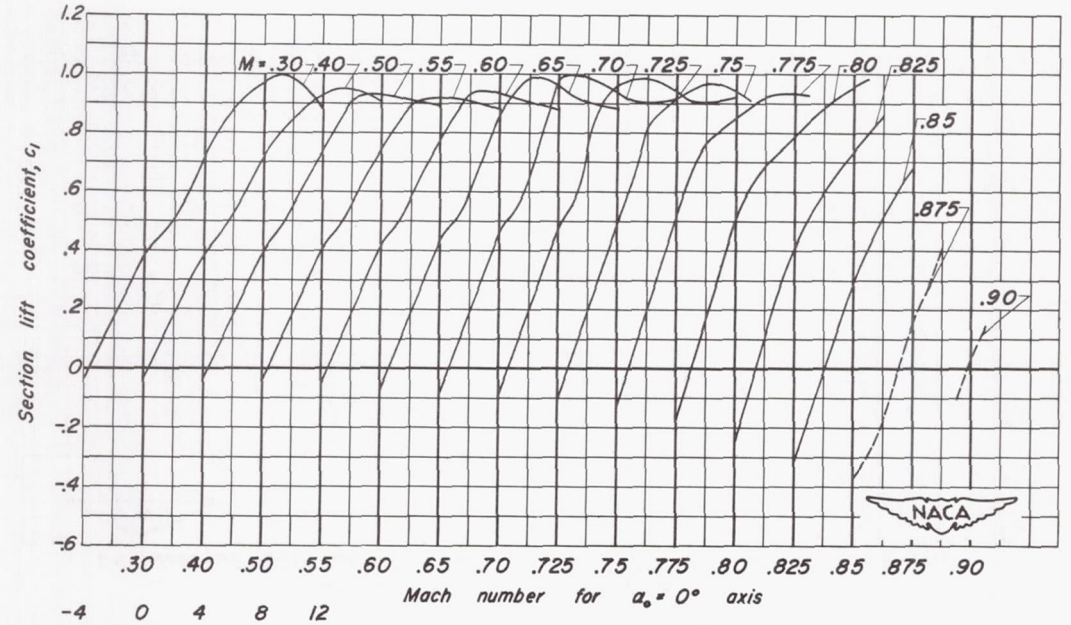

(j) δ_f, 6.1°

Figure 16.- Continued.

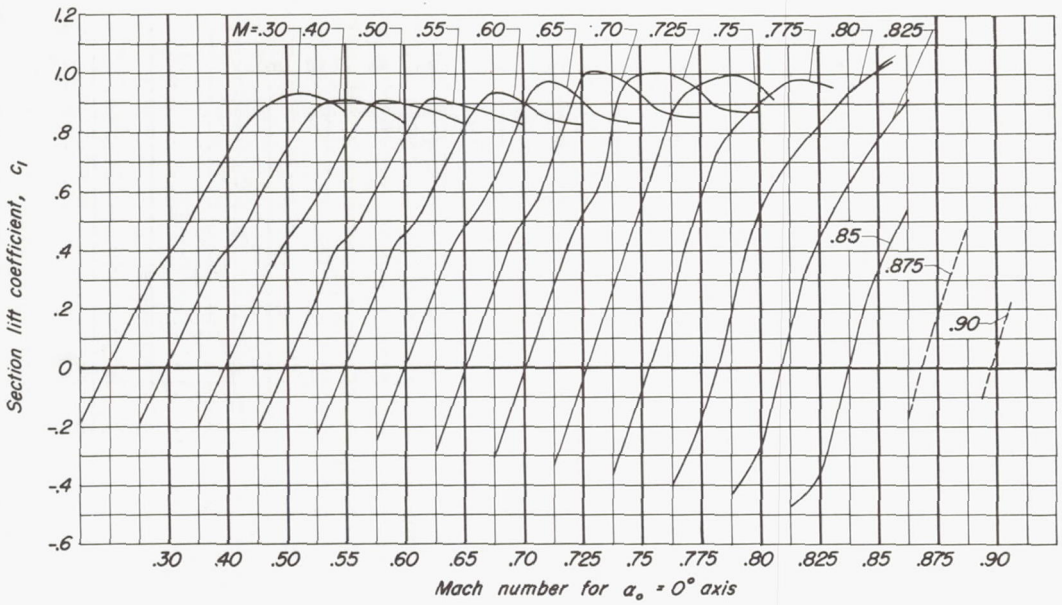

(k) δ_f, 6.8°

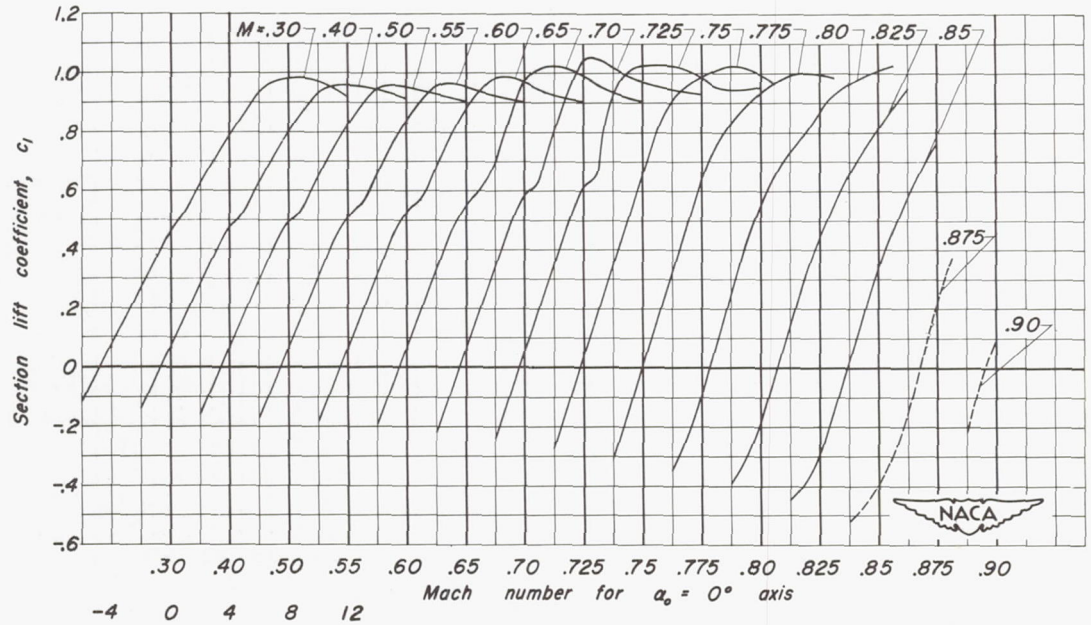

(l) δ_f, 8.1°

Figure 16.– Continued.

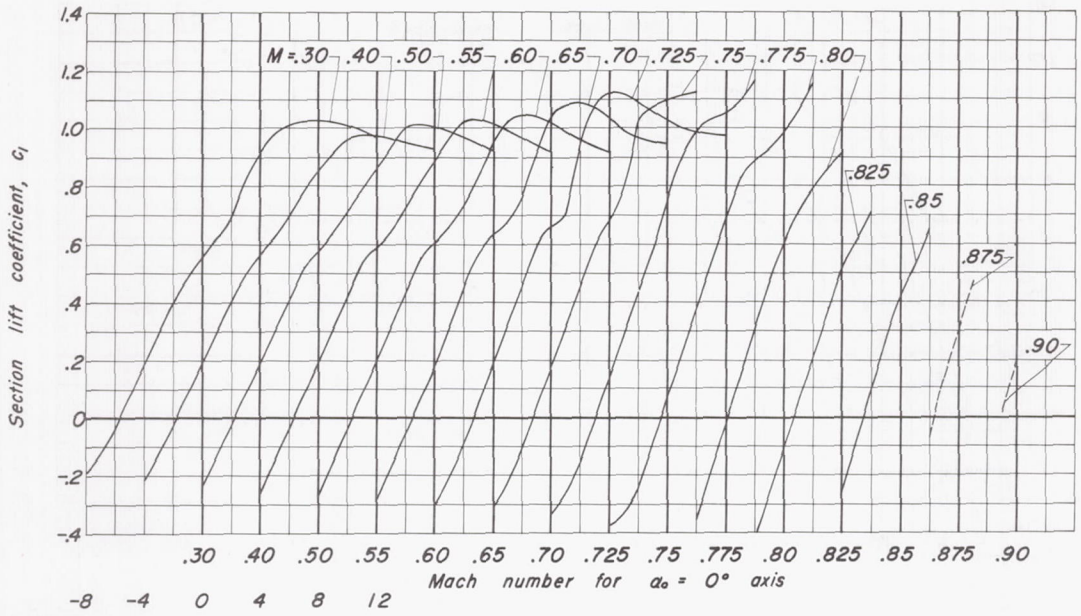

(m) δ_f, 10.1°

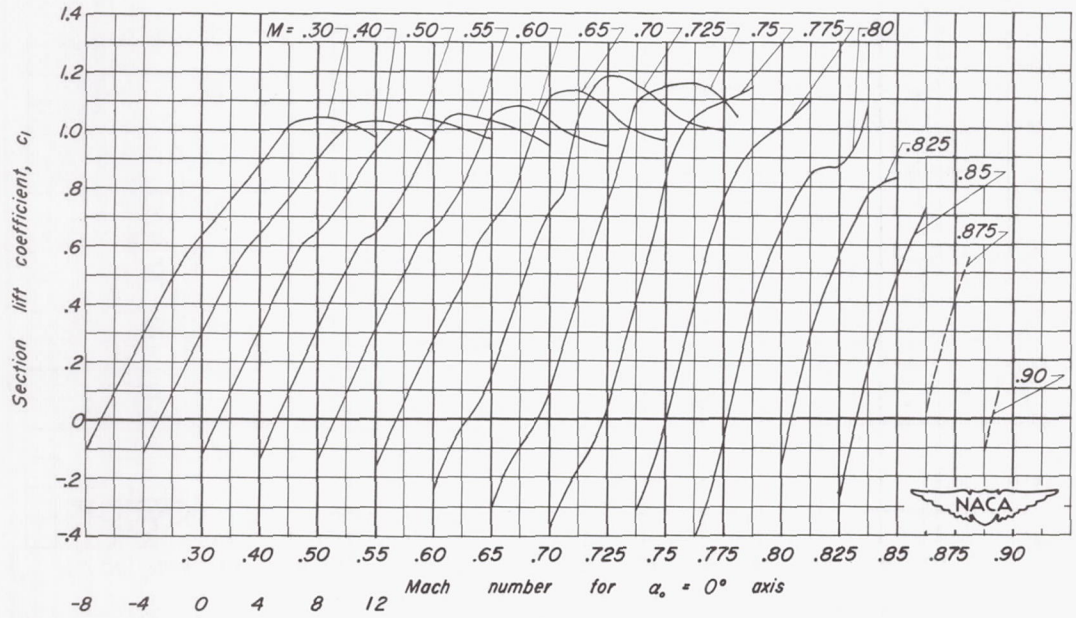

(n) δ_f, 12.1°

Figure 16.- Continued.

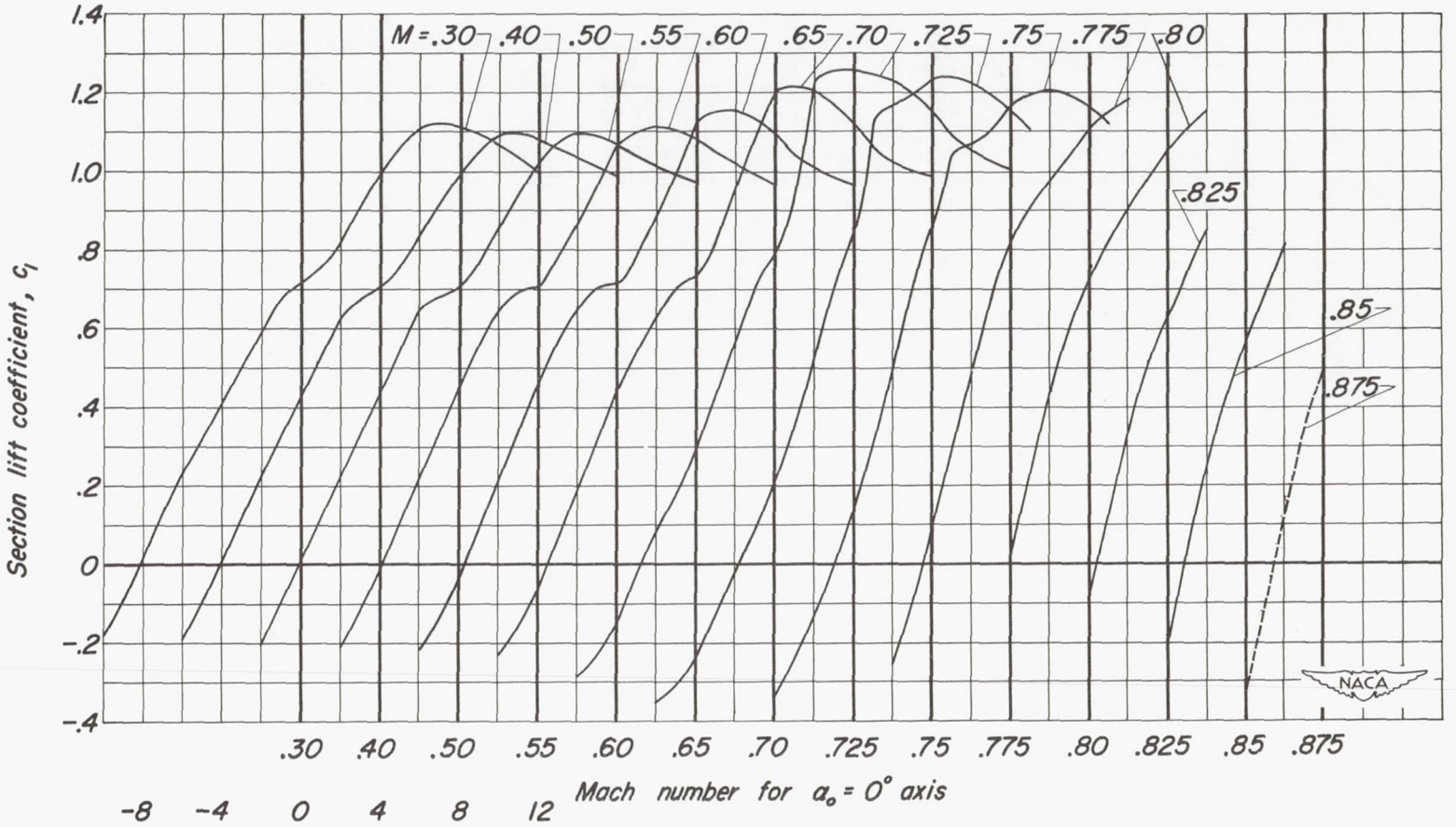

(o) δ_f, 14.4°

Figure 16. – Concluded.

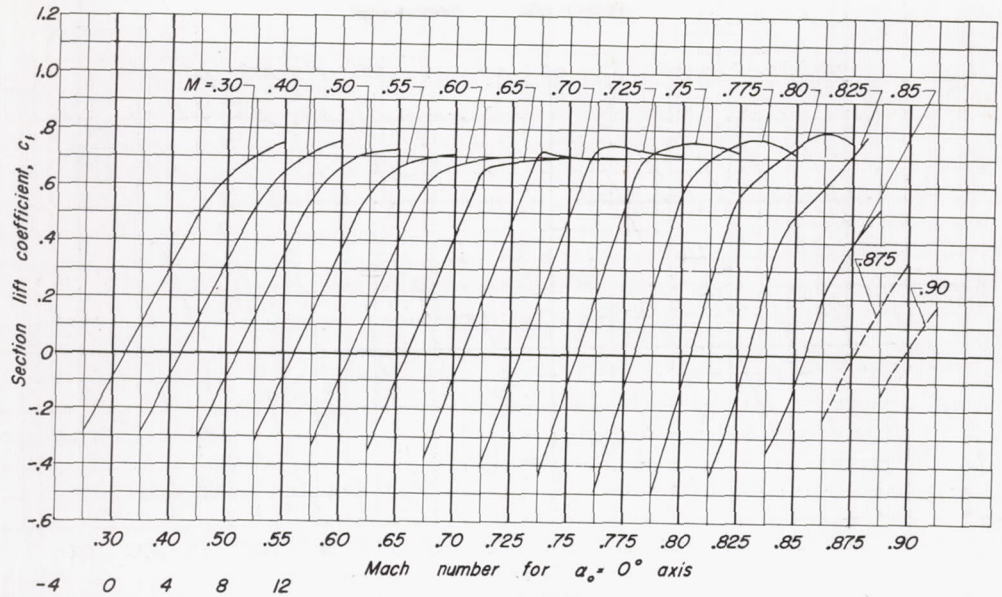

(a) δ_f, -1.3°

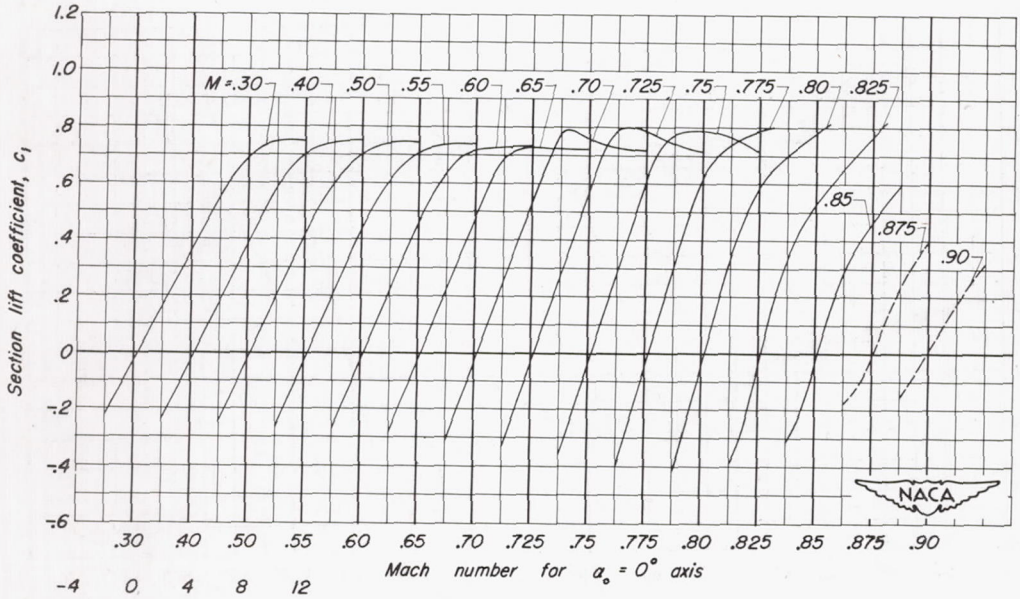

(b) δ_f, -0.5°

Figure 17.– Variation of section lift coefficient with angle of attack at various Mach numbers for the NACA 0010-0.70 40/1.051 airfoil section with a 25-percent-chord plain flap.

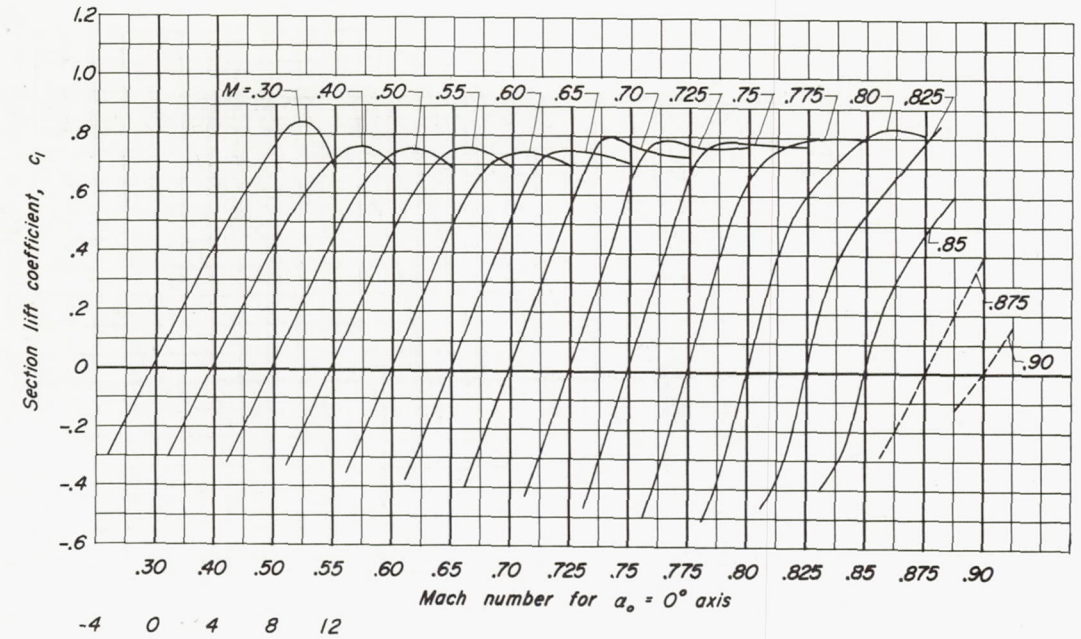

(c) δ_f, 0°

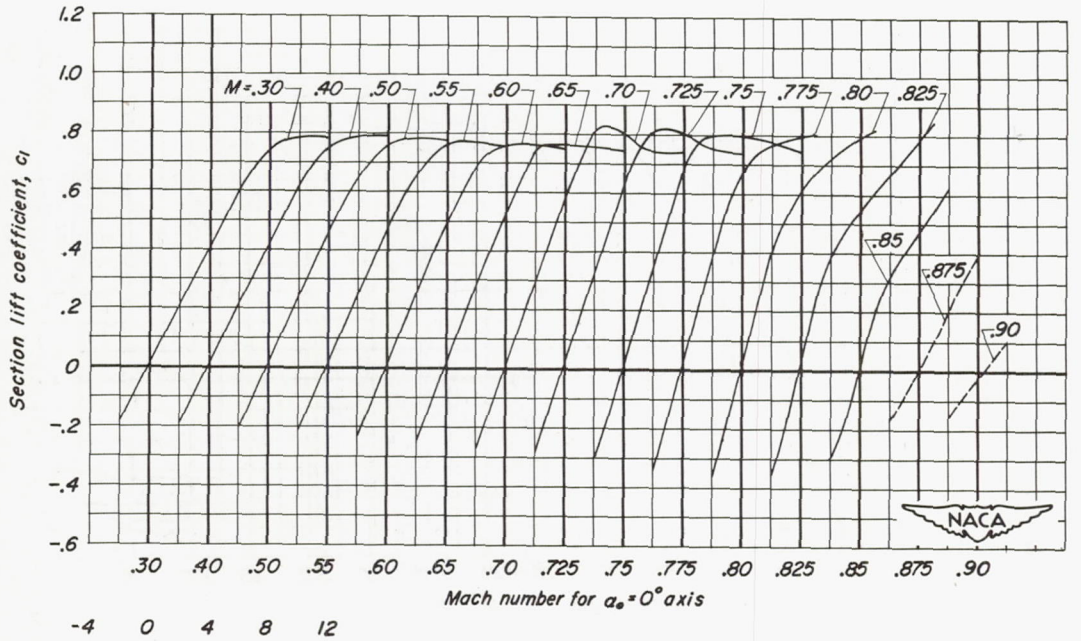

(d) δ_f, 0.5°

Figure 17.- Continued.

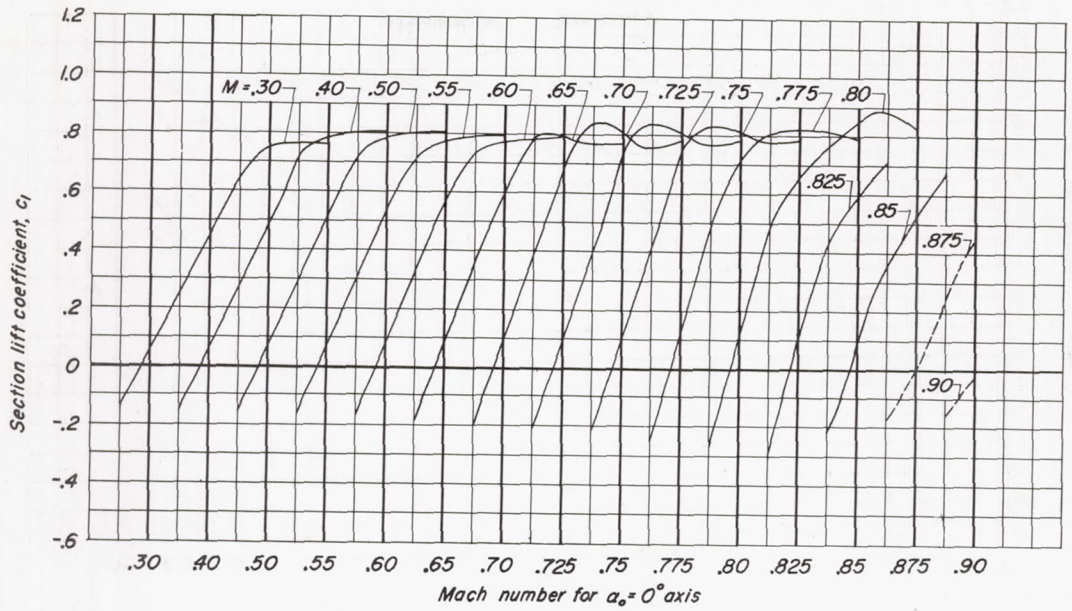

(e) δ_f, 1.3°

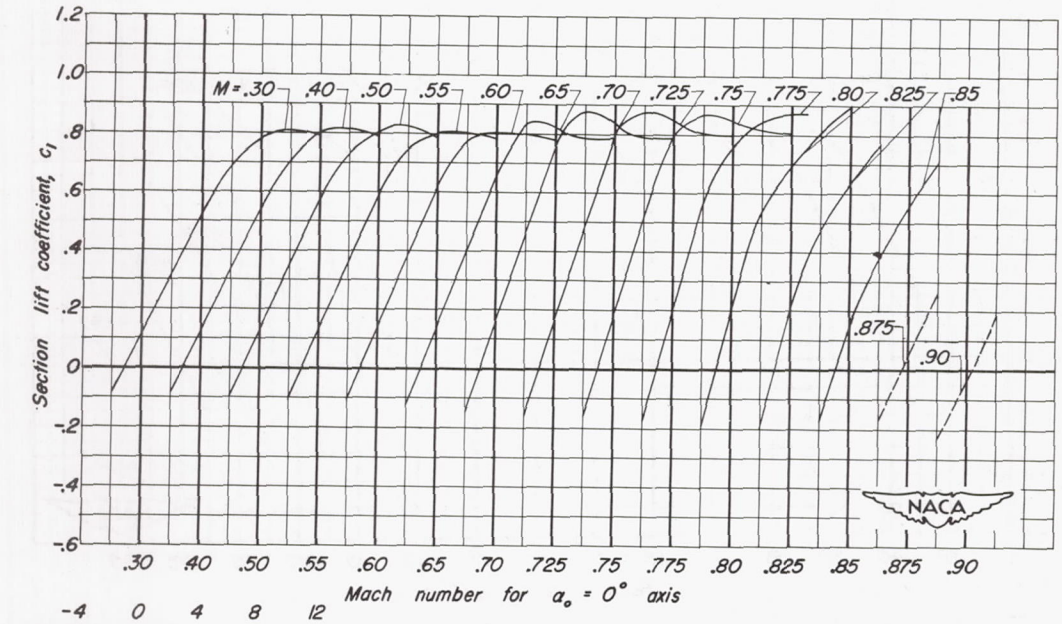

(f) δ_f, 2.3°

Figure 17.– Continued.

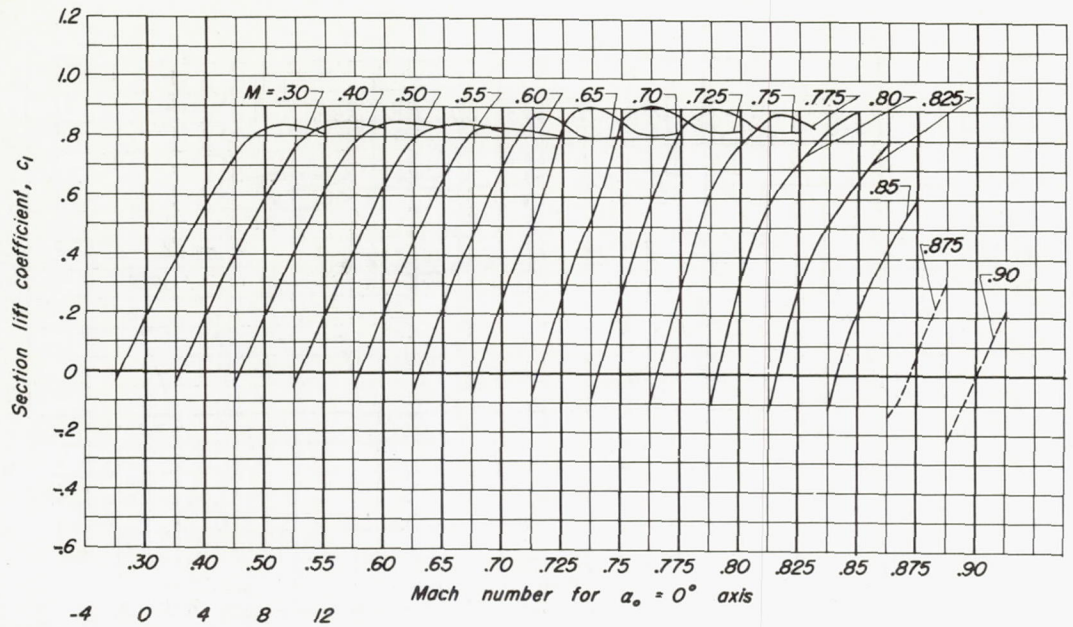

(g) δ_f, 3.0°

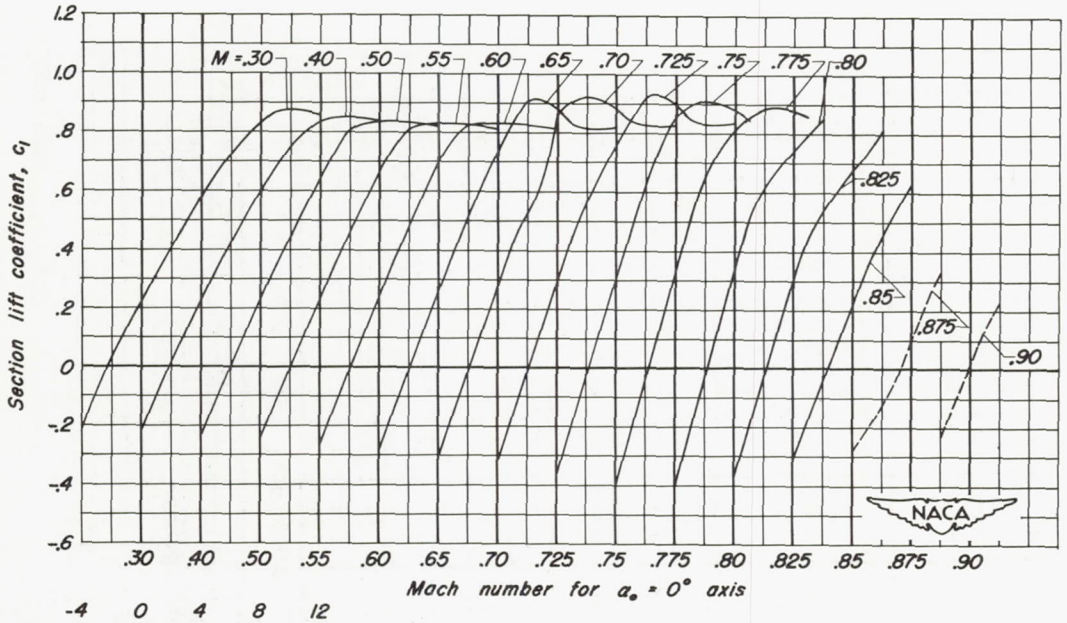

(h) δ_f, 3.7°

Figure 17.– Continued.

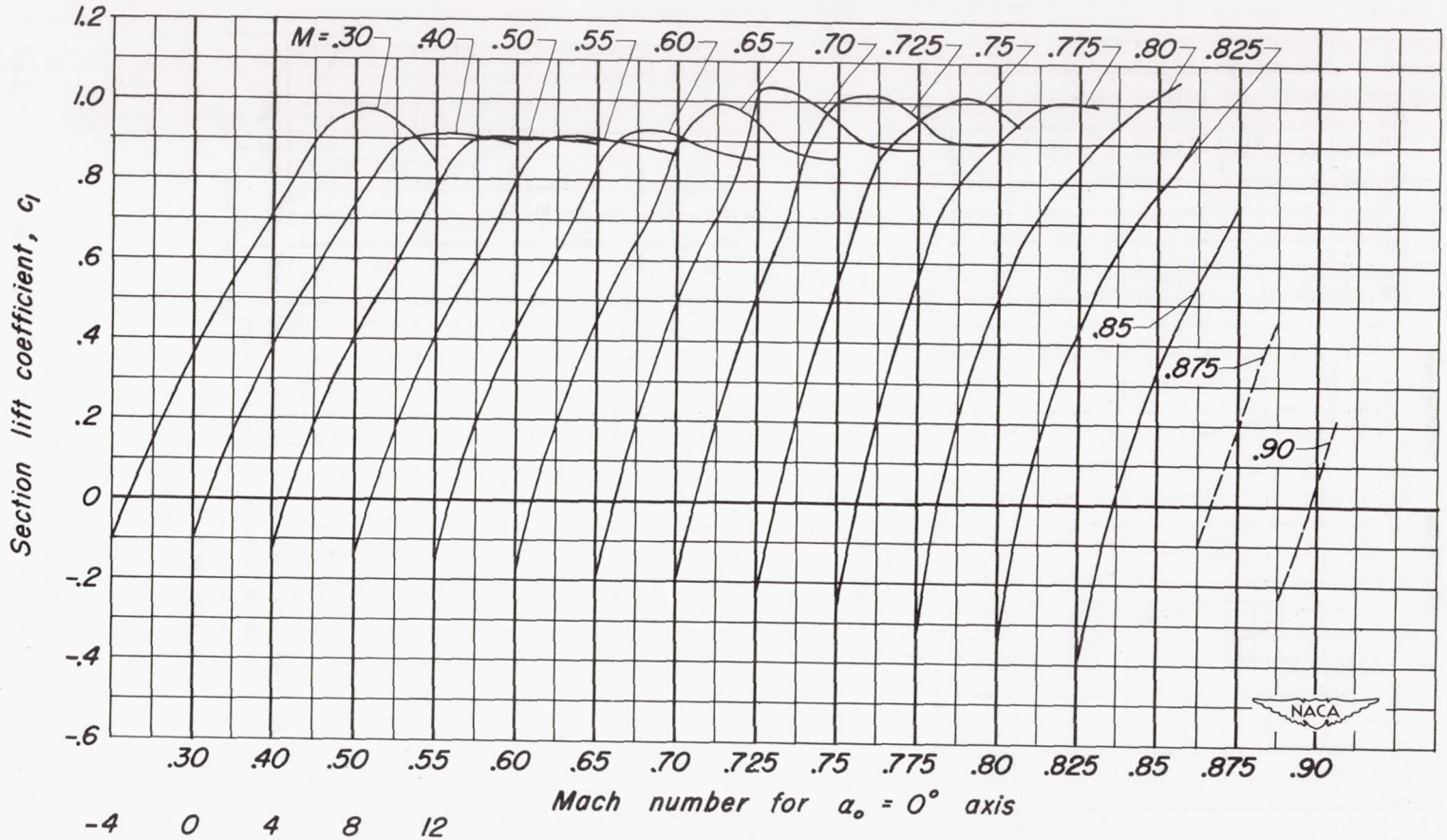

(i) δ_f, 6.1°

Figure 17.– Concluded.

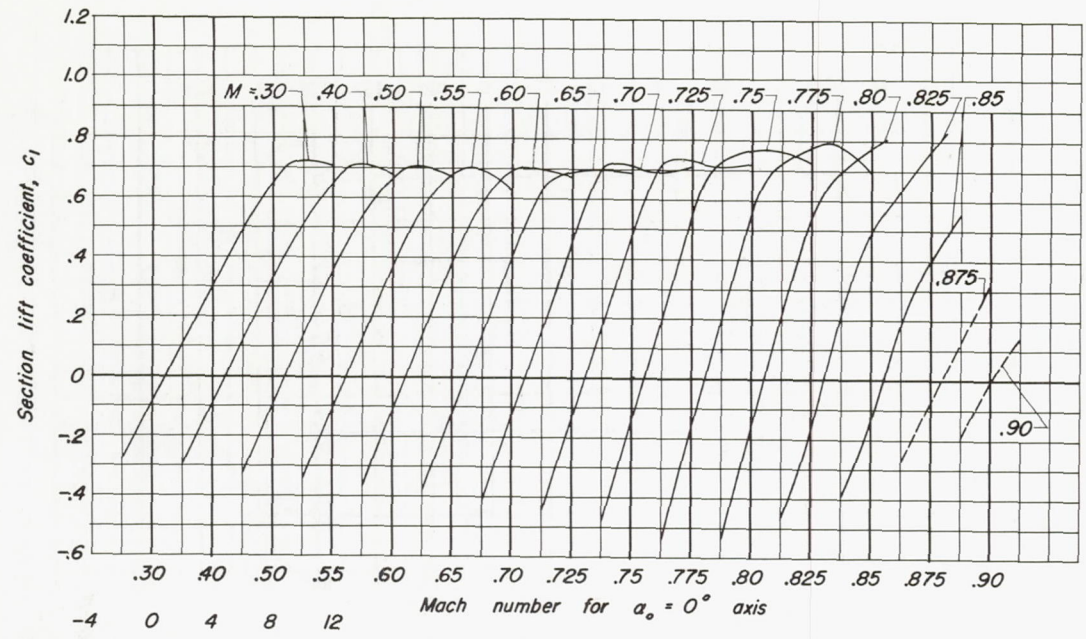

(a) δ_f, -1.2°

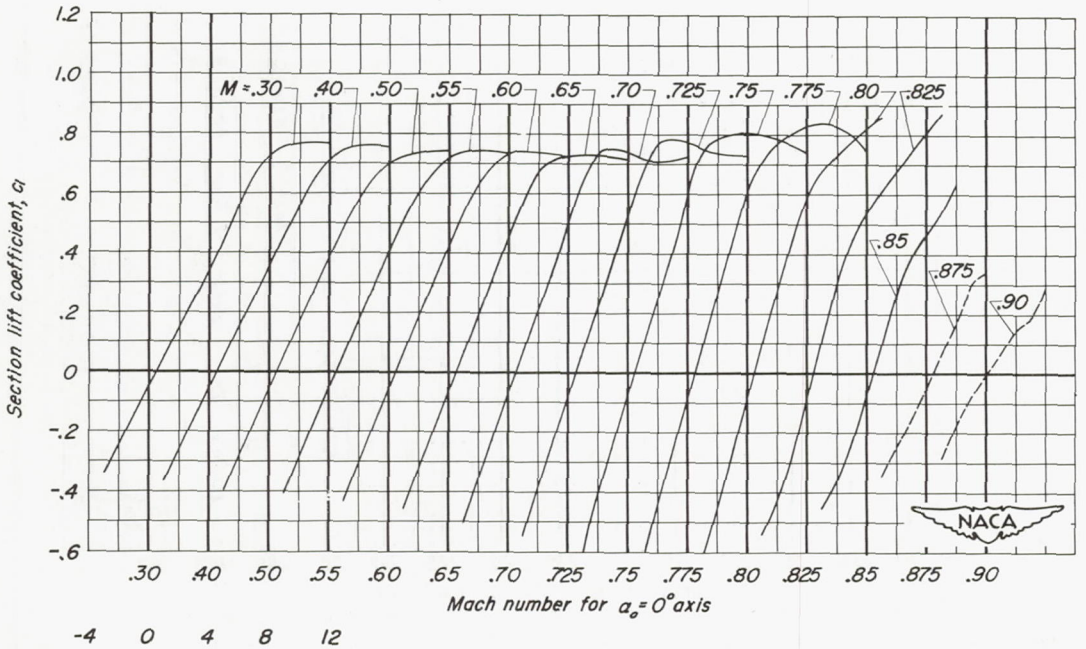

(b) δ_f, -0.5°

Figure 18.– Variation of section lift coefficient with angle of attack at various Mach numbers for the NACA 0010-0.70 40/0.524 airfoil section with a 25-percent-chord plain flap.

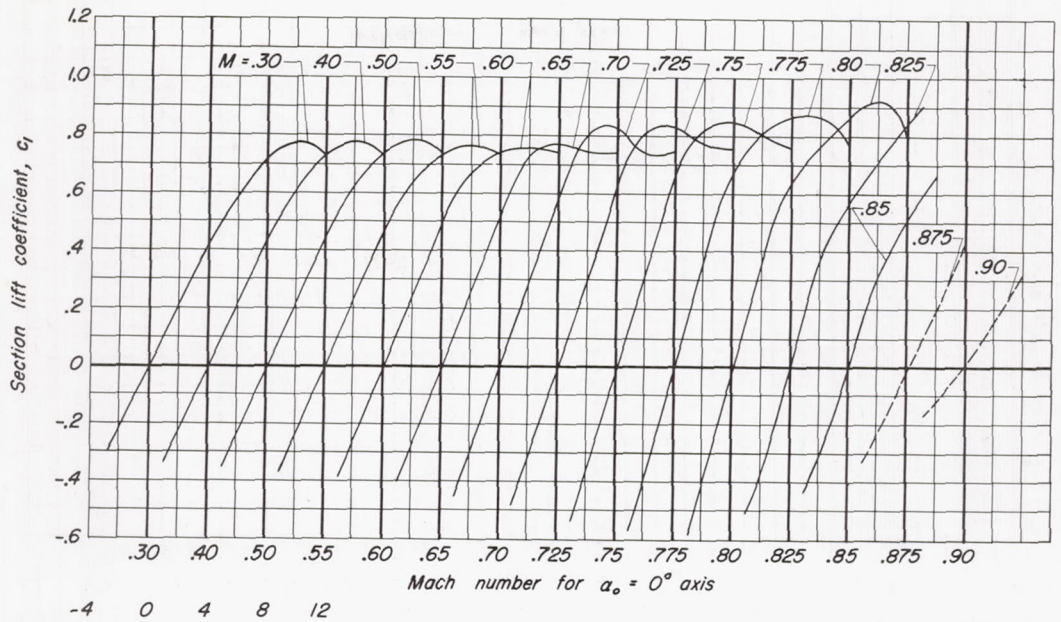

(c) δ_f, 0°

(d) δ_f, 0.5°

Figure 18.– Continued.

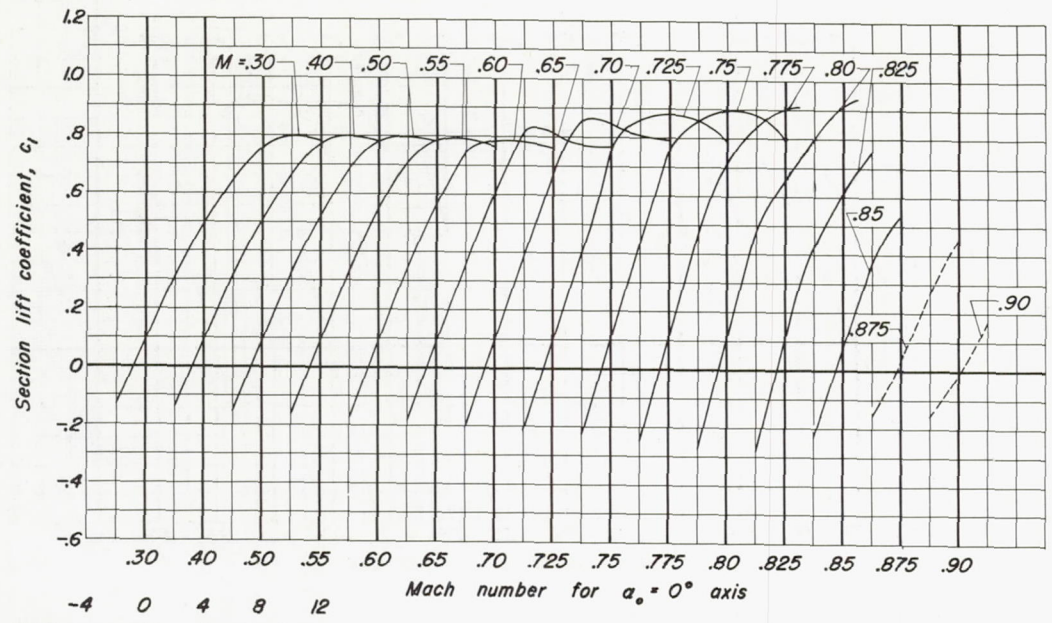

(e) δ_f, 1.2°

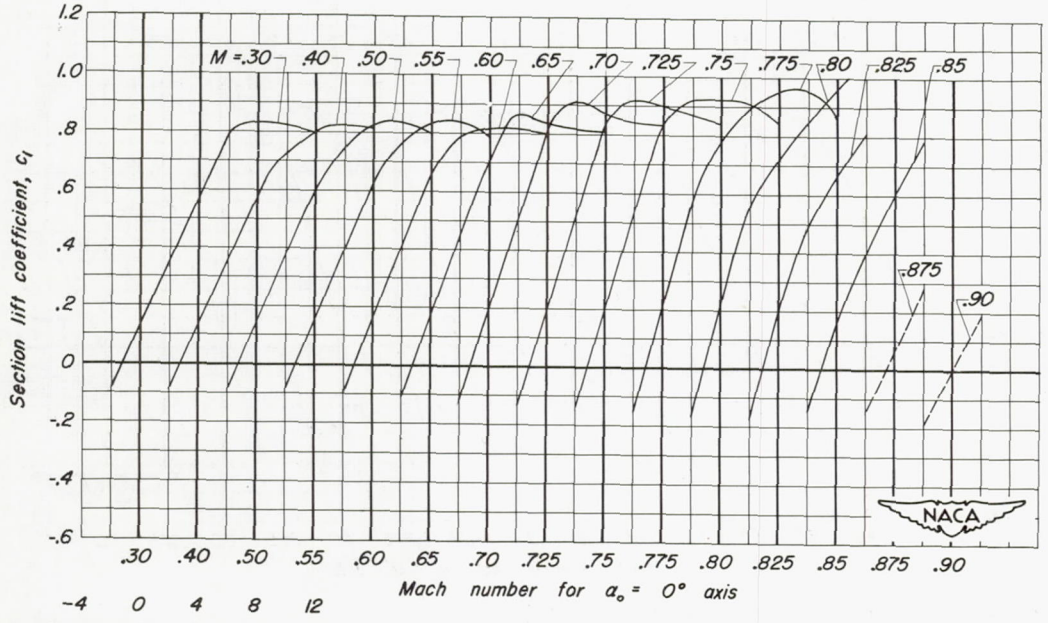

(f) δ_f, 2.3°

Figure 18.- Continued.

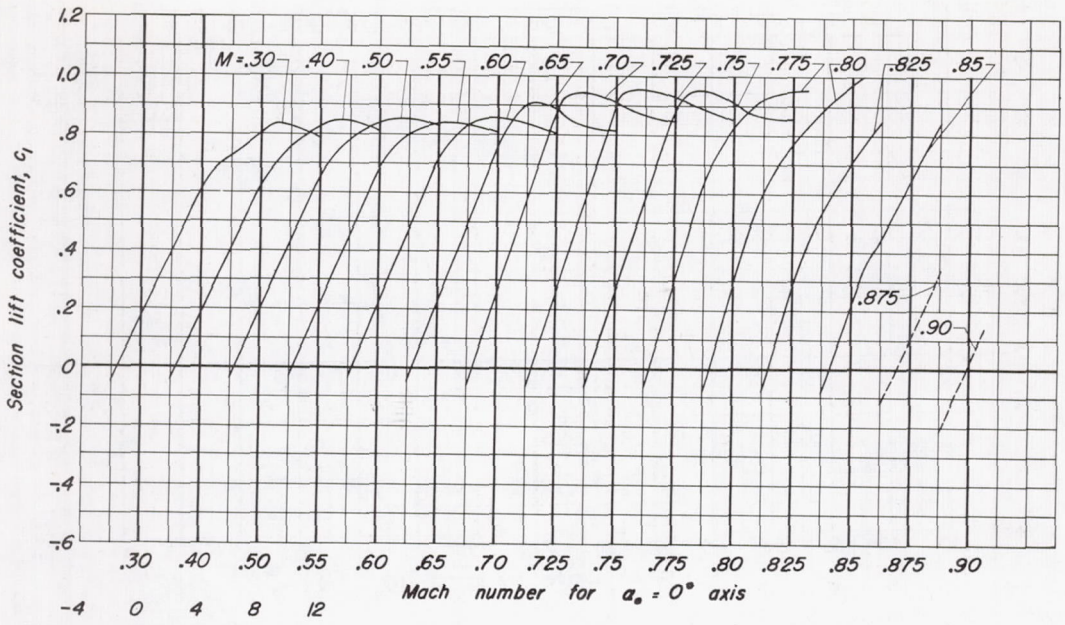

(g) δ_f, 3.4°

(h) δ_f, 4.2°.

Figure 18.- Continued.

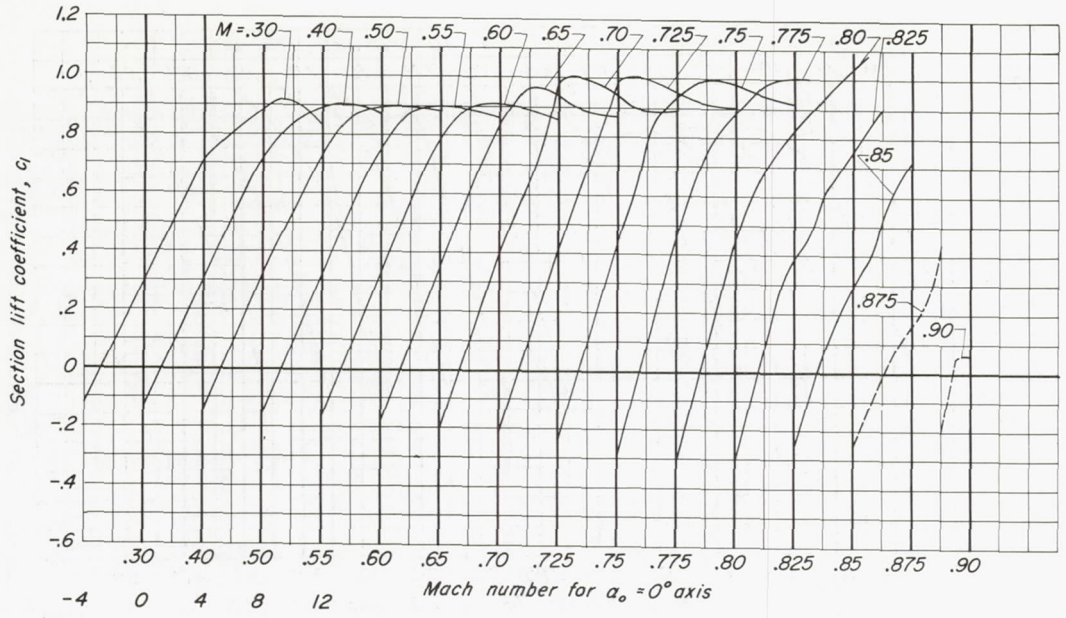

(i) δ_f, 5.0°

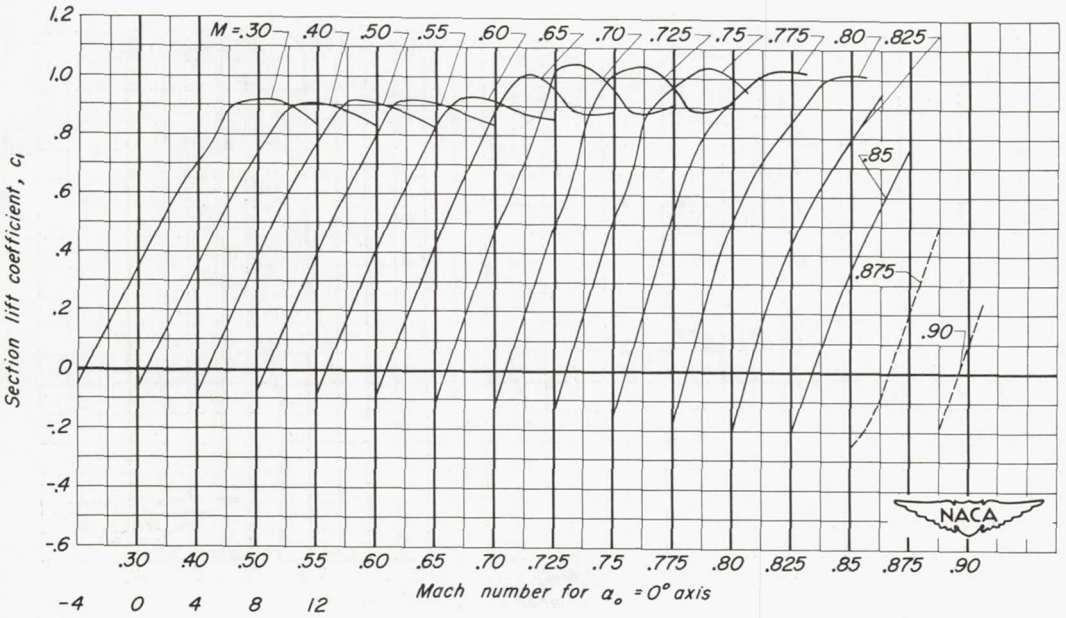

(j) δ_f, 6.0°

Figure 18. – Concluded.

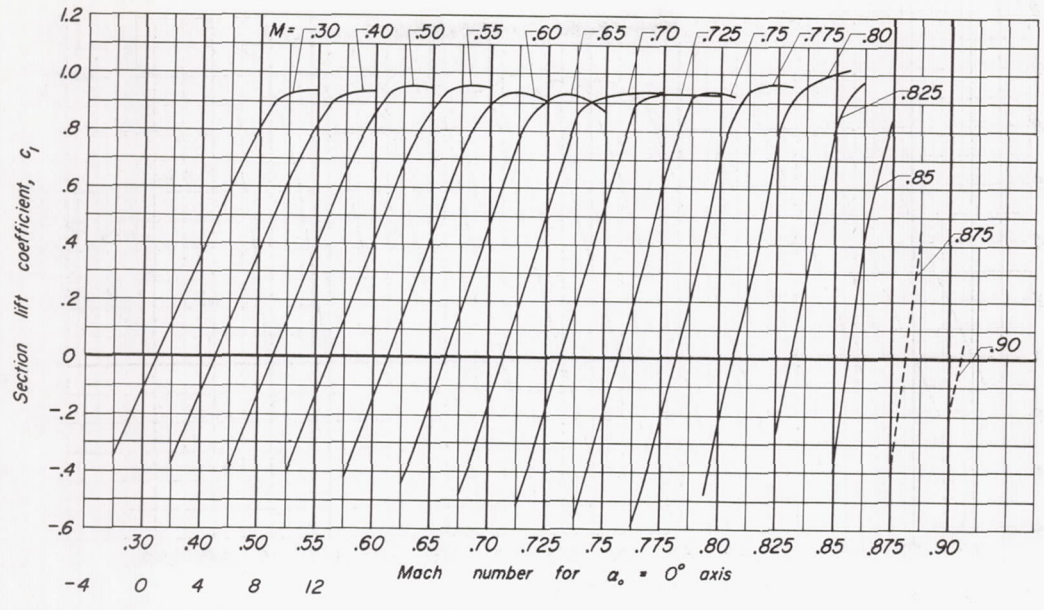

(a) δ_f, -1.2°

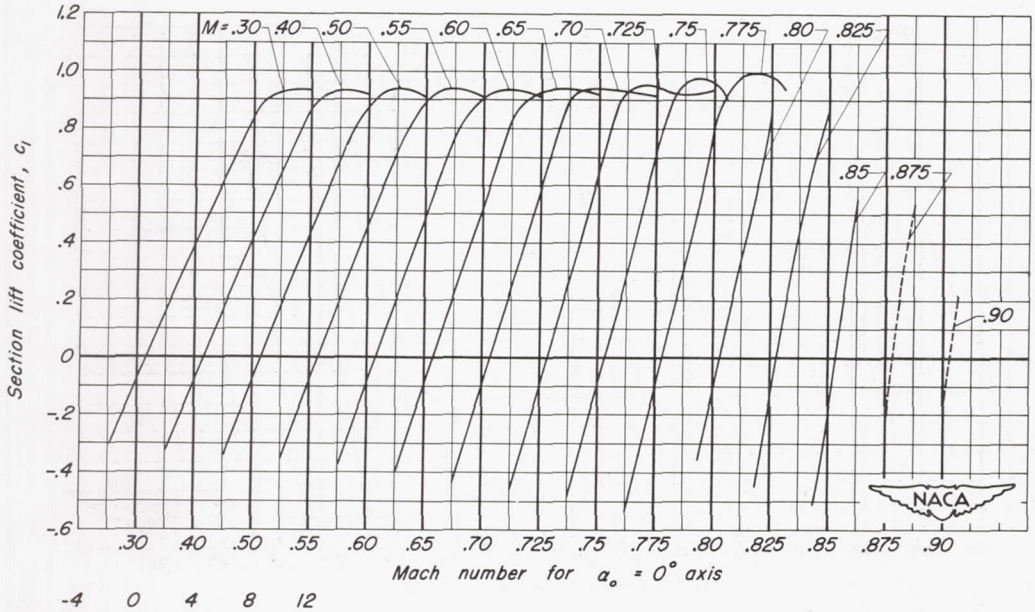

(b) δ_f, -0.4°

Figure 19.- Variation of section lift coefficient with angle of attack at various Mach numbers for the NACA 0010-0.70 40/1.575 (modification A) airfoil section with a 25-percent-chord plain flap.

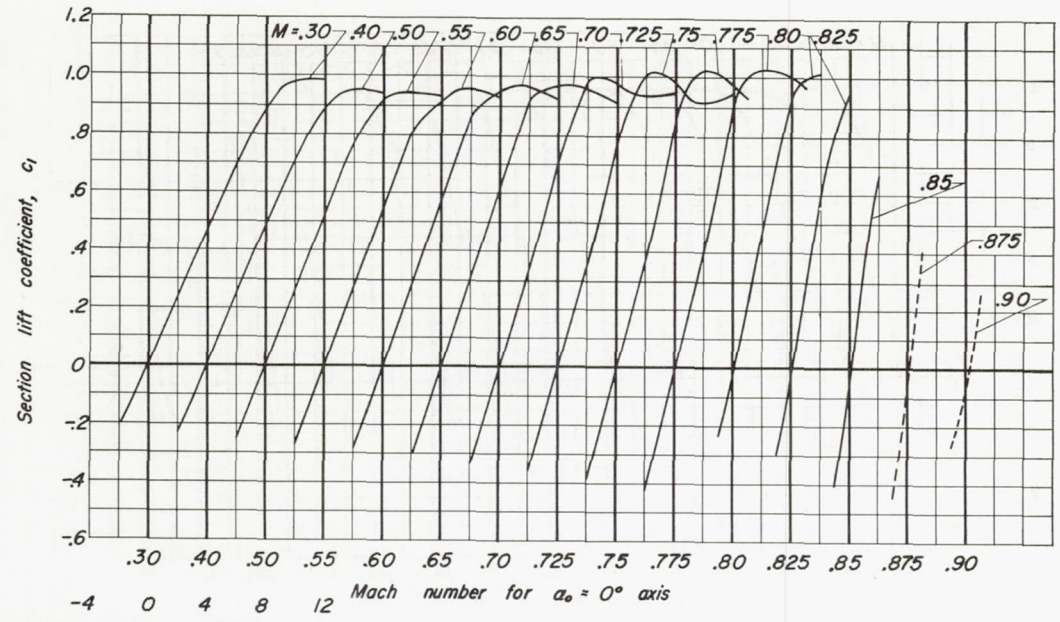

(c) δ_f, 0°

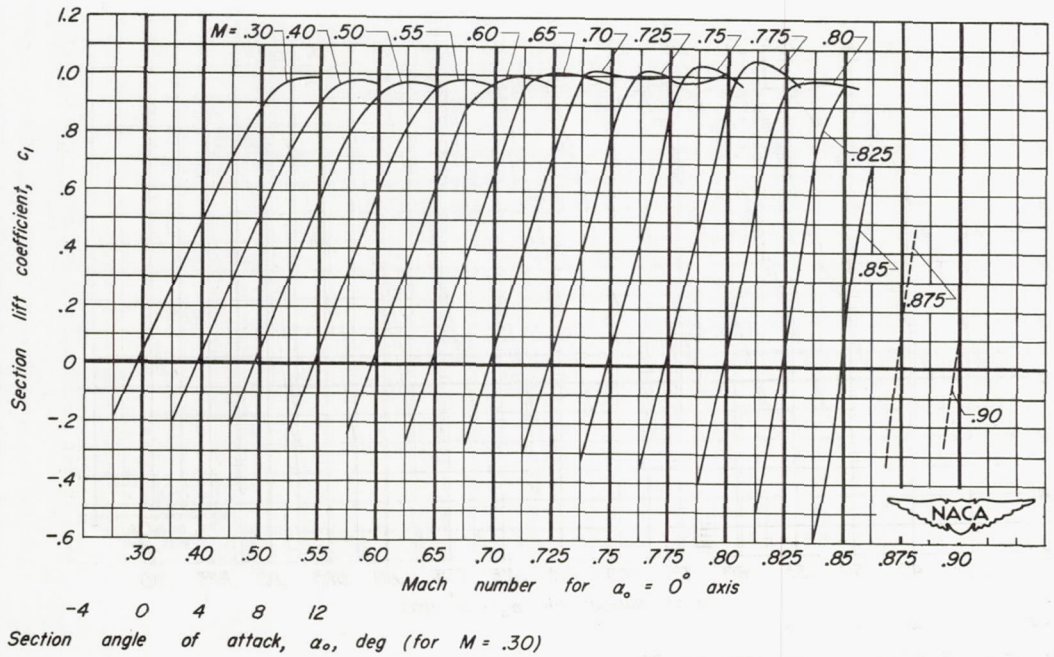

(d) δ_f, 0.4°

Figure 19.– Continued.

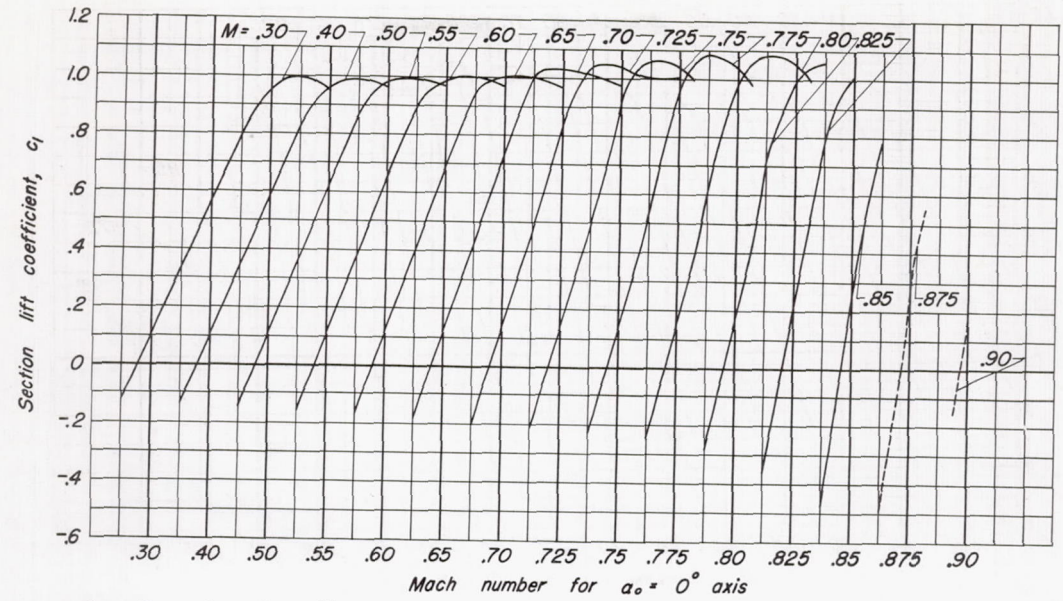

(e) δ_f, 1.2°

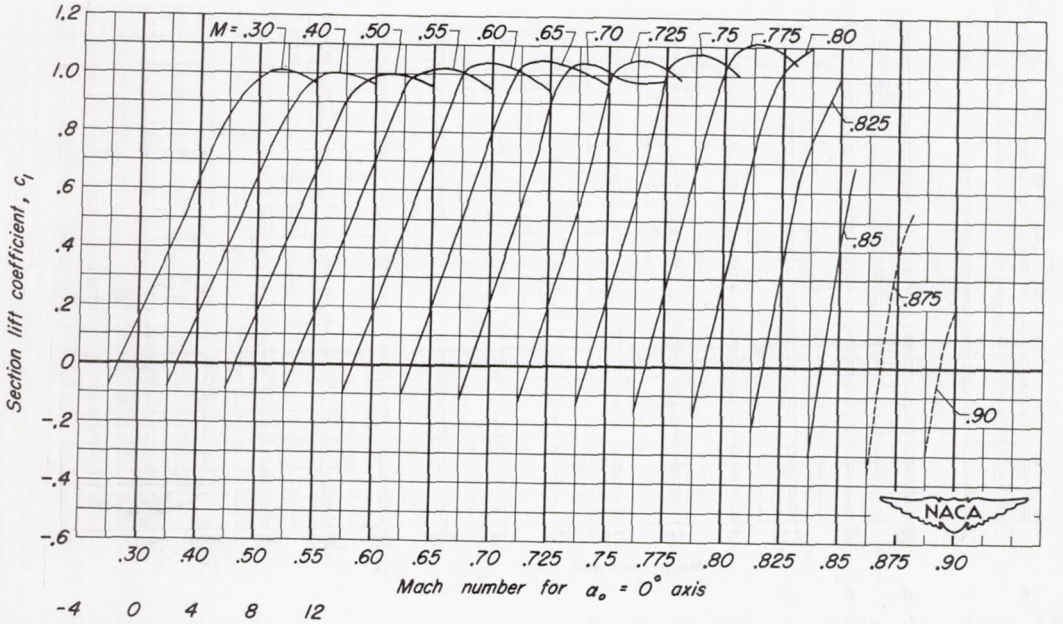

(f) δ_f, 2.0°

Figure 19.- Continued.

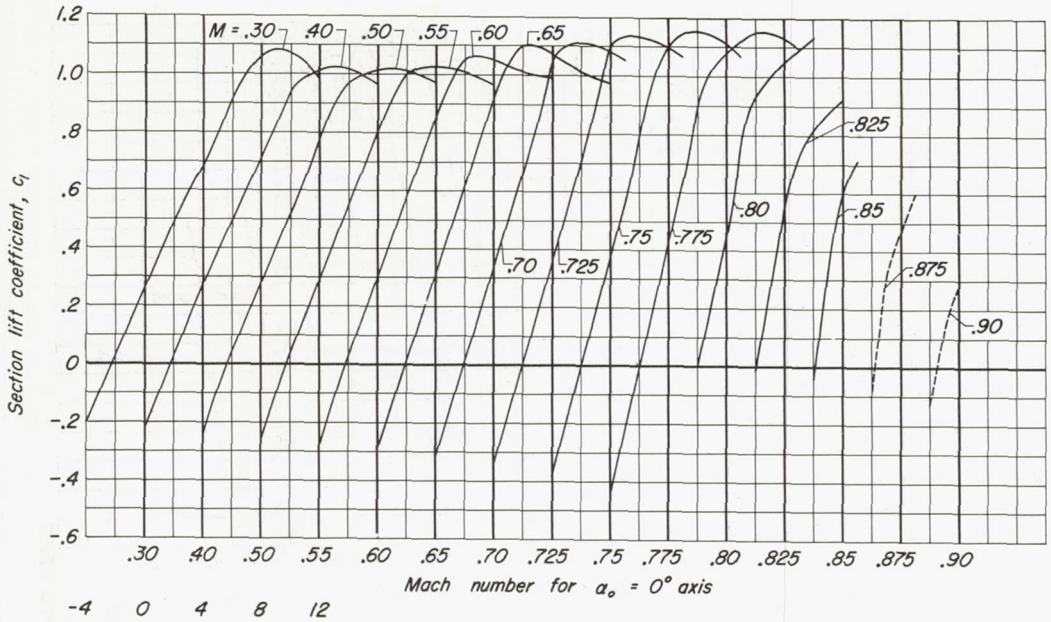

(g) δ_f, 3.2°

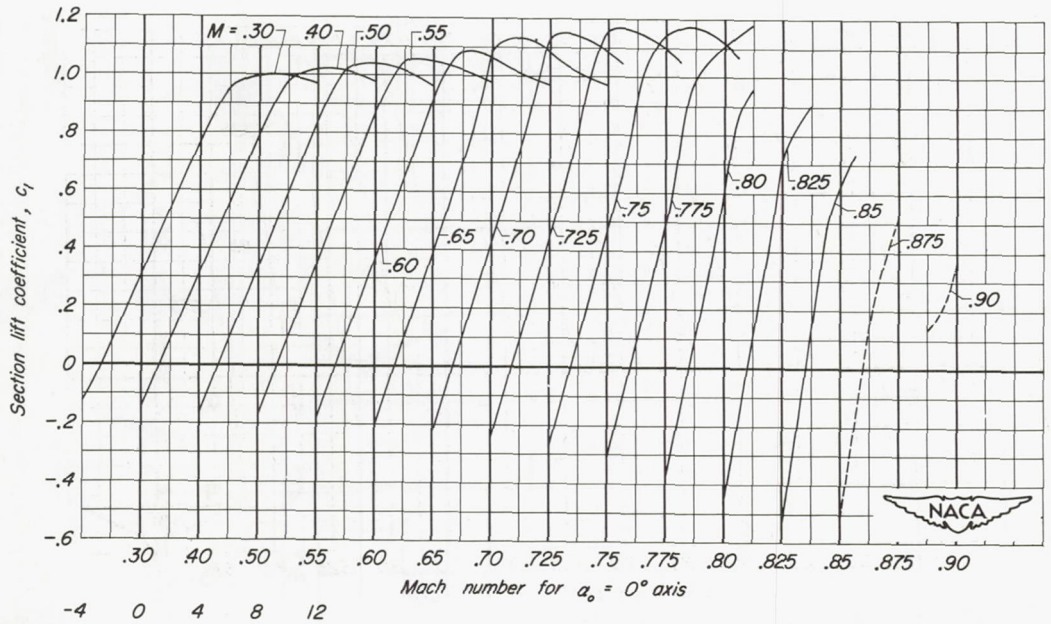

(h) δ_f, 4.2°

Figure 19.- Continued.

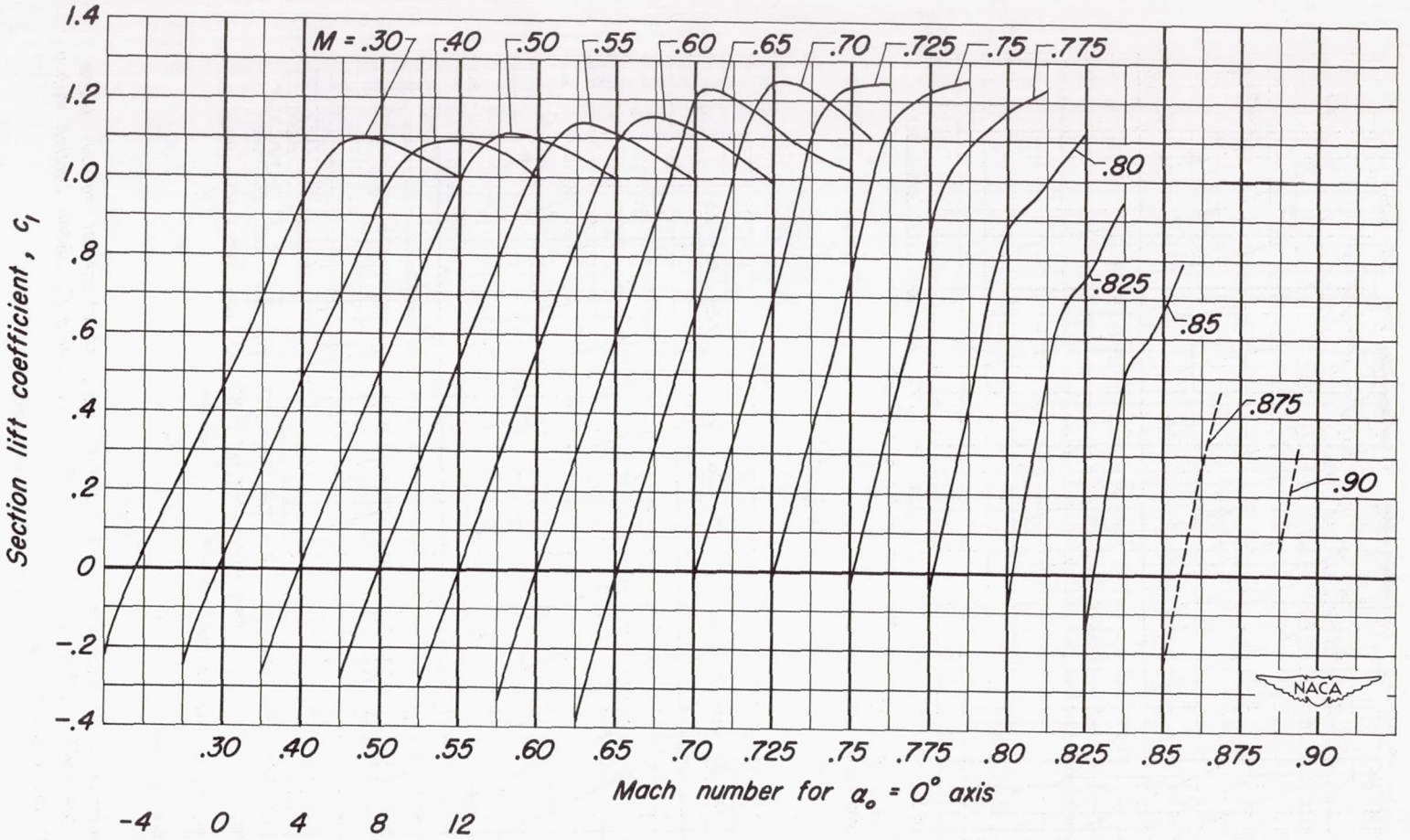

(i) δ_f, 6.8°

Figure 19.- Concluded.

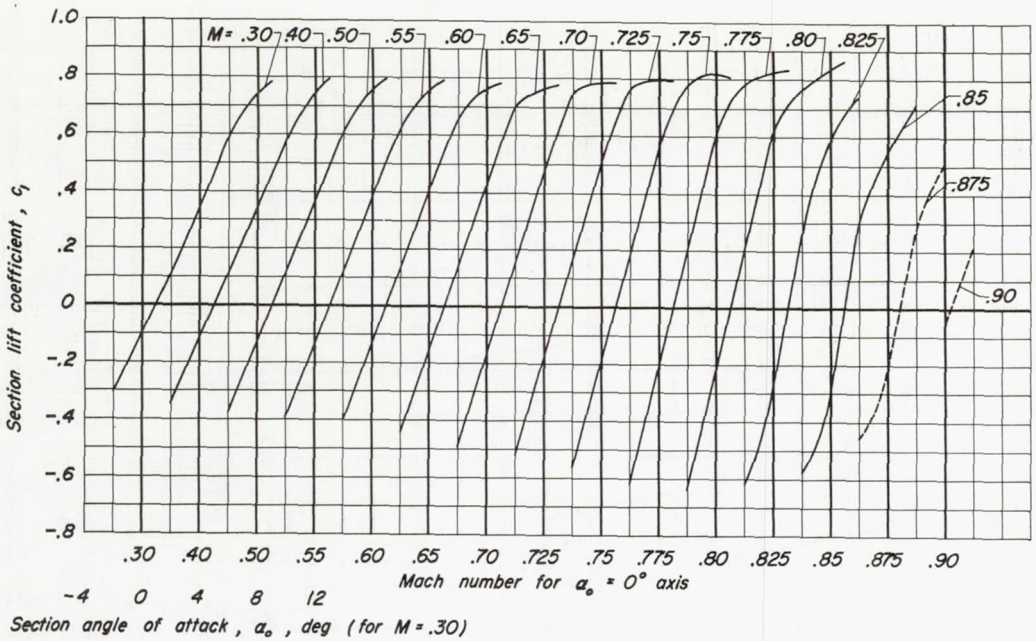

(a) δ_f, -1.5°

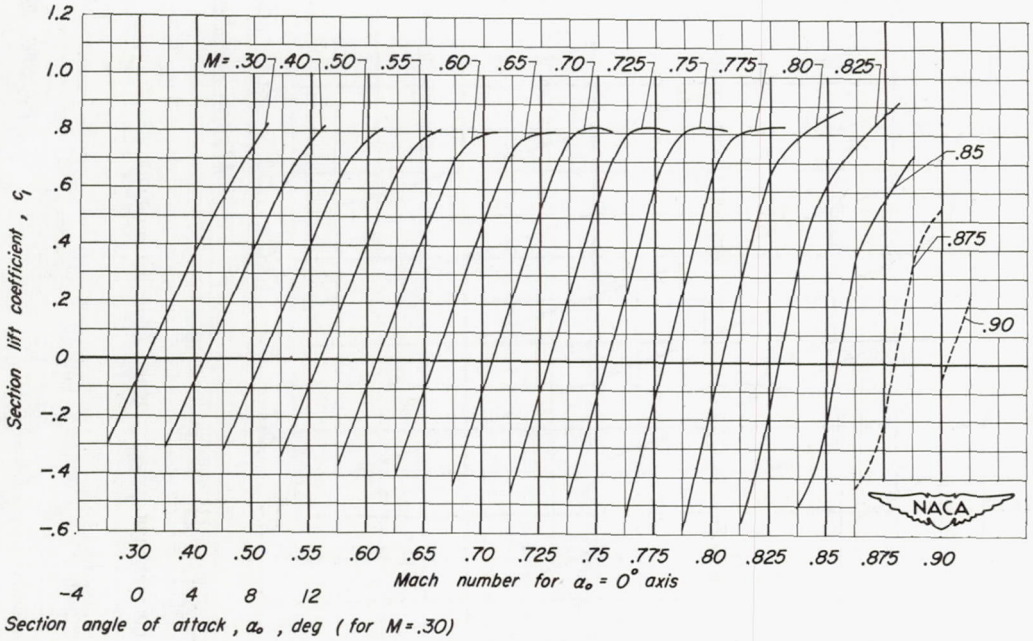

(b) δ_f, -0.6°

Figure 20.- Variation of section lift coefficient with angle of attack at various Mach numbers for the NACA 0010-0.70 40/1.575 (modification B) airfoil section with a 25-percent-chord plain flap.

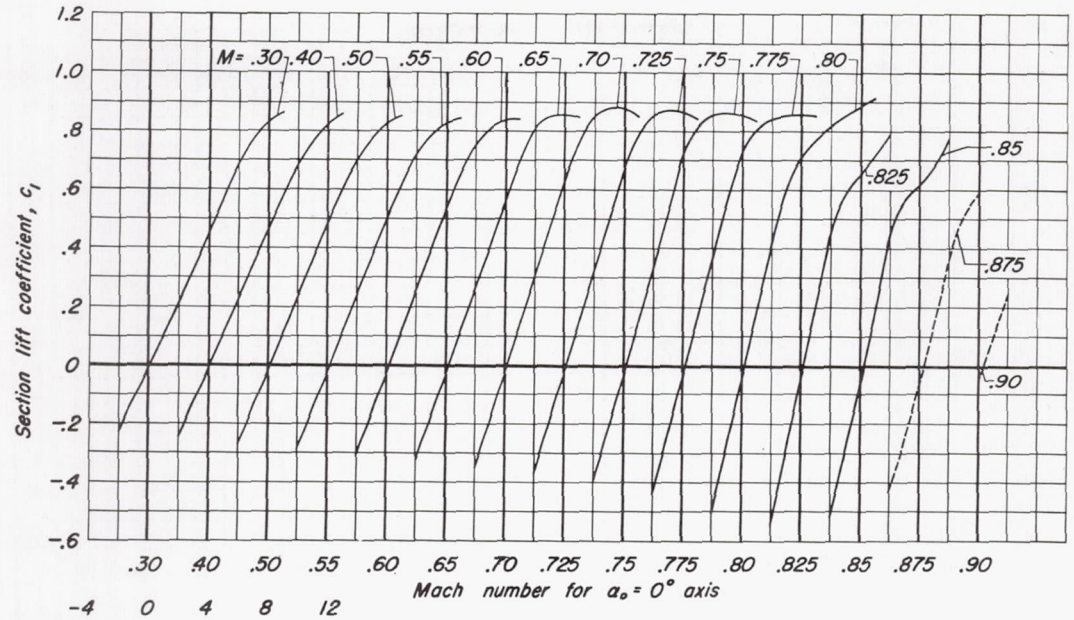

(c) δ_f, 0°

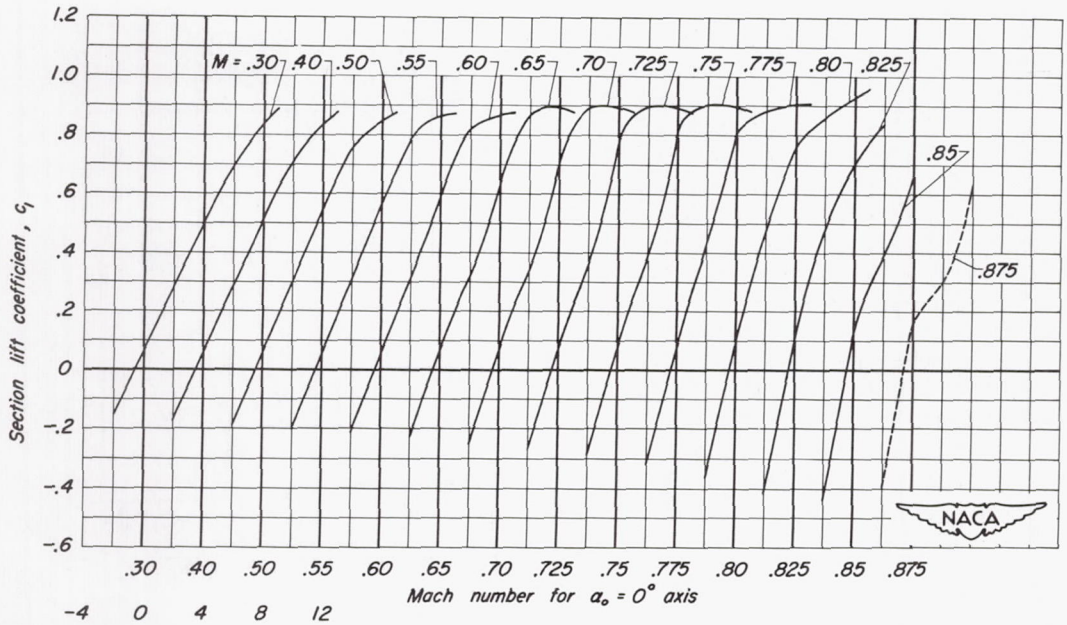

(d) δ_f, 0.6°

Figure 20.- Continued.

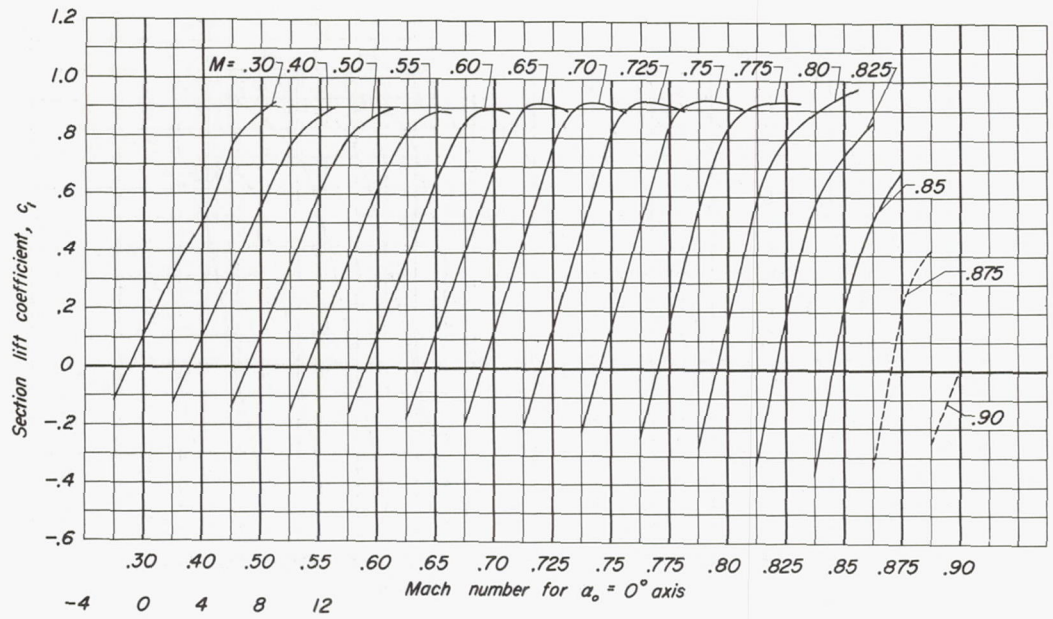

(e) δ_f, 1.5°

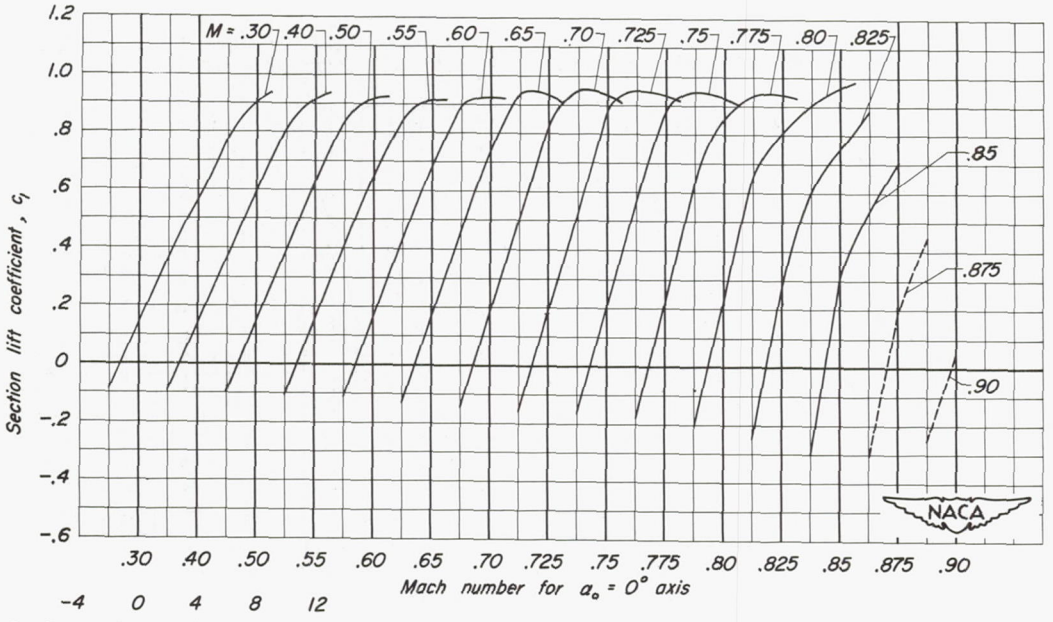

(f) δ_f, 2.3°

Figure 20.- Continued.

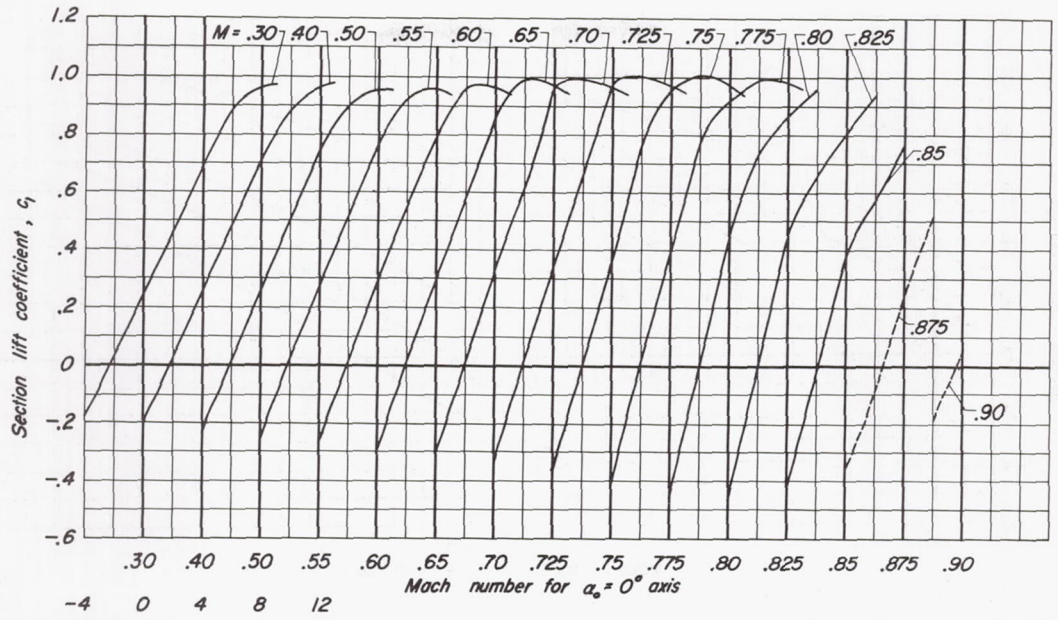

(g) δ_f, 4.0°

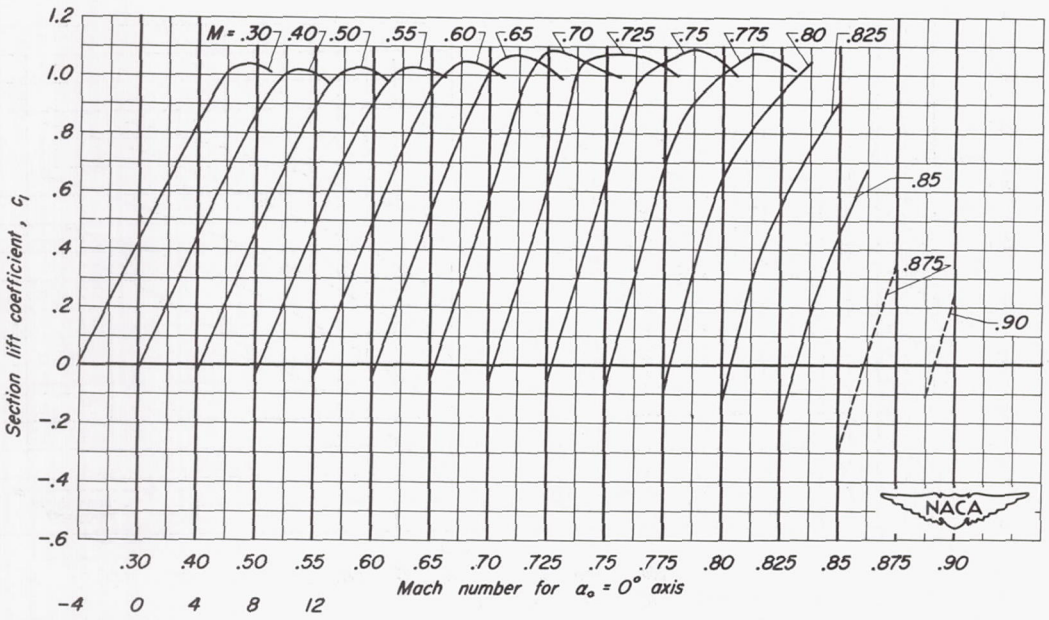

(h) δ_f, 6.5°

Figure 20.- Concluded.

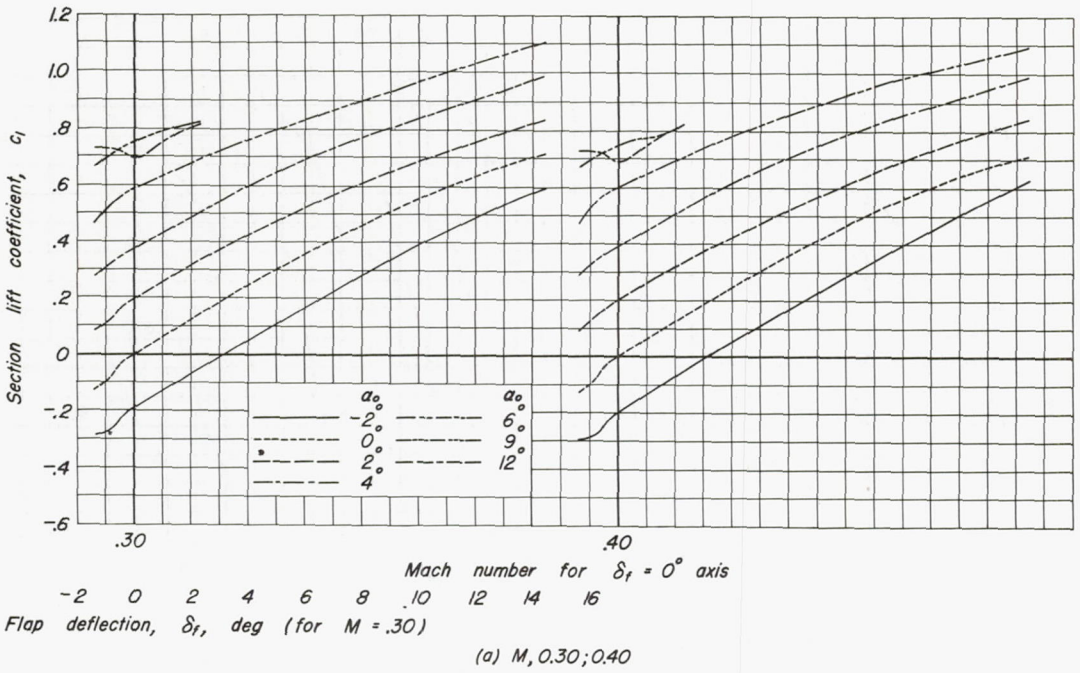

(a) M, 0.30; 0.40

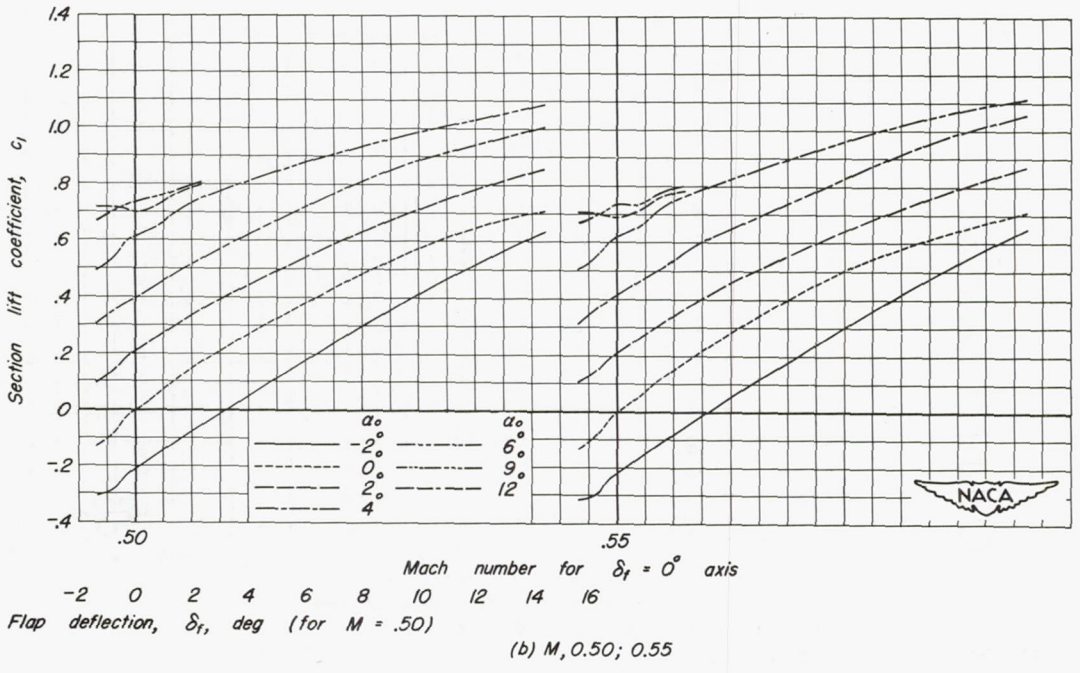

(b) M, 0.50; 0.55

Figure 21.– Variation of section lift coefficient with flap deflection at various Mach numbers for the NACA 0010 – 0.70 40/1.575 airfoil section with a 25-percent-chord plain flap.

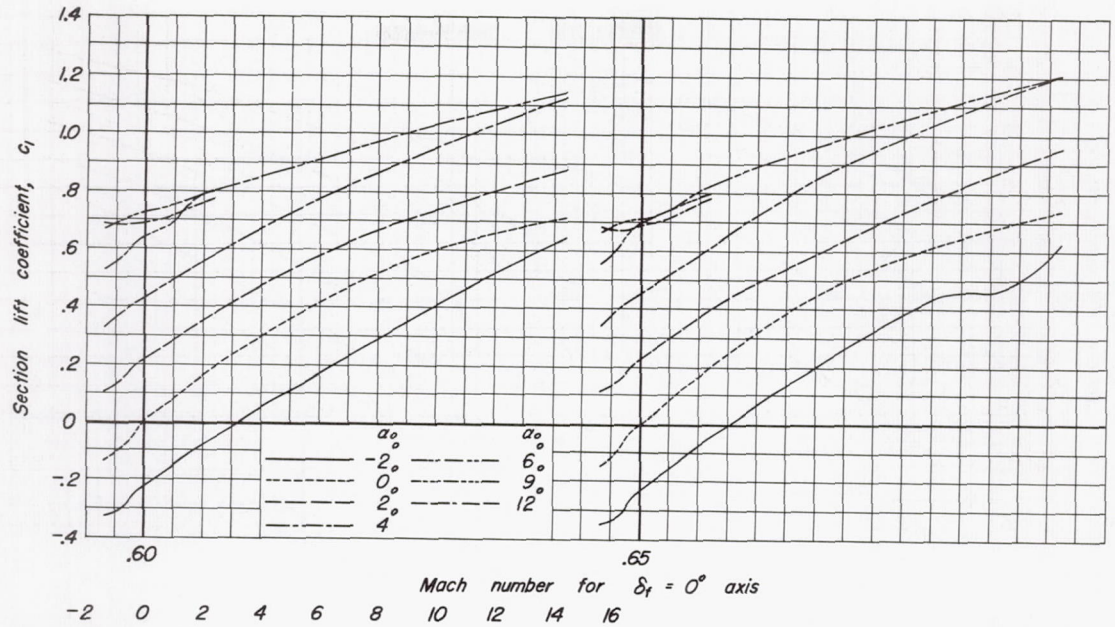

(c) M, 0.60 ; 0.65

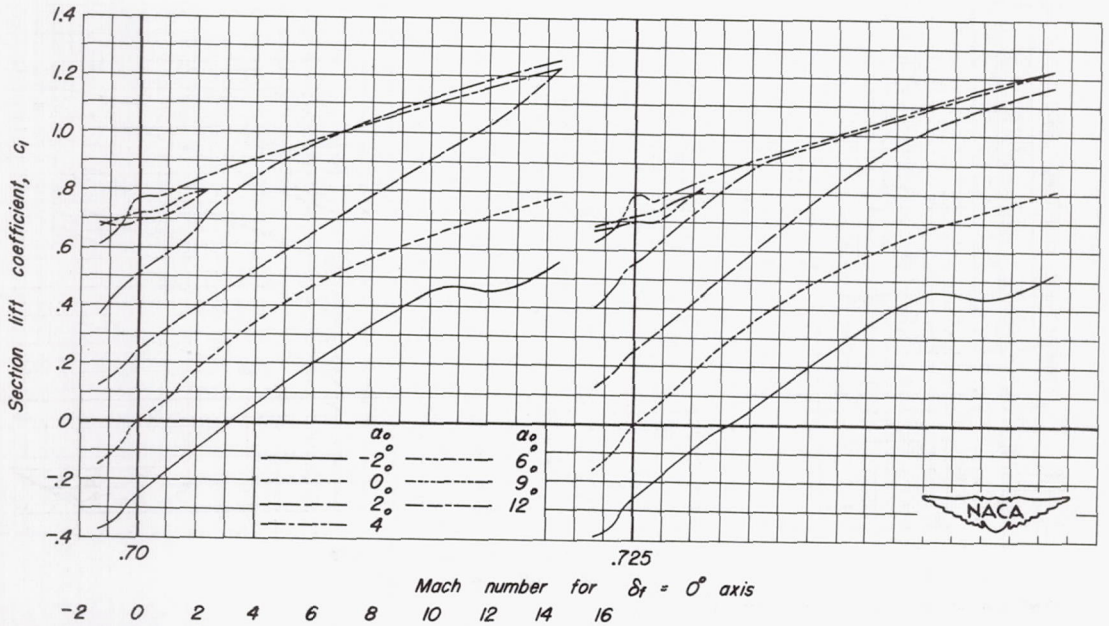

(d) M, 0.70; 0.725

Figure 21.- Continued.

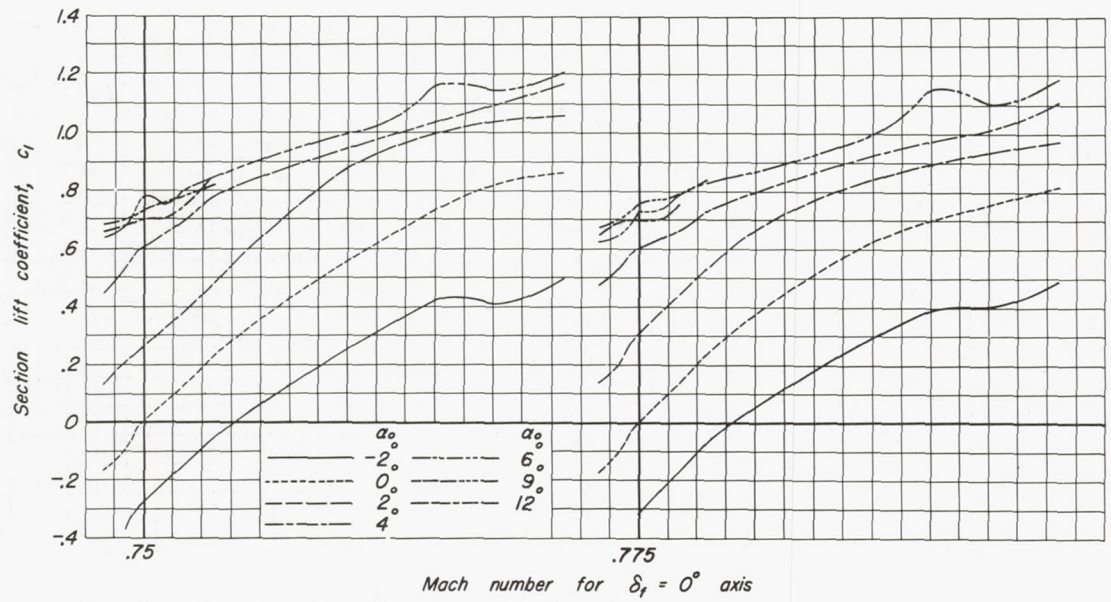

(e) M, 0.75 ; 0.775

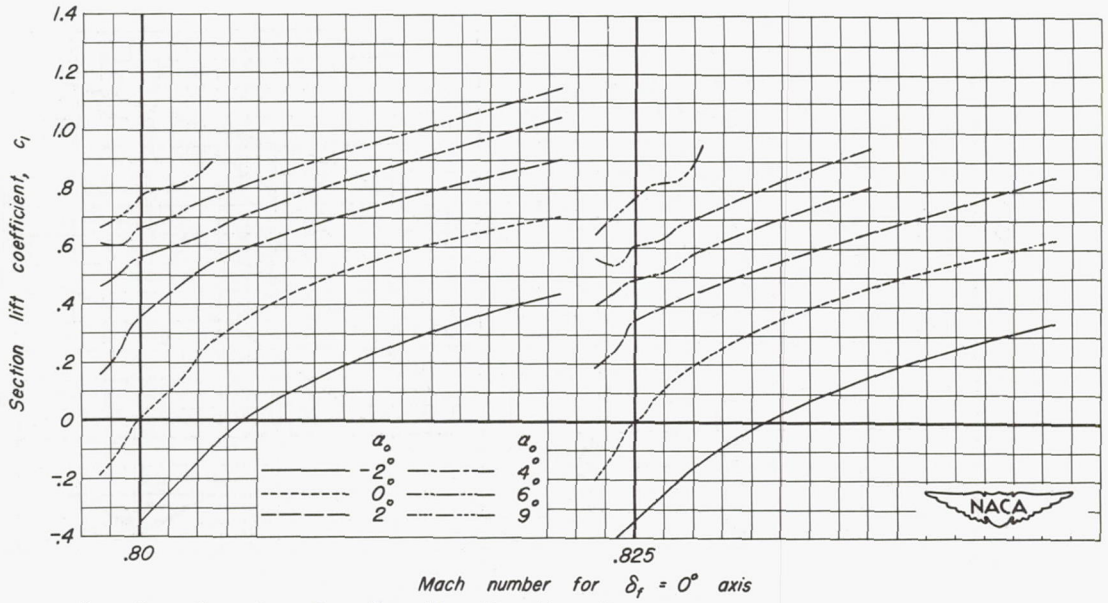

(f) M, 0.80; 0.825

Figure 21.- Continued.

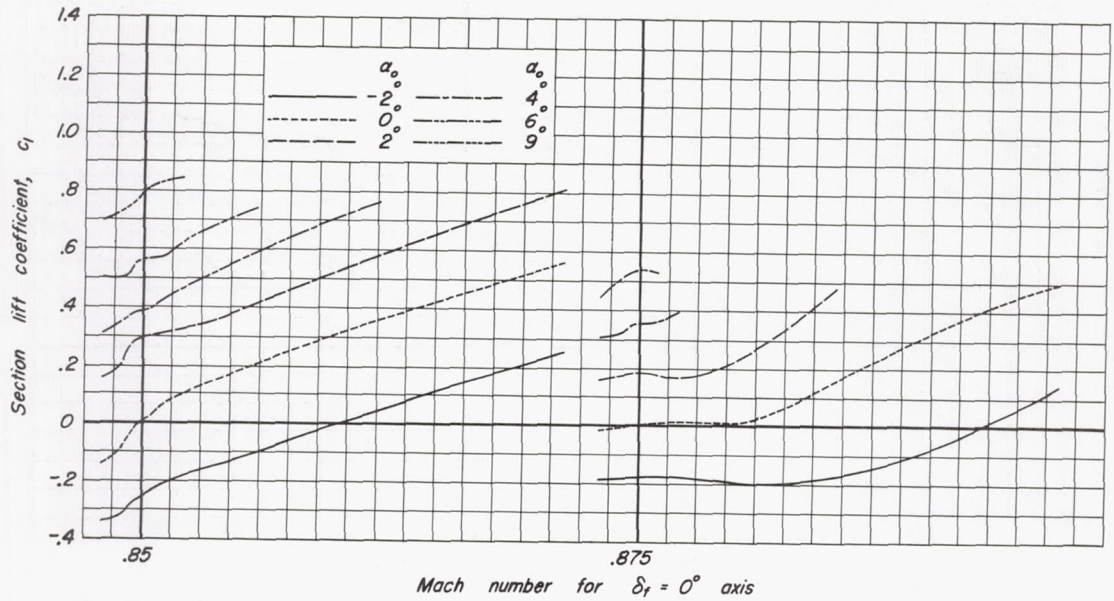

(g) M, 0.85 ; 0.875

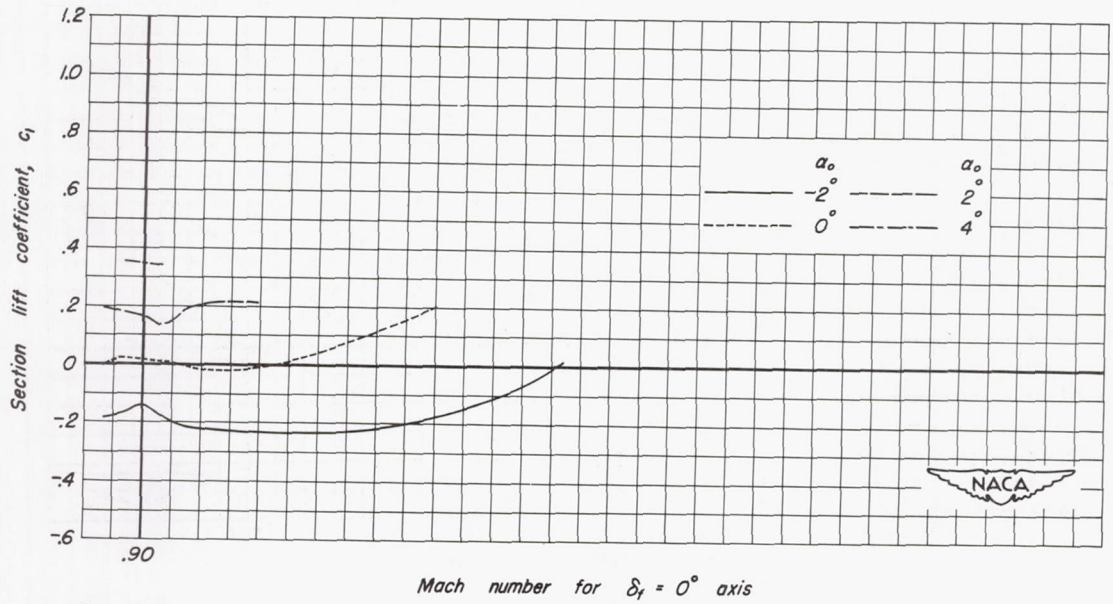

(h) M, 0.90

Figure 21.- Concluded.

(a) M,0.30;0.40;0.50;0.55

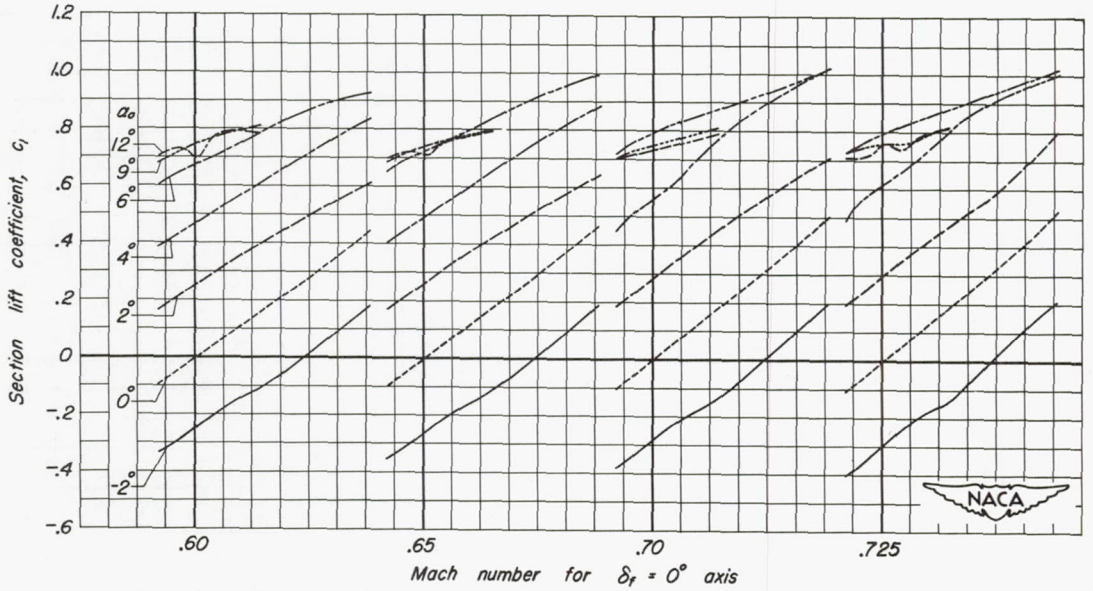

(b) M,0.60;0.65;0.70;0.725

Figure 22.- Variation of section lift coefficient with flap deflection at various Mach numbers for the NACA 0010-0.70 40/1.051 airfoil section with a 25-percent-chord plain flap.

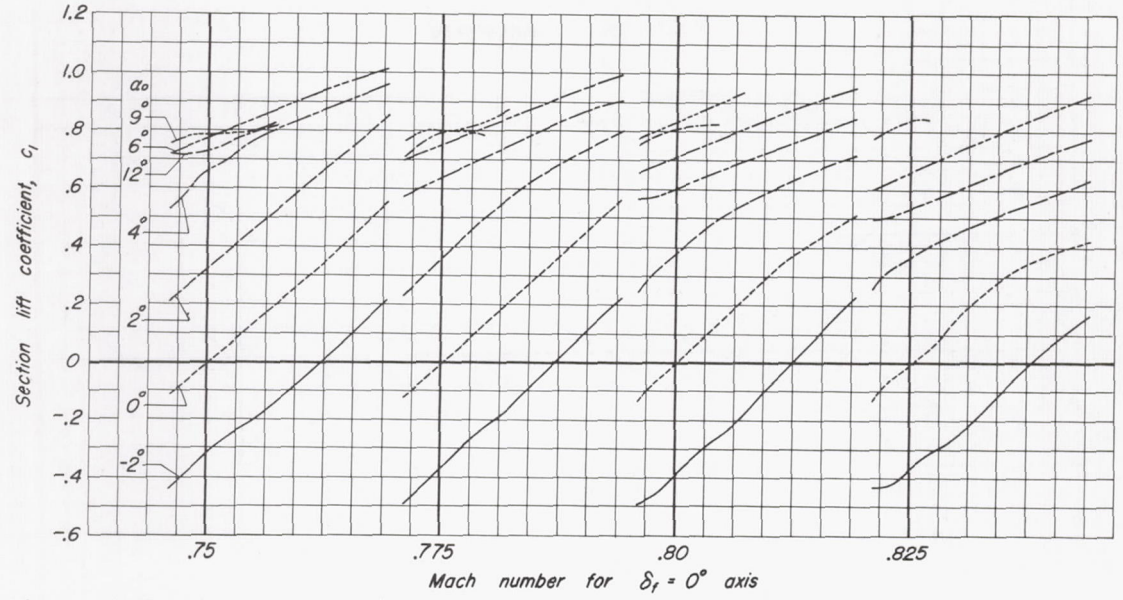

(c) M, 0.75; 0.775; 0.80; 0.825

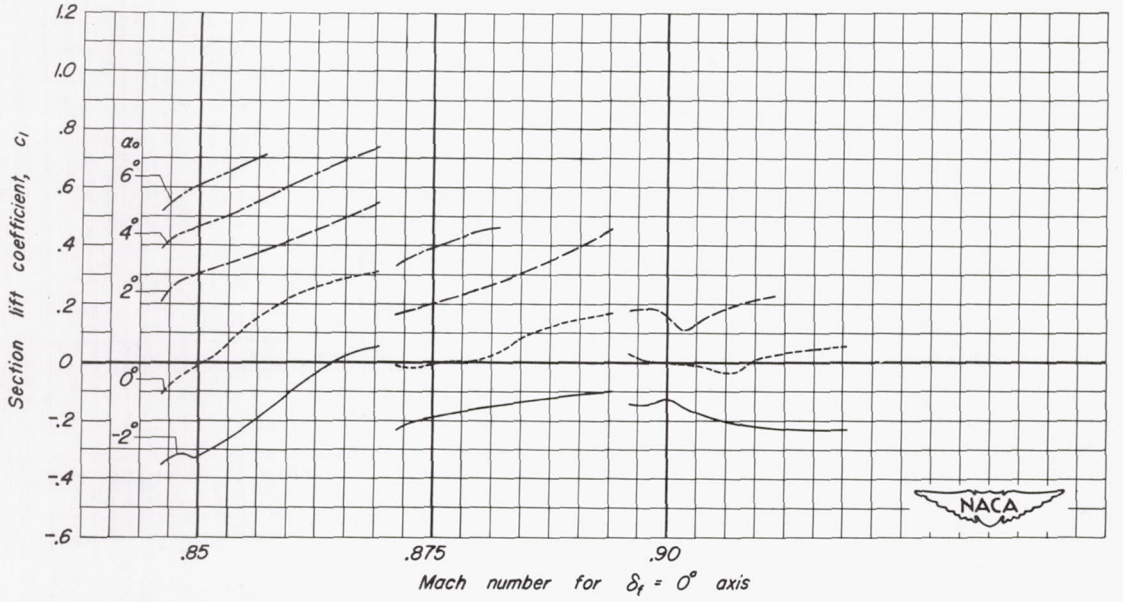

(d) M, 0.85; 0.875; 0.90

Figure 22.- Concluded.

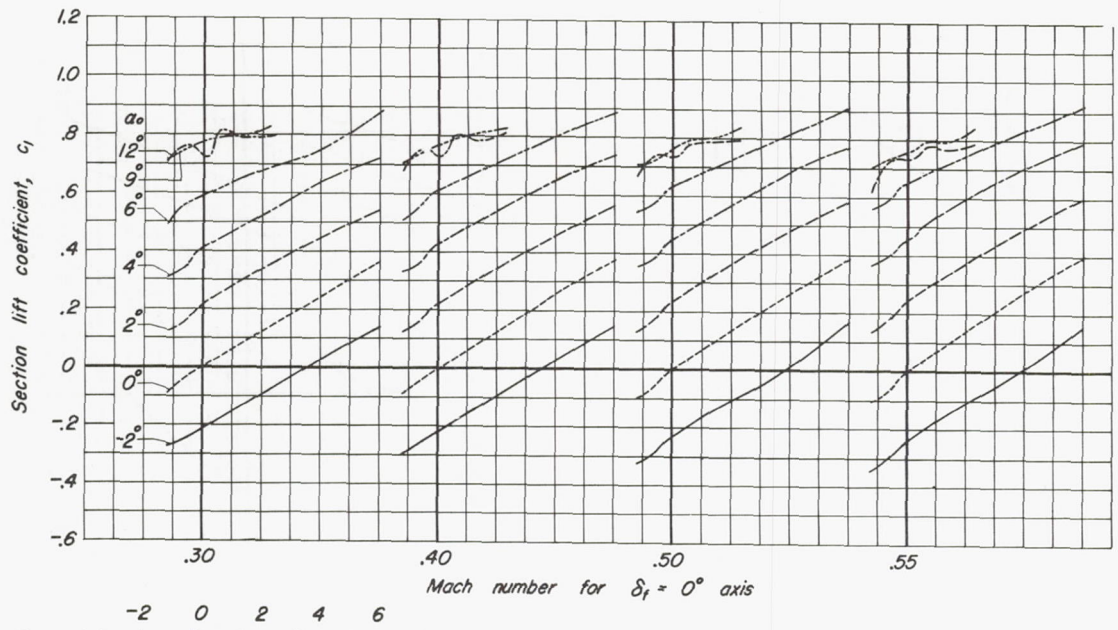

(a) M,0.30;0.40;0.50;0.55

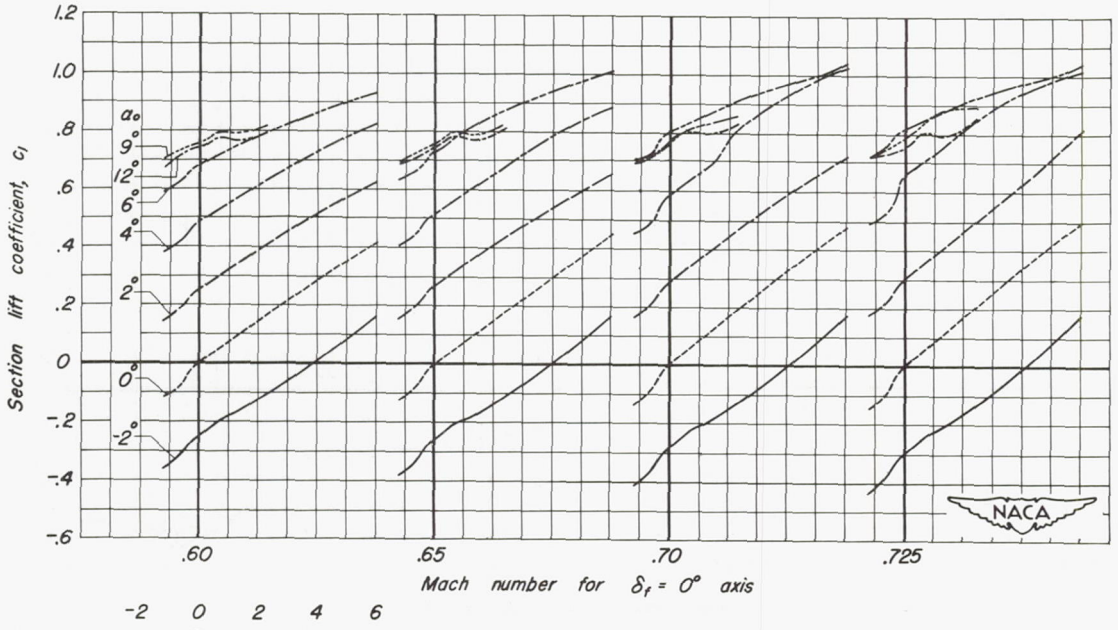

(b) M,0.60;0.65;0.70;0.725

Figure 23.- Variation of section lift coefficient with flap deflection at various Mach numbers for the NACA 0010-0.70 40/0.524 airfoil section with a 25-percent-chord plain flap.

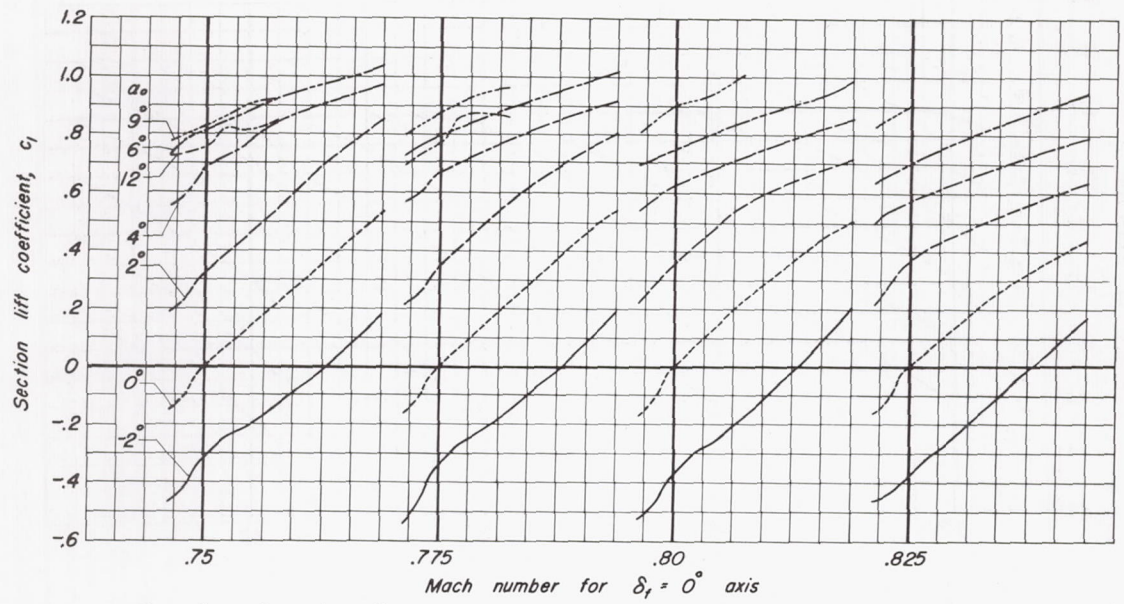

(c) M, 0.75; 0.775; 0.80; 0.825

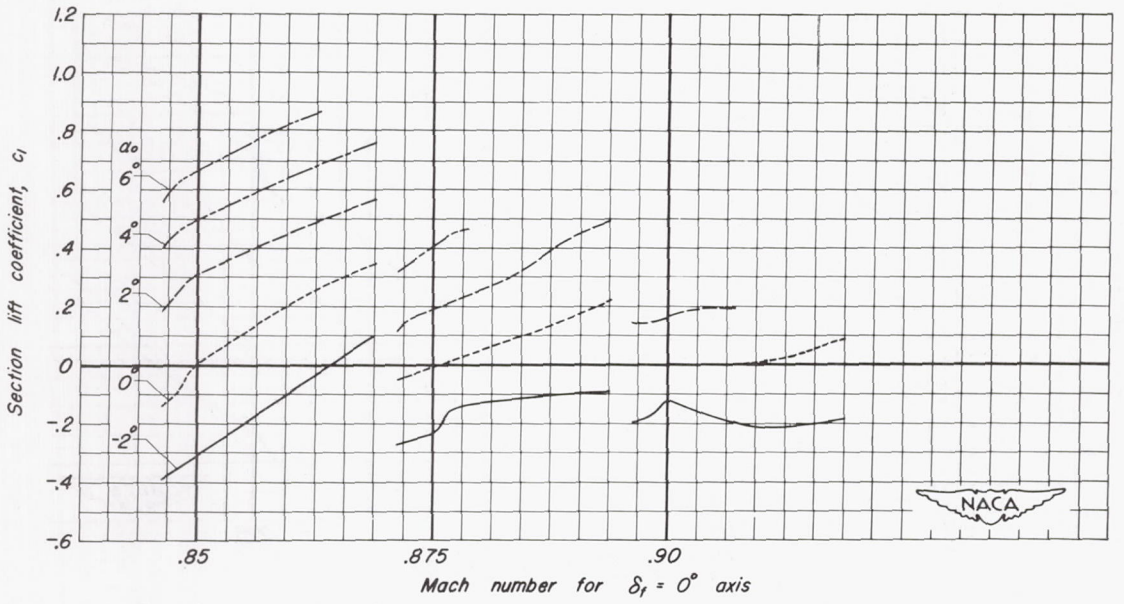

(d) M, 0.85; 0.875; 0.90

Figure 23.– Concluded.

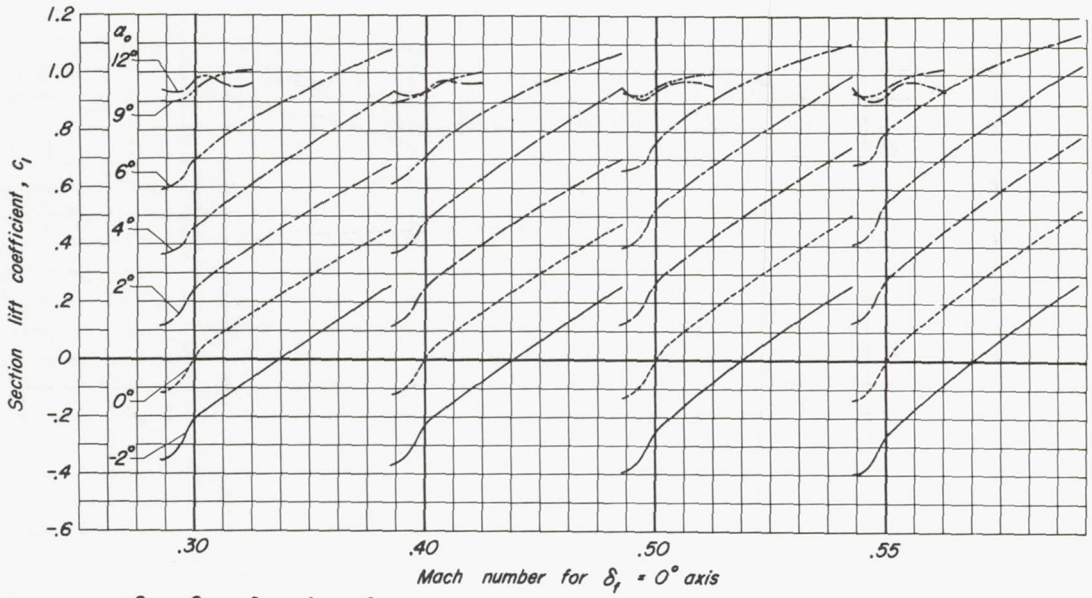

(a) M, 0.30; 0.40; 0.50; 0.55

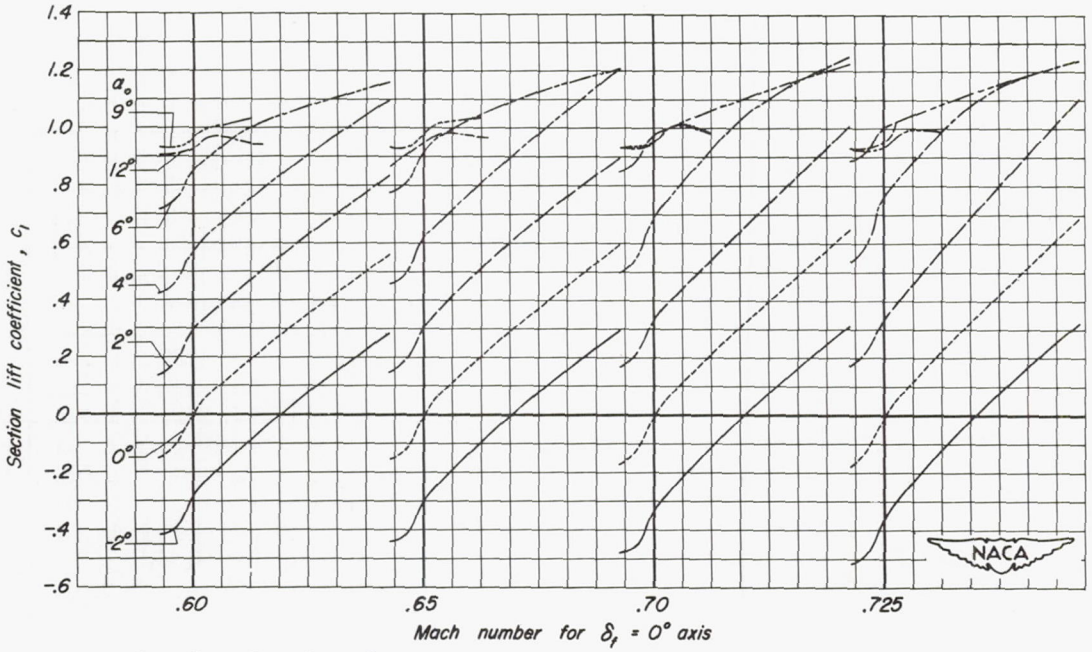

(b) M, 0.60; 0.65; 0.70; 0.725

Figure 24.- Variation of section lift coefficient with flap deflection at various Mach numbers for the NACA 0010 - 0.70 40/1.575 (modification A) airfoil section with a 25-percent-chord plain flap.

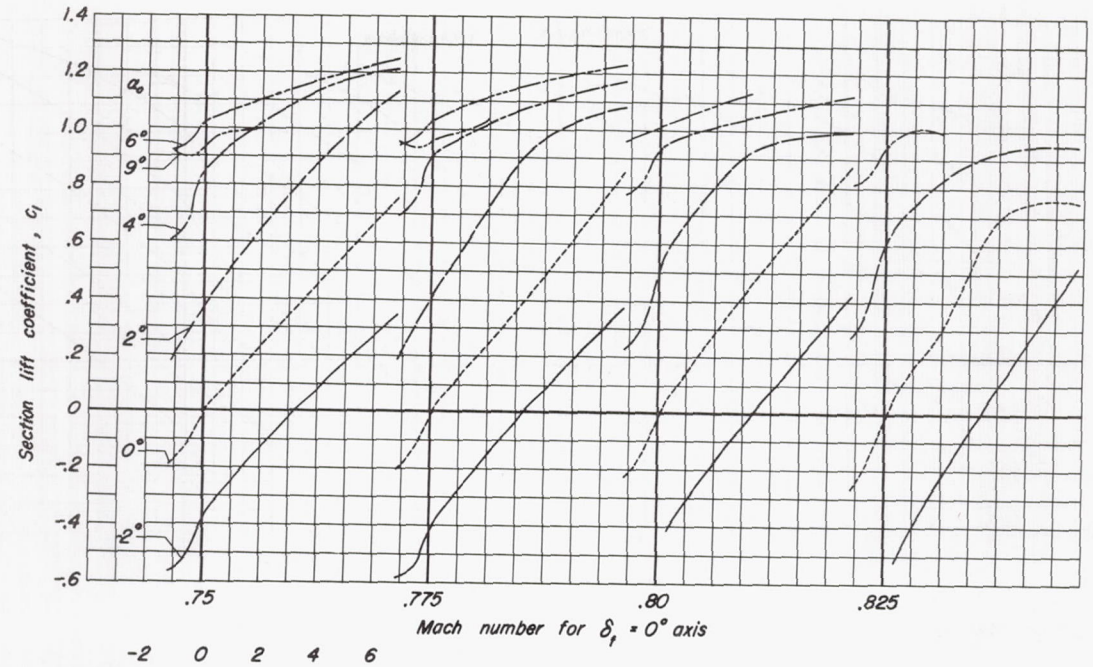

(c) M, 0.75; 0.775; 0.80; 0.825

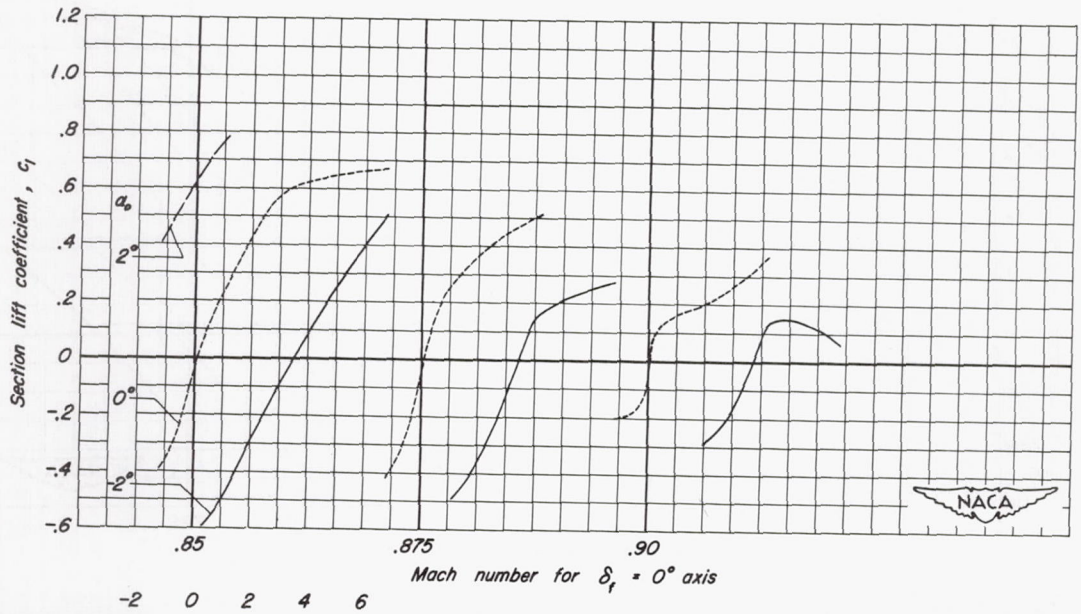

(d) M, 0.85; 0.875; 0.90

Figure 24.– Concluded.

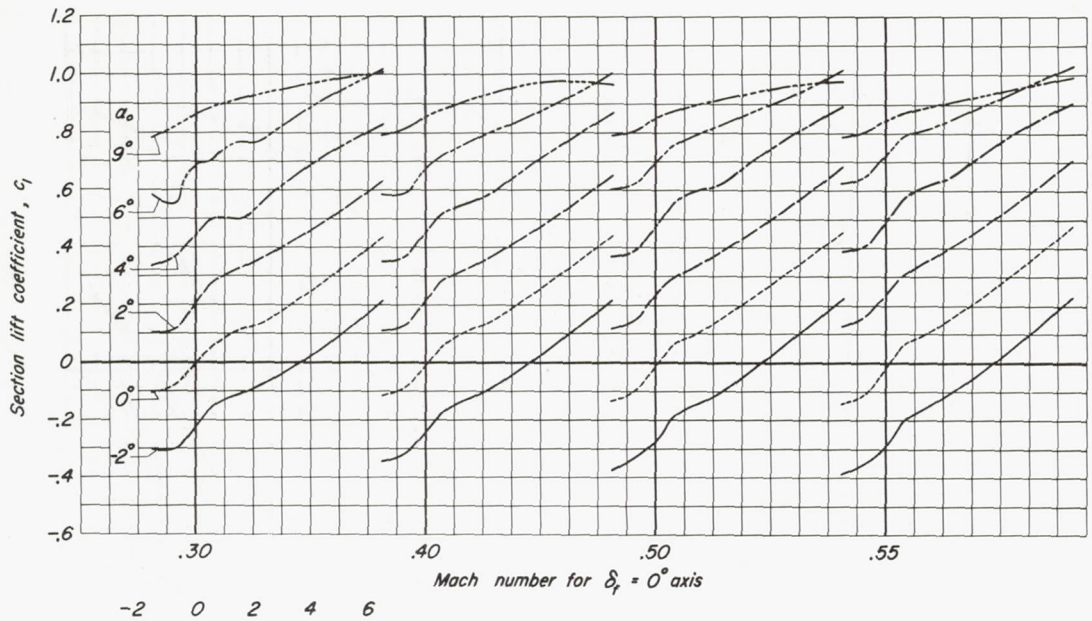

(a) M, 0.30; 0.40; 0.50; 0.55

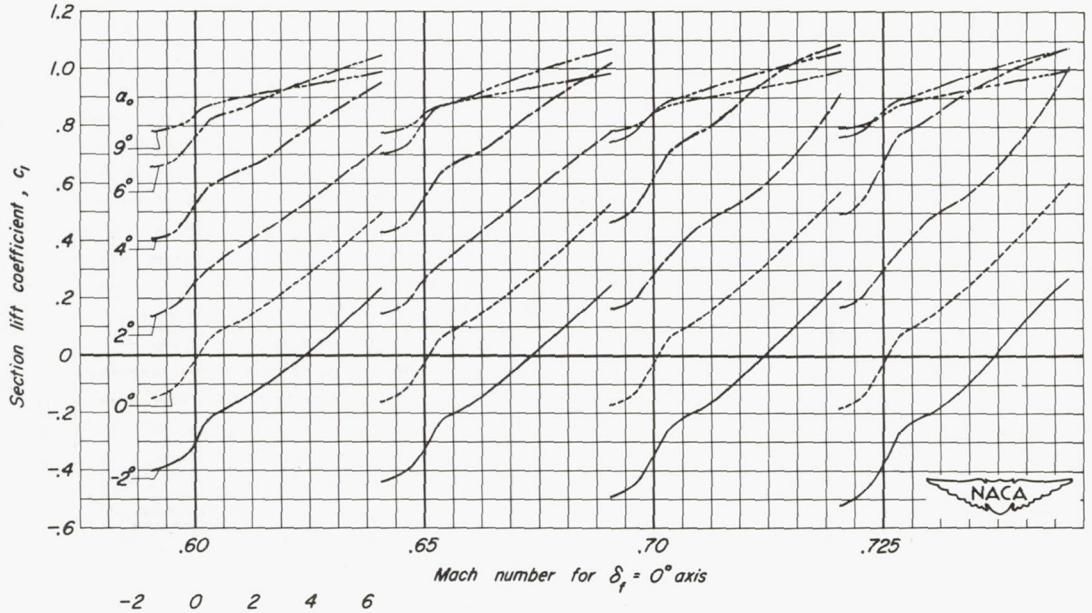

(b) M, 0.60; 0.65; 0.70; 0.725

Figure 25.– Variation of section lift coefficient with flap deflection at various Mach numbers for the NACA 0010 – 0.70 40/1.575 (modification B) airfoil section with a 25-percent-chord plain flap.

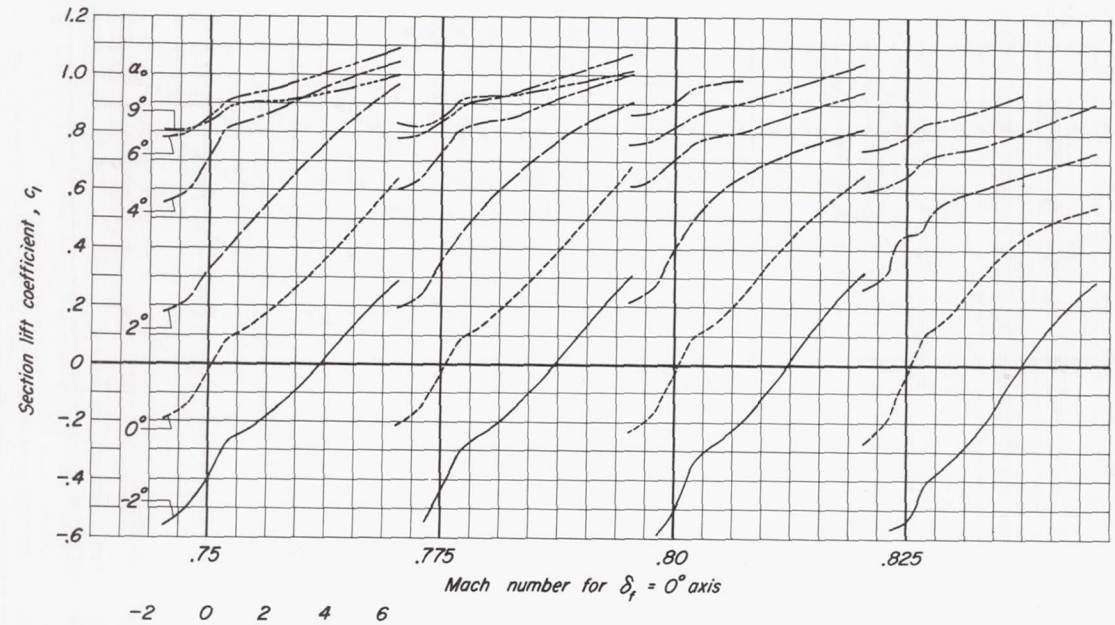

(c) M, 0.75; 0.775; 0.80; 0.825

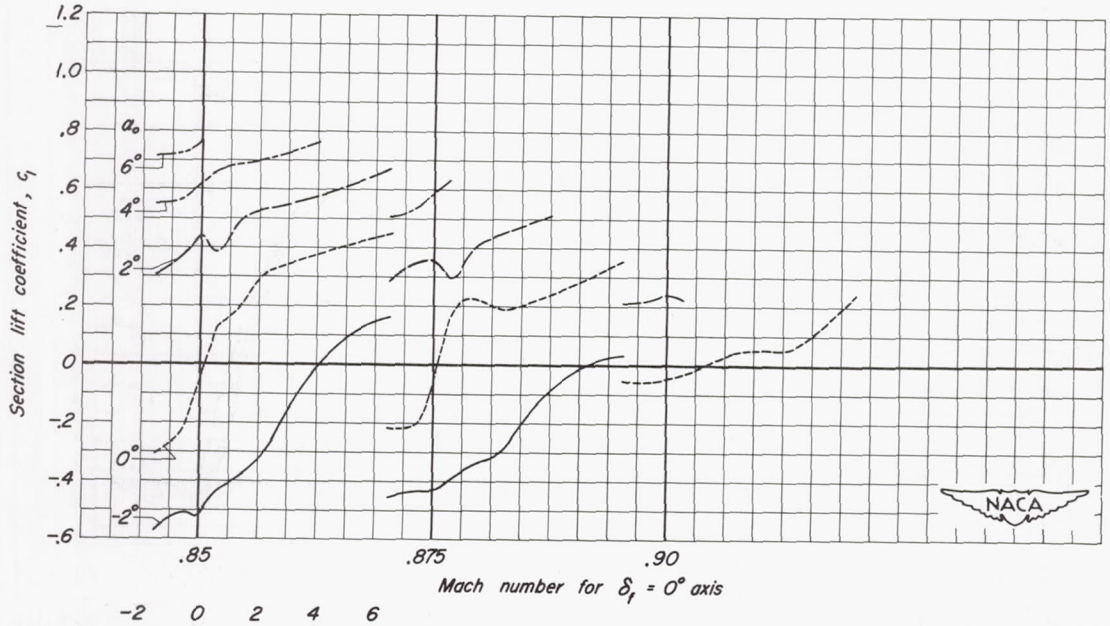

(d) M, 0.85; 0.875; 0.90

Figure 25.- Concluded.

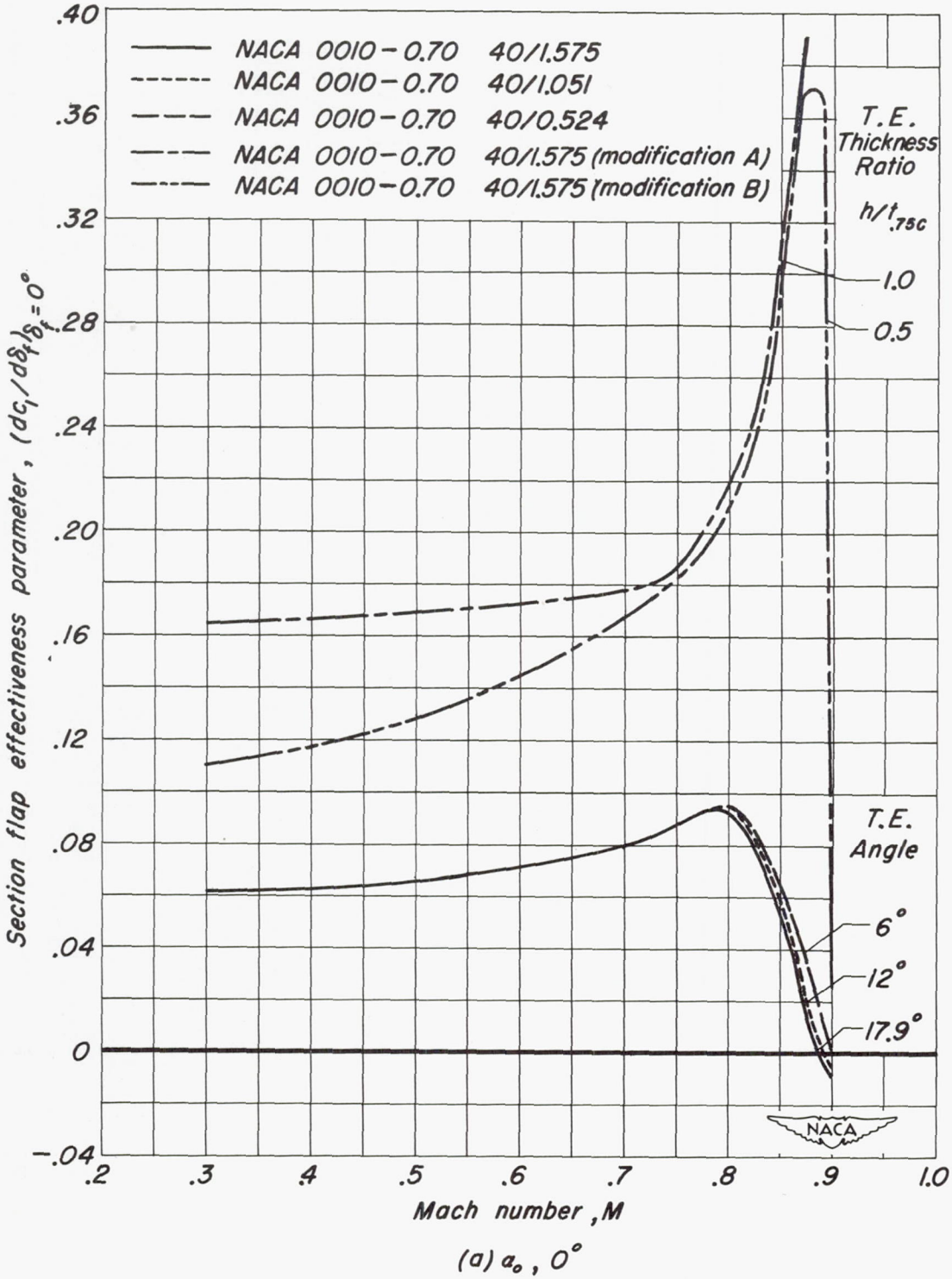

(a) a_o, 0°

Figure 26.- Variation of flap effectiveness with Mach number.

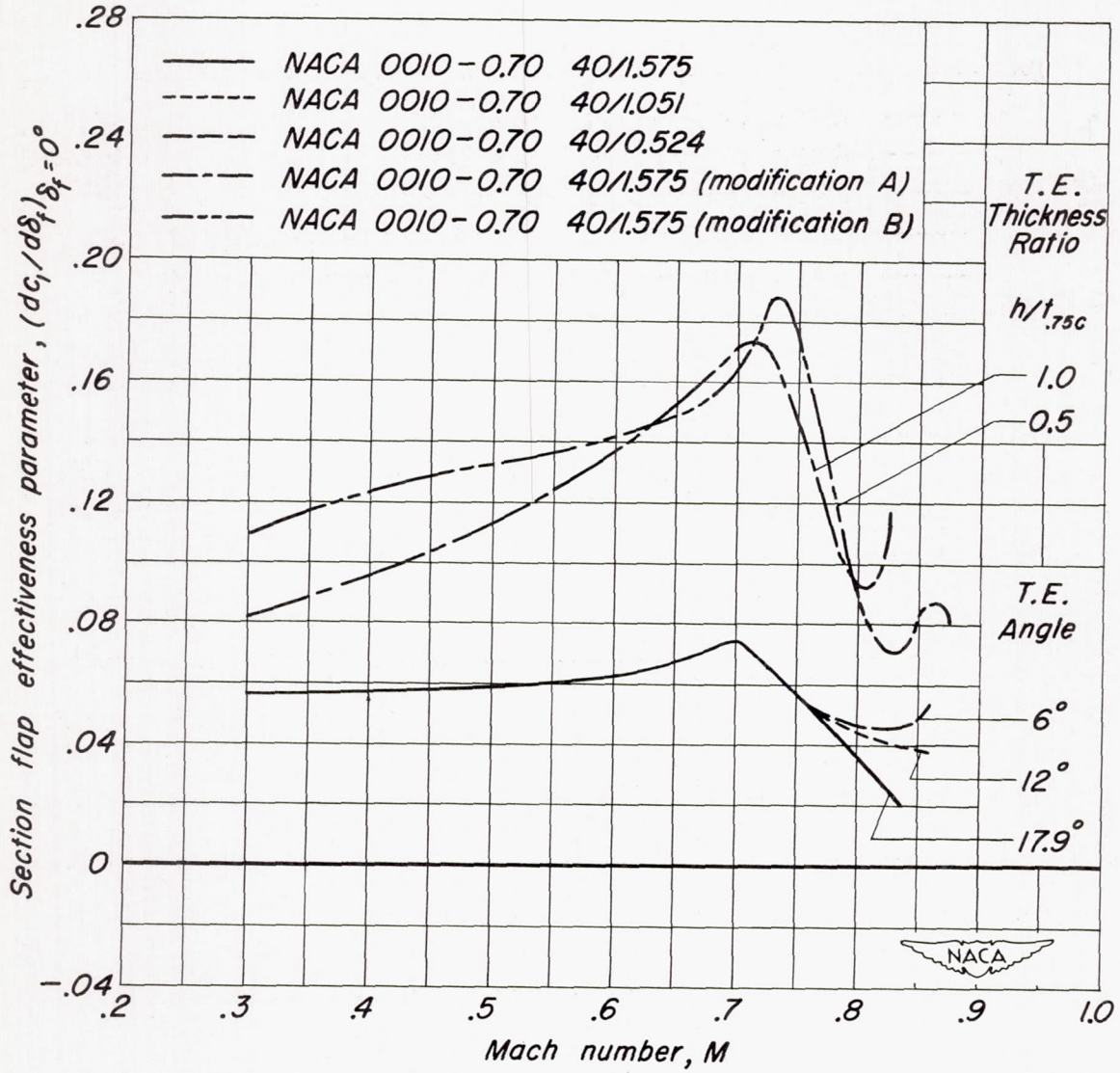

(b) a_o, 4°

Figure 26.- Continued.

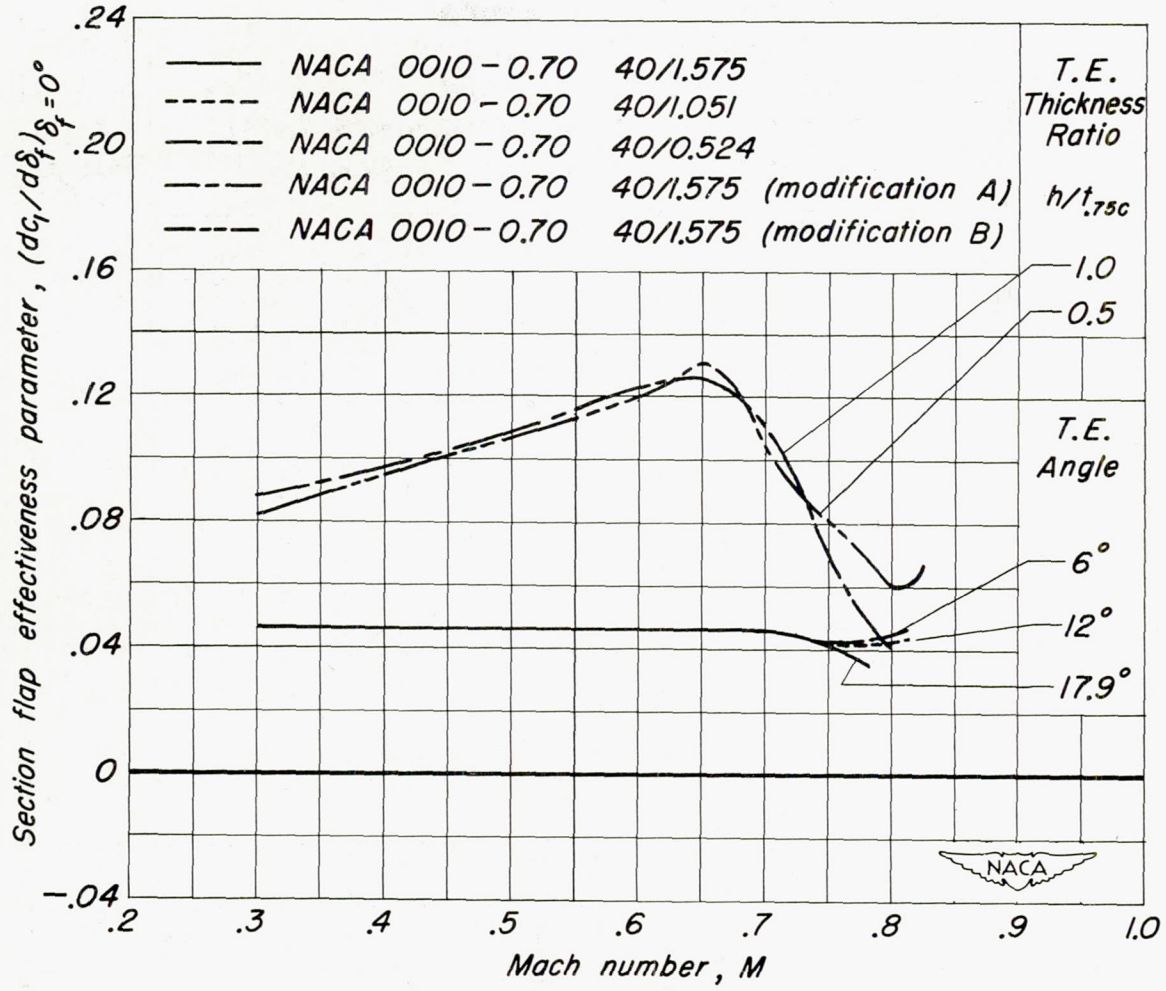

(c) a_o, 6°

Figure 26.- Concluded.

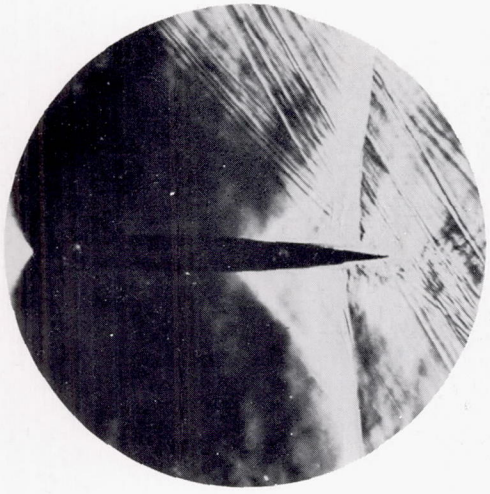

(a) Trailing-edge angle, 17.9°;
M, 0.89

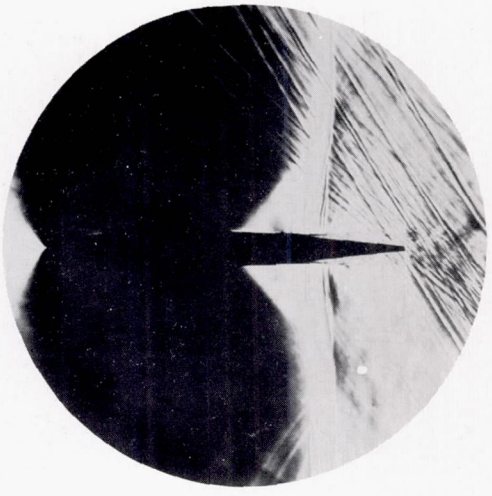

(b) Trailing-edge angle, 12°;
M, 0.88

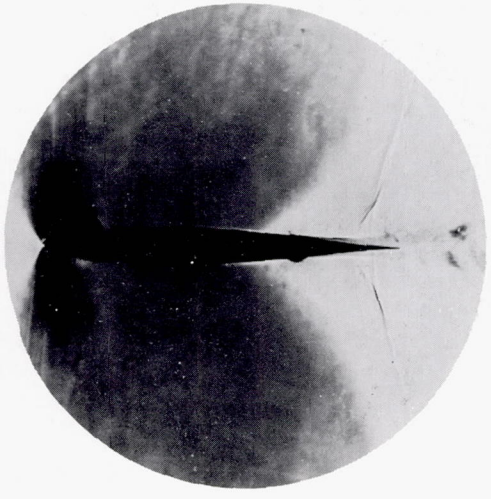

NACA
A-15845

(c) Trailing-edge angle, 6°;
M, 0.88

Figure 27.- Schlieren photographs of flow over the various profiles at zero angle of attack and zero flap deflection.

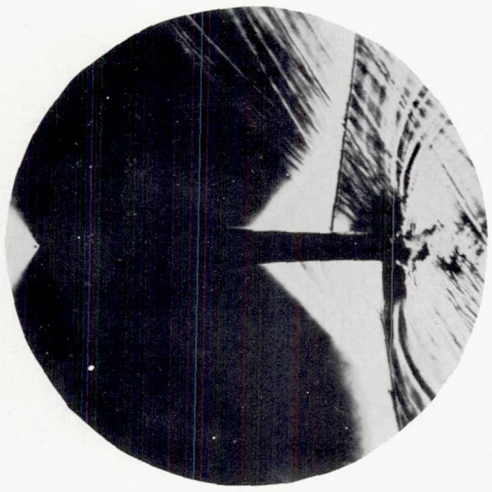

(d) Trailing-edge thickness ratio, $h/t_{0.75c}$, 1.0;
M, 0.89

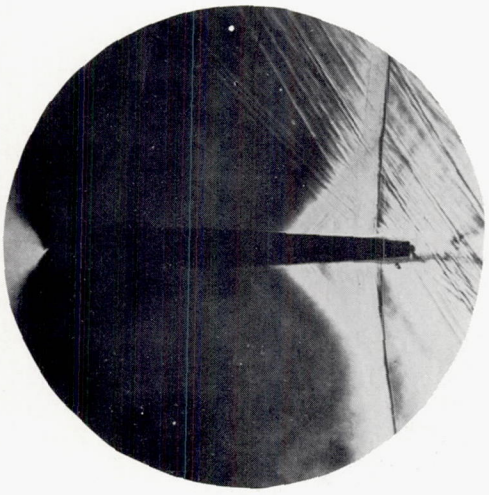

NACA
A-15846

(e) Trailing-edge thickness ratio, $h/t_{0.75c}$, 0.5;
M, 0.88

Figure 27.- Concluded.

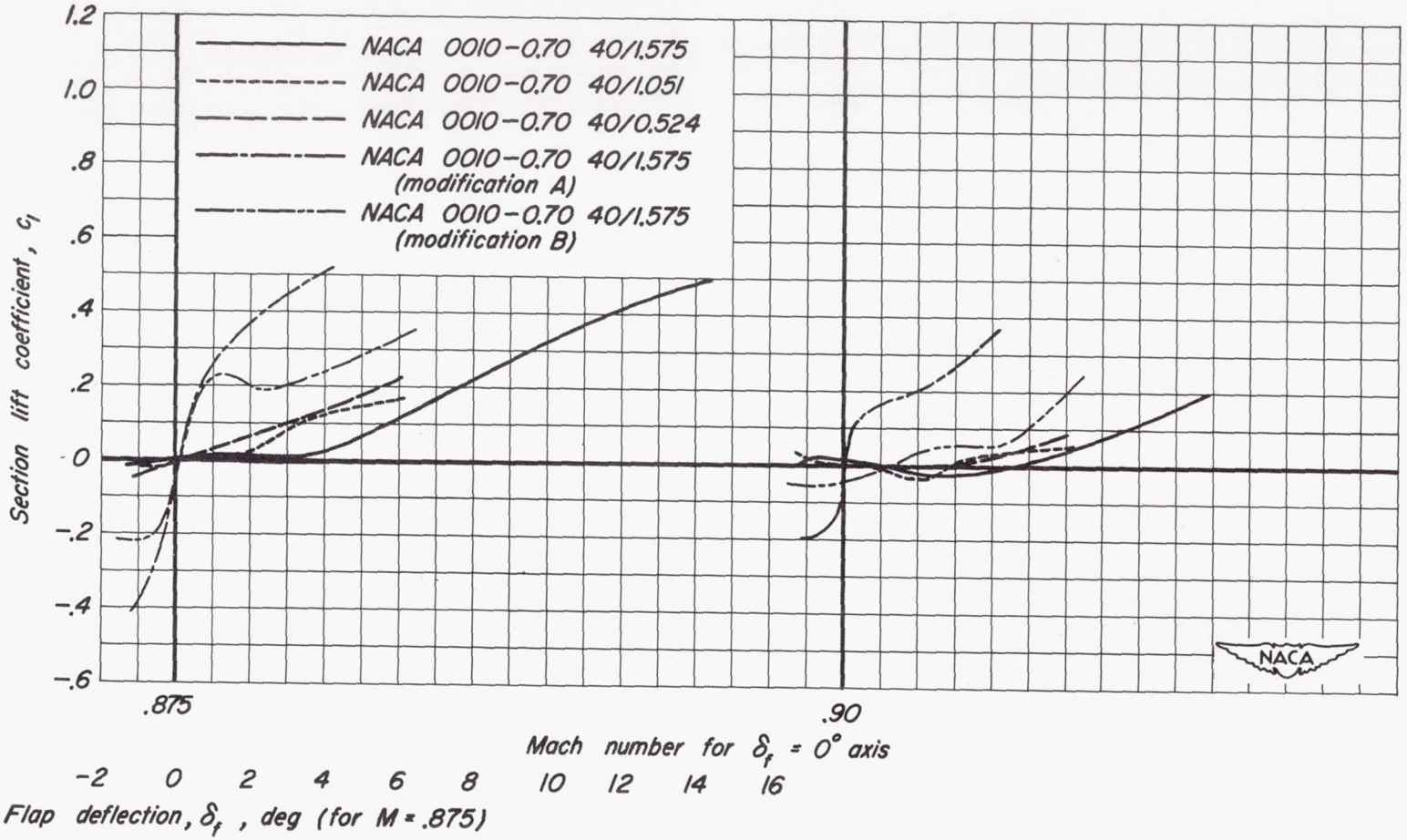

Figure 28.– Variation of section lift coefficient with flap deflection for the various profiles at zero angle of attack; M,0.875 and M,0.90.

NACA-Langley - 6-3-54 - 1000